

**Preparation and Evaluation of Small Peptide Binding Boronic Acid Probes for
Bioconjugation**

by

Negar Mokhtarihaj

A thesis submitted in partial fulfillment of the requirements for the degree of

Master of Science

Department of Chemistry
University of Alberta

© Negar Mokhtarihaj, 2014

Abstract

The study of target proteins in live cells is fundamentally important to understanding their molecular roles in biological processes. Applications of cell permeable small molecules in bioorthogonal reactions have been improved to selectively label proteins tag for the purpose of protein interaction analysis. Bioorthogonal reaction is defined as the chemical reactions that do not react or interfere with biological systems. Functional groups that involve in bioorthogonal reactions must selectively react with each other under physiologically conditions. Also using a small reactive molecule in bioorthogonal reactions can prevent the structural perturbation of the proteins that wants to be monitored. Molecule fluorophores can provide dynamic information on cell surface interactions due to their small size, low detection limits and environmental sensitivity. Boronic acids have been applied in the construction of receptors and chemosensors for a range of biologically important species, especially saccharides. In 2009, for the first time, Schepartz utilized a rhodamine-derived bisboronic acid sensor (RhoBo) as a reversible, selective and non-toxic sensor to selectively label a specific tetraserine peptide. In this thesis, simple monoarylboronic acids with potentially four covalent, reversible points of attachment were designed and synthesized to test their binding affinity to a small peptide tag in a sequence specific manner. Boronate ester formation between serines and the boronic acid part of the molecule was believed to potentially increase the selectivity and stability of imine formation between the lysine and ketone part of the molecule. Binding affinity of designed boronic acids towards a selection of chosen peptides was evaluated *via* the Alizarin Red S colorimetric assay and UV spectrophotometry and fluorescence spectroscopy. In Chapter 2 small boronic acid molecules with Michael acceptors were

designed in which the boronic acid part of the molecule was employed as a way to increase site-specificity of the thiol-Michael addition reactions towards small peptide tag containing cysteine and serine residues. 3-Maleimidophenylboronic acid was found to be reactive towards small peptides containing cysteine and terminal serine residues. Reaction kinetics were performed to monitor its reactivity towards the peptide by HPLC-MS and ^1H NMR spectroscopy.

Acknowledgements

I would never have been able to finish my dissertation without the collaborative effort. I deeply want to thank all the people whom helped me during my research work.

First I am especially grateful to my supervisor Dennis G. Hall for his guidance, advice, caring and support throughout my research studies. My appreciation and thanks are also offered to the rest of my Supervisory Committee and my Examination Committee members: Professor Robert Campbell, Professor Frederick West, Professor Todd Lowary, and Professor Mariusz Klobukowski.

Thanks to the Hall group members, both past and present, for being so great. A special thanks to Burcin Akgun for her great friendship, useful advice and help in my research projects, with her my work in the lab was such a great time, also Dr. Sylvain Bernard for computational calculations, Taras Rybak, Sergiy Vshyvenko and Kaitlyn Lopushinsky for proof reading this manuscript.

Moreover, my research greatly benefited from the great research services with amazing people at the University of Alberta. I would like to thank the NMR lab especially to Nupur Dabral, the Mass Spectrometry lab especially to Ed Fu and Wayne Moffat, the machine shop and storeroom. I would also like to thank Dr. Hayley Wan and Dr. Norman Gee for their wonderful work as undergraduate lab coordinators.

The research presented in this thesis would not have been possible without the help of various funding agencies. My gratitude goes to the Natural Research and Engineering Research Council (NSERC) and the University of Alberta for supporting my research.

I would like to thank my parents for all the support they have provided me over the years and always being there for me. I would like to thank my fiancé for all his support; my life has become so great after meeting him during my graduate studies.

Table of Contents

Chapter 1 Introduction: Bioconjugation, Preparation	
1.1 Background and significance	1
1.2 Bioorthogonal chemistry	2
1.2.1 Nucleophilic substitution	2
1.2.2 Bioorthogonal reactions by using small peptide tag	4
1.2.3 Use of azide in bioorthogonal reactions	6
1.2.3.1 Staudinger ligation	6
1.2.3.2 Cu-catalyzed [3+2] azide-alkyne cycloaddition (CuAAC)	8
1.2.3.3 Strain-promoted alkyne-azide cycloaddition	9
1.2.4 Diels-Alder cycloadditions	10
1.3 Chemoselective sensors of saccharides using simple boronic acids	12
1.4 Boronic acid sensors for selective recognition of proteins	18
1.5 Thesis research objectives	20
1.6 References	21
Chapter 2 Design and Synthesis of Small Aryl Boronic Acid Reporters with Potentially Four Covalent, Reversible Points of Attachment to Peptides	
2.1 Introduction	32
2.2 Design and synthesis of small monoboronic acid probes	33
2.3 Design of a peptide array	35
2.4 Alizarin Red S (ARS) as a competitive assay for the complexation of boronic acids	40
2.5 Other methods for the determination of binding affinity between boronic acids and peptides	46
2.5.1 Binding studies with UV spectrophotometry	46
2.5.2. Binding studies with fluorescence spectroscopy	49
2.5.3. Binding studies by HPLC-MS analysis	52
2.6 Summary	52
2.7 Future work	53
2.8 Experimental	53
2.8.1 General information	53
2.8.2 General procedure for the preparation of aryl boronic acids using the Miyaura reaction	54
2.8.3 Synthesis of 2-benzoylphenyl boronic acid (BA1)	55
2.8.4 Synthesis of 3-benzoylphenyl boronic acid (BA2)	55
2.8.5 Synthesis of 4-benzoylphenyl boronic acid (BA3)	56
2.8.6 Synthesis of 2-bromo-9-fluorenone	56
2.8.7 Synthesis of 9-fluorenone-2-boronic acid (BA4)	57
2.8.8 Peptides 1-10: Synthesis and characterization	58

2.8.9 Resin cleavage with TFA	59
2.9 References	59
Chapter 3 Design and Synthesis of Boronic Acids Containing Michael Acceptor Units for Selective Labeling of Proteins	
3.1 Introduction	61
3.2 Design and synthesis of functionalized boronic acids	62
3.3 Design of peptide array	65
3.4 ¹H NMR kinetic analysis	67
3.5 Kinetic study by HPLC-MS	79
3.6 Summary	82
3.7 Future work	82
3.8 Experimental	83
3.8.1 General information	83
3.8.2 Synthesis of (<i>E</i>)-2-boronic acid-chalcone (BA5)	83
3.8.3 Synthesis of (<i>E</i>)-4-boronic acid-chalcone (BA6)	84
3.8.4 Synthesis of 3-acrylamidophenyl boronic acid (BA7)	85
3.8.5 Synthesis of N-phenylmaleimide	86
3.8.6 Synthesis of 3-maleimidophenylboronic (BA8)	87
3.8.7 Synthesis of peptide 2	87
3.8.8 Synthesis of peptides by solid phase peptide synthesis	88
3.8.9 ¹ H NMR kinetic analysis	89
3.8.10 HPLC-MS kinetic analysis	89
3.3 References	90
Chapter 4 Conclusions and Future Perspectives	
4.1 Thesis summary and conclusions	92
4.2 Future perspectives	93
Bibliography	95
Appendices	
Appendix 1 Selected copies of NMR spectra	107
Appendix 2 HPLC-MS data for peptides	116

List of Tables

Table 2-1: Click Diels–Alder cycloadditions	11
Table 2-2: Calculated and observed mass of peptides 1-11	39

List of Figures

Figure 1-1: A general scheme for a bioorthogonal chemical reporter strategy	2
Figure 1-2: Reaction of tetracysteine containing peptide or protein domain with FlAsH–EDT ₂ or ReAsH–EDT	4
Figure 1-3: Condensation between RhoBo and tetraserines peptide tag	5
Figure 1-4: Cyclooctynes synthesized for Cu–free click chemistry in living cells	10
Figure 1-5: Boronic acid sensors	13
Figure 1-6: Diboronic acids sensors	14
Figure 1-7: Flexible diboronic acid tweezer sensors	15
Figure 1-8: Structure of benzoboroxole library and Gal-β-1,3-GalNAc	16
Figure 1-9: Different aggregation behavior of boronic acid probe with fructose and glucose. Reprinted with permission from <i>J. Am. Chem. Soc.</i> , 2013, 135, 1700–1703. Copyright 2013 American Chemical Society	17
Figure 1-10: Recognition of sialic acid on virus surface by modifying quantum dots with phenyl boronic acid	18
Figure 1-11: A Stable iminoboronate with reversible linkage	19
Figure 1-12: Iminoboronate probe for labeling cancer cells	20
Figure 2-1: A designed boronic acid with potentially four covalent bonds with a peptide tag	33
Figure 2-2: Boronic acid functionalized benzophenone derivatives	34
Figure 2-3: Molecular modeling for interaction of peptide 11 and 9-fluorenone-2-boronic acid (BA4)	40
Figure 2-4: Solutions of ARS (10 ⁻⁴ M in 0.1 M phosphate buffer) and A) phenylboronic acid with D-glucamine B) boronic acid (BA1) with D-glucamine C) boronic acid (BA2) with D-glucamine D) boronic acid (BA3) with D-glucamine and E) boronic acid (BA4) with D-glucamine	43
Figure 2-5: Solutions of ARS (10 ⁻⁴ M in 0.1 M phosphate buffer) and A) phenylboronic acid with fructose B) boronic acid (BA1) with fructose C) boronic acid (BA2) with fructose D) boronic acid (BA3) with fructose and E) boronic acid (BA4) with fructose	43
Figure 2-6: Solutions of ARS (10 ⁻⁴ M in 0.1 M phosphate buffer) and boronic acid (BA1) (0.02 M) containing: A, 0.5 M peptide 1; B, 0.5 M peptide 2; C, 0.5 M peptide 3; D, 0.5 M peptide 4; E, 0.5 M peptide 5; F, 0.5 M peptide 6; G, 0.5 M peptide 7	44
Figure 2-7: Solutions of ARS (10 ⁻⁴ M in 0.1 M phosphate buffer) and boronic acid (BA2) (0.02 M) containing: A, 0.5 M peptide 1; B, 0.5 M peptide 2; C, 0.5 M peptide 3; D, 0.5 M peptide 4; E, 0.5 M peptide 5; F, 0.5 M peptide 6; G, 0.5 M peptide 7	44
Figure 2-8: Solutions of ARS (10 ⁻⁴ M in 0.1 M phosphate buffer) and boronic acid (BA3) (0.02 M) containing: A, 0.5 M peptide 1; B, 0.5 M peptide 2; C, 0.5 M peptide 3; D, 0.5 M peptide 4; E, 0.5 M peptide 5; F, 0.5 M peptide 6; G, 0.5 M peptide 7	45

Figure 2-9: Solutions of ARS (10^{-4} M in 0.1 M phosphate buffer) and boronic acid (BA4) (0.02 M) containing: A, 0.5 M D-glucamine; B, 0.5 M peptide 1; C, 0.5 M peptide 2; D, 0.5 M peptide 3; E, 0.5 M peptide 4, F; 0.5 M peptide 5, G, 0.5 M peptide 6, H, 0.5 M peptide 7; I, no peptide	45
Figure 2-10: UV absorbance of 2-benzoylphenyl boronic acid (BA1) in pH = 7 with peptides 1-7, peptide GGSS-NH ₂ and peptide Ac-SPGS-NH ₂ , fructose and D-glucamine	47
Figure 2-11: UV absorbance of 3-benzoylphenyl boronic acid (BA2) in pH = 7 with peptides 1-7, peptide GGSS-NH ₂ and peptide Ac-SPGS-NH ₂ , fructose and D-glucamine	47
Figure 2-12: UV absorbance of 4-benzoylphenyl boronic acid (BA3) in pH = 7 with peptides 1-7, peptide GGSS-NH ₂ and peptide Ac-SPGS-NH ₂ , fructose and D-glucamine	48
Figure 2-13: UV absorbance of 9-fluorenone-2-boronic acid (BA4) in pH = 7 with peptides 1-7, peptide GGSS-NH ₂ and peptide Ac-SPGS-NH ₂ , fructose and D-glucamine	48
Figure 2-14: Fluorescence response of 9-fluorenone-2-boronic acid towards peptides	49
Figure 2-15: Fluorescent response of 9-fluorenone-2-boronic acid towards peptide 3	50
Figure 2-16: Fluorescent response of ARS (10^{-4}) to A) 9-fluorenone-2-boronic acid (10^{-3}) and peptide Ac-SGPS-NH ₂ (10^{-2}) B) 9-fluorenone-2-boronic acid (10^{-3}) and C) D-glucamine (10^2)	51
Figure 2-17: Vials of ARS (10^{-4} M in 0.1 M phosphate buffer) and boronic acid (BA4) (0.02 M) containing: A, 0.5 M D-glucamine; B, no peptide; C, peptide Ac-SGPS-NH ₂	52
Figure 2-18: General strategy for SPPS on Rink Amide resin	58
Figure 3-1: Proposed boronic acids functionalized with a Michael acceptor	62
Figure 3-2: Library of peptides 1-5	66
Figure 3-3: a) The reaction between 3-maleimidophenylboronic acid and peptide 2 was monitored at ~0.5 mM concentrations in 30 % CD ₃ CN: D ₂ O by ¹ H NMR at room temperature. b) The second-order rate constant was calculated by plotting 1/[3-maleimidophenylboronic acid] as a function of time. The slope of the resulting line is the rate constant. Data is plotted to within 76% and 82% conversion to the product. c) Calculated second-order rate constants for each trial	69
Figure 3-4: a) The reaction between N-phenylmaleimide and peptide 2 was monitored at ~0.5 mM concentrations in 30 % CD ₃ CN: D ₂ O by ¹ H NMR at room temperature. b) The second-order rate constant was calculated by plotting 1/[N-phenylmaleimide] as a function of time. The slope of the resulting line is the rate constant. Data is plotted to within 67% and 71% conversion to the product. c) Calculated second-order rate constants for each trial	70
Figure 3-5: a) The reaction between 3-maleimidophenylboronic acid and peptide 1 was monitored at ~0.5 mM concentrations in 30 % CD ₃ CN: D ₂ O by ¹ H NMR at room	71

temperature. b) The second-order rate constant was calculated by plotting $1/[3\text{-maleimidophenyl boronic acid}]$ as a function of time. The slope of the resulting line is the rate constant. Data is plotted to within 62% and 67% conversion to the product. c) Calculated second-order rate constants for each trial

Figure 3-6: a) The reaction between N-phenylmaleimide and peptide **1** was monitored at ~ 0.5 mM concentrations in 30 % $\text{CD}_3\text{CN}:\text{D}_2\text{O}$ by ^1H NMR at room temperature. b) The second-order rate constant was calculated by plotting $1/[\text{N-phenylmaleimide}]$ as a function of time. The slope of the resulting line is the rate constant. Data is plotted to within 62% and 67% conversion to the product. c) Calculated second-order rate constants for each trial 72

Figure 3-7: a) The reaction between 3-maleimidophenylboronic acid and peptide **3** was monitored at ~ 0.5 mM concentrations in 30 % $\text{CD}_3\text{CN}:\text{D}_2\text{O}$ by ^1H NMR at room temperature. b) The second-order rate constant was calculated by plotting $1/[3\text{-maleimidophenylboronic acid}]$ as a function of time. The slope of the resulting line is the rate constant. Data is plotted to within 79% and 80% conversion to the product. c) Calculated second-order rate constants for each trial 73

Figure 3-8: a) The reaction between N-phenylmaleimide and peptide **3** was monitored at ~ 0.5 mM concentrations in 30 % $\text{CD}_3\text{CN}:\text{D}_2\text{O}$ by ^1H NMR at room temperature. b) The second-order rate constant was calculated by plotting $1/[\text{N-phenylmaleimide}]$ as a function of time. The slope of the resulting line is the rate constant. Data is plotted to within 74% and 79% conversion to the product. c) Calculated second-order rate constants for each trial 74

Figure 3-9: a) The reaction between 3-maleimidophenylboronic acid and peptide **4** was monitored at ~ 0.5 mM concentrations in 30 % $\text{CD}_3\text{CN}:\text{D}_2\text{O}$ by ^1H NMR at room temperature. b) The second-order rate constant was calculated by plotting $1/[3\text{-maleimidophenylboronic acid}]$ as a function of time. The slope of the resulting line is the rate constant. Data is plotted to within 70% and 78% conversion to the product. c) Calculated second-order rate constants for each trial 75

Figure 3-10: a) The reaction between N-phenylmaleimide and peptide **4** was monitored at ~ 0.5 mM concentrations in 30 % $\text{CD}_3\text{CN}:\text{D}_2\text{O}$ by ^1H NMR at room temperature. b) The second-order rate constant was calculated by plotting $1/[\text{N-phenylmaleimide}]$ as a function of time. The slope of the resulting line is the rate constant. Data is plotted to within 76% and 81% conversion to the product. c) Calculated second-order rate constants for each trial 76

Figure 3-11: a) The reaction between 3-maleimidophenylboronic acid and peptide **5** was monitored at ~ 0.5 mM concentrations in 30 % $\text{CD}_3\text{CN}:\text{D}_2\text{O}$ by ^1H NMR at room temperature. b) The second-order rate constant was calculated by plotting $1/[3\text{-maleimidophenylboronic acid}]$ as a function of time. The slope of the resulting line is the rate constant. Data is plotted to within 76% and 81% conversion to the product. c) Calculated second-order rate constants for each trial 77

- Figure 3-12:** a) The reaction between N-phenylmaleimide and peptide **5** was monitored at ~0.5 mM concentrations in 30 % CD₃CN: D₂O by ¹H NMR at room temperature. b) The second-order rate constant was calculated by plotting 1/[N-phenylmaleimide] as a function of time. The slope of the resulting line is the rate constant. Data is plotted to within 76% and 81% conversion to the product. c) Calculated second-order rate constants for each trial 78
- Figure 3-13:** Reaction between 1/[3-maleimidophenylboronic acid] and peptide **2** in ammonium acetate buffer (pH = 5.5) was monitored by HPLC by monitoring the disappearance of both starting materials and appearance of the product. N-Methylacetanilide was used as an internal standard. Second order rate constant for the reaction was determined by plotting the 1/[3-maleimidophenylboronic acid] versus time and analyzing by linear regression. Second order rate constant corresponds to the slope. a) Trial 1 b) Trial 2 80
- Figure 3-14:** Reaction between 1/[N-phenylmaleimide] and peptide **2** in ammonium acetate buffer (pH = 5.5) was monitored by HPLC by monitoring the disappearance of both starting materials and appearance of the product. N-Methylacetanilide was used as an internal standard. Second order rate constant for the reaction was determined by plotting the 1/[N-phenylmaleimide] versus time and analyzing by linear regression. Second order rate constant corresponds to the determined slope. a) Trial 1 b) Trial 2 81

List of Schemes

Scheme 1-1: Stable imine formation with hydrazide and aminoxy functionalized groups	3
Scheme 1-2: Pictet–Spengler type reaction	3
Scheme 1-3: Staudinger ligation of a 2–(diphenylphosphoryl)benzoic ester derivatives with an alkyl azide	7
Scheme 3-4: Synthesis of borane protected phosphine and subsequent coupling to acetylalanine and deprotection with DABCO	8
Scheme 1-5: Amide bond formation with a modified Staudinger ligation	8
Scheme 1-6: (A) The terminal 1,3–dipolar cycloaddition of azides (B) The Cu(I)–catalyzed formal azide–alkyne cycloaddition (C) The strain–promoted cycloaddition between azides and cyclooctynes	9
Scheme 1-7: Thermodynamic cycle of boronic acid interaction with cis–1,2–diols	12
Scheme 1-8: B–N bond interaction after boronic ester formation	14
Scheme 2-1: Synthesis of 3-benzoylphenyl boronic acid (BA2)	34
Scheme 2-2: Synthesis of 9-fluorenone-1-boronic acid (BA4)	35
Scheme 2-3: Mechanism for Fmoc deprotection in SPPS	36
Scheme 2-4: Mechanism for coupling amino acids in SPPS	37
Scheme 2-5: Mechanism of peptide cleavage from resin with TFA	38
Scheme 2-6: Alizarin Red S binding with a boronic acid	41
Scheme 3-1: Preparation of (<i>E</i>)-2-boronic acid-chalcone (BA5)	63
Scheme 3-2: Synthesis of 3-acrylamidophenylboronic acid (BA7)	63
Scheme 3-3: Preparation of 3-maleimidophenylboronic acid (BA8)	65
Scheme 3-4: Synthesis of peptide 2	65

List of Abbreviations

Ac	Acetyl
ACS	American Chemical Society
AM1	Austin Model 1
Ar	Aryl group
AZT	Azidothymidine
ARS	Alizarin Red S
BA	Boronic Acid
Bn	Benzyl
br s	Broad singlet
<i>t</i> -Boc	<i>tert</i> -Butyloxycarbonyl
<i>t</i> -Bu	<i>tert</i> -Butyl
calcd	Calculated
cm ⁻¹	Wavenumbers
DCC	<i>N,N'</i> -Dicyclohexylcarbodiimide
DCM	Dichloromethane
DCU	Dicyclohexyl urea
DIC	<i>N,N'</i> -Diisopropylcarbodiimide
dd	Doublet of doublets
DIPEA	<i>N,N</i> -Diisopropylethylamine
DMAP	4-Dimethylaminopyridine
DMF	<i>N,N</i> -Dimethylformamide
DMSO	Dimethyl sulfoxide
DNA	Deoxyribonucleic acid
dppf	1,1'-Bis(diphenylphosphino)ferrocene
EI	Electron impact
equiv	Equivalents
ESI	Electrospray ionization
Et	Ethyl

Et ₂ O	Diethyl ether
EtOAc	Ethyl acetate
EtOH	Ethanol
FlAsH-EDT ₂	4,5-Bis(1,3,2-dithiarsolan-2-yl)fluorescein
Fmoc	9-Fluorenylmethoxycarbonyl
h	Hour
HBTU	<i>N,N,N',N'</i> -Tetramethyl-O-(1H-benzotriazol-1-yl)uranium hexafluorophosphate
HPLC	High performance liquid chromatography
HRMS	High resolution mass spectrometry
HOAt	1-Hydroxy-7-azabenzotriazole
HOBt	Hydroxybenzotriazole
IR	Infrared spectroscopy
m	Multiplet
MALDI-TOF	Matrix-Assisted Laser Desorption Ionization-Time of Flight
Me	Methyl
MeCN	Acetonitrile
MeOH	Methanol
NMR	Nuclear magnetic resonance
Ph	Phenyl
pin	Pinacolato
<i>i</i> -Pr	Isopropyl
ReAsH-EDT ₂	4,5-Bis(1,3,2-dithiarsolan-2-yl)-resorufin
rt	Room temperature
SPPS	Solid phase peptide synthesis
TIPS	Triisopropylsilane
TCEP	Tris(2-carboxyethyl)phosphine
TFA	Trifluoroacetic acid
THF	Tetrahydrofuran
TIPS	Triisopropylsilyl chloride

Chapter 1

Introduction: Bioconjugation, Preparation

1.1 Background and significance

Living systems are composed of numerous biopolymers and small molecule metabolites. The ability to track molecules in their native environment has provided better understanding of biological processes through *in vivo* studies.^{1,2} During the past century, biological chemistry has evolved in the field of cellular event monitoring. An early attempt to monitor ongoing biological processes involved visualization by fluorescence microscopy whereby Green Fluorescent Protein (GFP) was fused to a protein of interest. In 2008, the Nobel Prize in Chemistry was awarded to Osamu Shimomura, Martin Chalfie and Roger Y. Tsien for the discovery, development and application of the green fluorescent proteins.¹ Genetic engineering has progressed dramatically and now provides several methods for the incorporation of various Fluorescent Proteins (FPs) into model systems and living organisms.³ Introduction of the FP gene into cellular DNA allows the cell to incorporate an FP into a protein. These proteins of interest can be monitored by fluorescence spectroscopy by exciting the FP tag using a suitable wavelength. These proteins have been widely used to visualize gene expression, protein localization, interaction and degradation within live cells and organisms. While FPs techniques continue to be valuable tools for cell biology, this method is not without its limitations. FPs can form unwanted aggregates and could also interfere with the function, interaction and assembly of the labeled proteins.^{4,5} Also many biomolecules such as nucleic acids, lipids, glycans and other non-proteinaceous biomolecules cannot be monitored with genetically encoded reporters.^{2,6} Small molecule probes can be used to circumvent these problems. A central role in bioorthogonal chemistry involves covalent modification of proteins, nucleic acids and carbohydrates with small synthetic molecules. In bioorthogonal reactions, two coupling partners including at least one biomolecule combine to form a biological and chemical linkage. These reactions must be kinetically fast, compatible with physiological pH and stable in a physiologically relevant solvent

environment. The reporter molecules involved in the bioorthogonal reaction must also produce a strong signal at low concentrations.^{7,8}

1.2 Bioorthogonal chemistry

Bioorthogonal reactions must take place under physiological conditions in an aqueous medium (neutral pH) with high selectivity and be non-perturbing or toxic to the biological system. For this purpose, a chemical reporter (yellow circle in Figure 1-1) with unique functionality can be introduced into a target system, followed by coupling to a small molecular probe (orange arc with labeling star in Figure 1-1).² Both the chemical reporter and the probe should not bring significant structural perturbations to the cell. Also they must avoid side reactions with non-target biomolecules (green shapes in Figure 1-1). For example, the cellular metabolic machinery can be used to transfer bioorthogonal functional groups into biomolecules using modified amino acids or monosaccharaides, of which translational machinery is tolerant to the modified structure.²

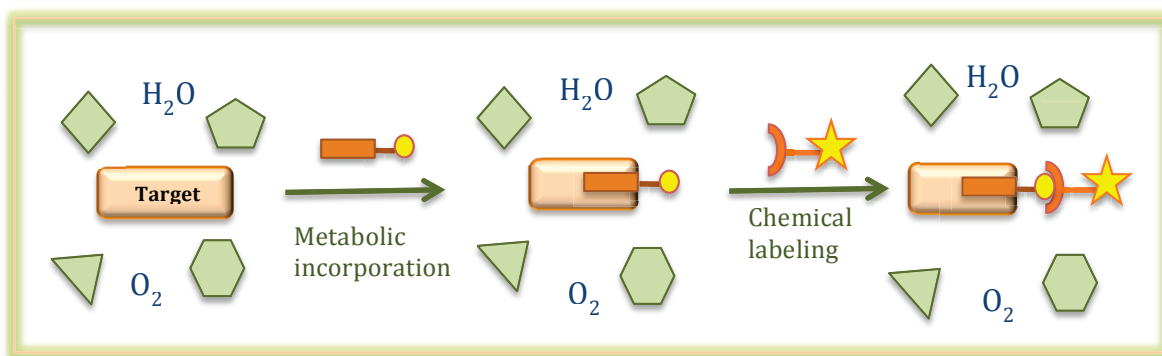
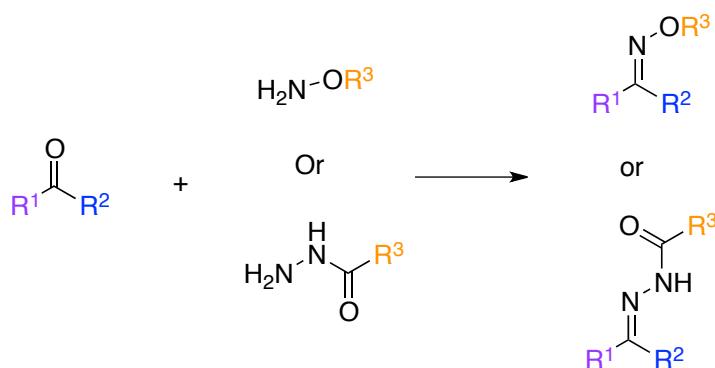


Figure 1-1: A general scheme for a bioorthogonal chemical reporter strategy

1.2.1 Nucleophilic substitution

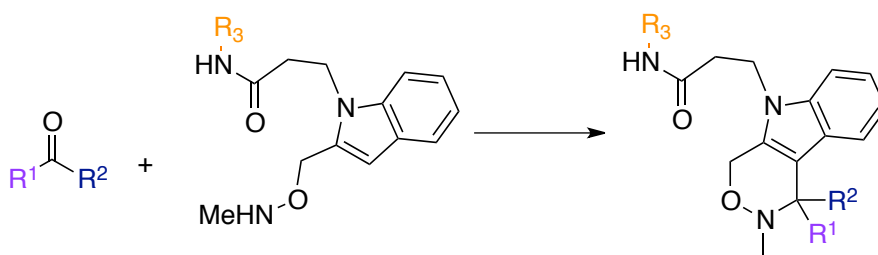
Aldehyde and ketone condensation reactions to form imines are considered to be the most prominent reactions, which have been used in bioconjugation studies. The reactivity of aldehydes and ketones has led them as traditionally applicable bioorthogonal reagents because of their mild electrophilicity, highly selective reactivity toward specific nucleophiles, and stability under physiological conditions.⁹⁻¹² Although these carbonyl

compounds react with primary amines such as lysine side chains to form imines, the equilibrium favors the formation of carbonyl compounds due to the pH of the physiological medium. On the other hand, the corresponding imine formed between carbonyl compounds with hydrazide or aminoxy groups to form hydrazones or oximes respectively are quite stable in physiological conditions because of the effect of strong electron donating groups attached to the nucleophile nitrogen (Scheme 1-1).^{11,13-16}



Scheme 1-1: Stable imine formation with hydrazide and aminoxy functionalized groups

While versatile, these reactions have some drawbacks, as the imine parts are susceptible to hydrolysis in cellular environments. Recently, Bertozzi and co-workers showed the modified aldehyde condensation of a Pictet–Spengler type reaction involving aldehydes and tryptamine nucleophiles (Scheme 1-2).¹⁷



Scheme 1-2: Pictet–Spengler type reaction

The oxycarboline product is stable to hydrolysis within one week. The authors also demonstrated the generality of this method using a variety of aldehyde–functionalized

proteins.

1.2.2 Bioorthogonal reactions by using small peptide tags

Sometimes, the FP tag is larger than the target protein, and this might affect the function of the protein of interest. Fusion of small peptide tags into the protein of interest has been applied for labeling with a variety of synthetic fluorescent molecules that have high affinity to the peptide tags and can satisfy the criteria for bioorthogonal chemistry. Additionally, carbohydrates or lipids that are conjugated to proteins can be monitored on the cell surface and inside of the cell.¹⁸ The most widely used class of genetic labeling strategies has been introduced by Tsien and co-workers by exploiting short peptide sequences containing a tetracysteine motif (CCXXCC), where XX are mostly proline and glycine, can be genetically incorporated into a protein of interest. In this approach, profluorescent biarsenical molecules can covalently label tetracysteine peptide tags in living cells.^{19,20} This system is based on small, cell-permeable organic dyes that can be functionalized with two arsenic atoms. The most common dyes used are fluorescein derivatives (FIAsH) and resorufin derivatives (ReAsH), due to their ability to bind to the peptide tags with high affinity (Figure 1-2).²¹

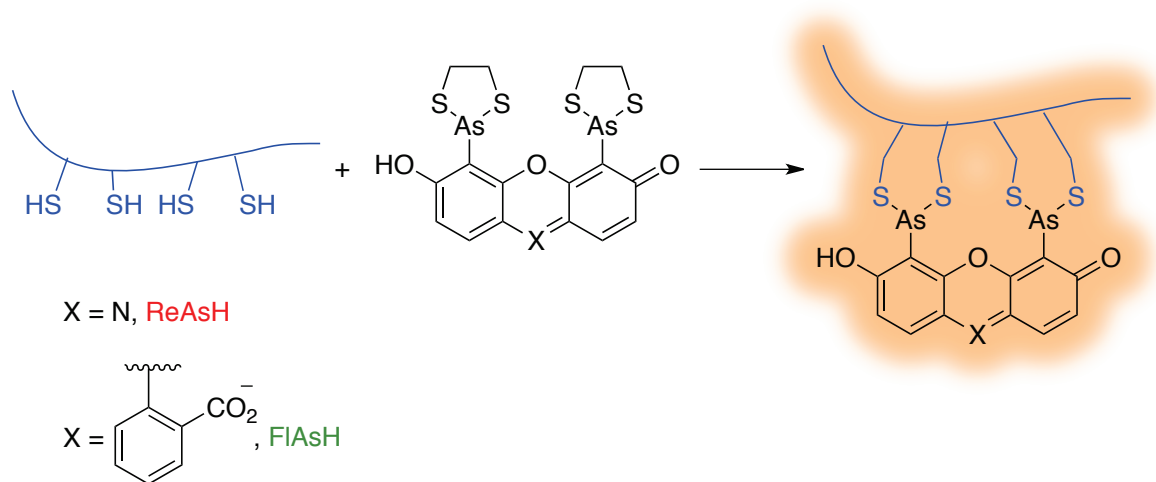


Figure 1-2: Reaction of tetracysteine containing peptide or protein domain with FIAsH-EDT₂ or ReAsH-EDT₂

These biarsenical probes are weakly fluorescent when free in solution, but increase up to

50-fold in fluorescent response when bound to a target sequence. The rarity of the hexapeptide motif affords target specificity among endogenous proteins. These systems have provided a powerful alternative to FP tagging without structural perturbation relative to the large size of these tags (Figure 1-2). However, biarsenicals have some disadvantages including high background signals and cytotoxicity, and can be hard to apply in oxidizing cellular environment.²¹ Other methods for peptide tagging include use of an oligohistidine sequence incorporated to the proteins of interest. The sequence can bind reversibly and specifically to a probe comprised of a chromophore and a metal-ion-chelating nitrilotriacetate (NTA) moiety.^{22,23} Libraries of constrained peptides that form stable folded aptamers bind with high affinity to the fluorescent dye, Texas red, and provide tools for in vivo imaging and analysis.²⁴ The engineering of a lanthanide (Ln) binding site into a protein either by utilization of an intrinsic metal ion-binding loop or by chemical modification of a nucleophilic amino acid provides useful luminescence properties for qualitative and quantitative analysis of proteins.^{25,26} Use of trans-splicing inteins for tagging probes to protein of interest in living cells have been reported by Muir and co-workers.²⁷ RhoBo, a rhodamine-derived bisboronic acid, has been reported as a non-toxic, cell permeable and turn-on fluorescent sensor for tetraserine motifs in engineered proteins (Figure 1-3).²⁸

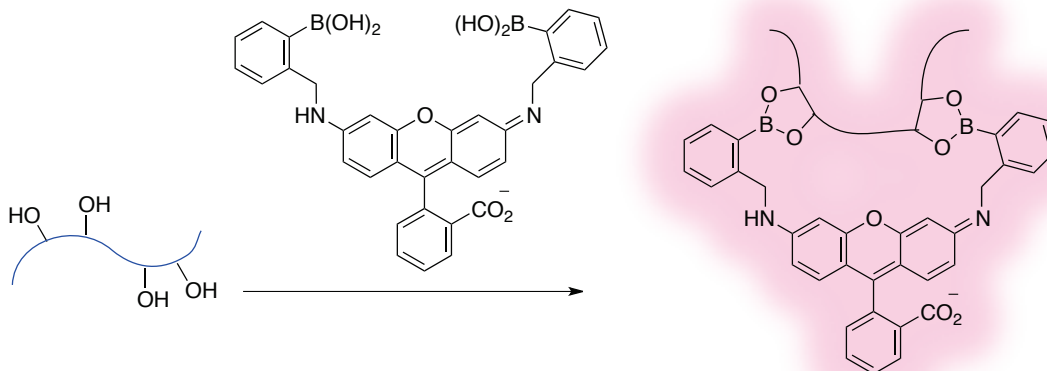


Figure 1-3: Condensation between RhoBo and tetraserines peptide tag

Proteins containing peptide tags with the sequence Ser-Ser-Pro-Gly-Ser-Ser have

shown the highest affinity complex with RhoBo ($K_{app}=452\pm 106$ nM). The bis-boronic acid functionalized dye forms boronate esters with the peptide, which then consequently emits at longer wavelengths under fluorescence. The affinity of RhoBo was examined in the presence of simple monosaccharides to evaluate the extent of competition between hydroxyl-rich functional groups and protein tetraserine motifs, of which RhoBo showed higher peptide affinity compared to monosaccharides.²⁸

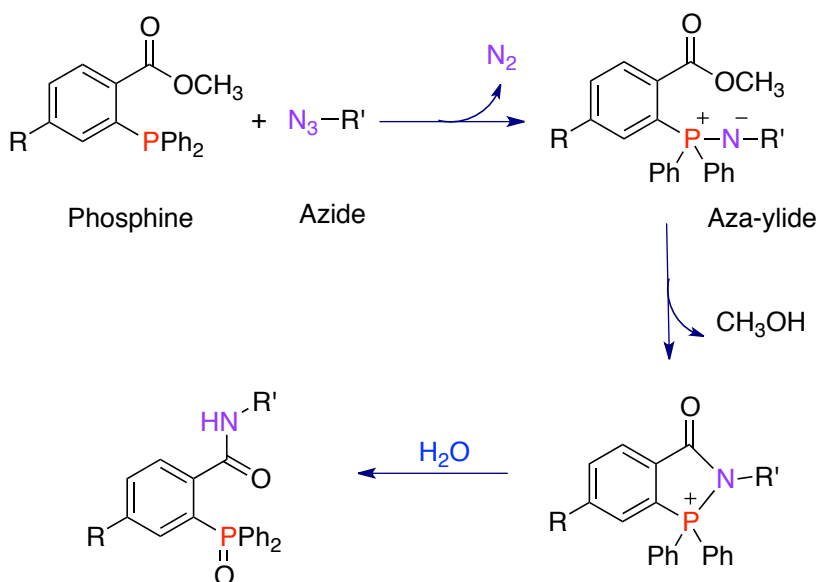
1.2.3 Use of azide in bioorthogonal reactions

Currently, organic azides are the most commonly used viable chemical reporters in the modification of all classes of biomolecules in any biological environment.² Azides are nearly absent from all naturally occurring species, not considerably reactive with water and are resistant to oxidation and stable at physiological temperature. Organic azides are mild electrophiles, but do not react with amines (hard nucleophile) and free thiols (soft nucleophile) unless they are subjected to vigorous heating or use of specific catalysts. Organic azides have no intrinsic toxicity and are present in FDA approved drugs, such as AZT.²⁹ They are also readily introduced in biomolecules *via* diazo-transfer of amines in lysines,³⁰ non-natural amino acids incorporation³¹ or expressed proteins by native chemical ligation.³² Azido metabolites have been used to target proteins,^{33,34} glycans,^{35,36} and lipids,^{37,38} among other biomolecules. As described below, in all cases, the azido species can be detected *via* covalent reactions with a complementary alkyne, cyclooctyne, or phosphine reagent.³⁹⁻⁴²

1.2.3.1 Staudinger ligation

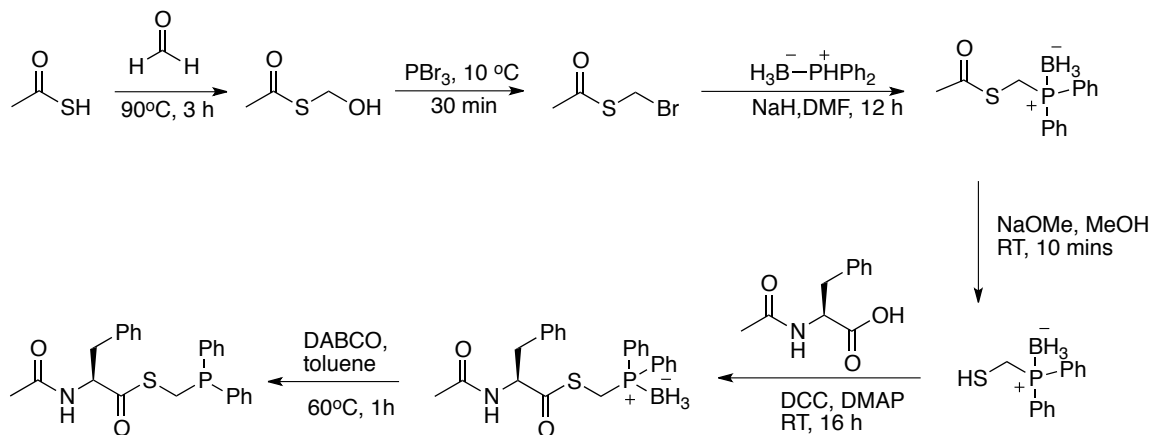
The Staudinger-Bertozzi ligation is a modification of the Staudinger reaction between an azide and a phosphine under mild conditions to produce aza-ylide intermediates. The later is traditionally hydrolyzed to give the corresponding amine and phosphine oxide.^{43,44} Bertozzi and co-workers modified the reaction through introduction of an intramolecular trap into the phosphine, which can be used in bioorthogonal transformations. An electrophile such as a carbonyl containing functional group (ester or thioester) reacts with the resulting azaphosphorane (aza-ylide) to give a secondary amide linkage and phosphine oxide (Scheme 1-3).^{2,44,45} The Staudinger ligation has been used as a probe, in

which phosphine derivatives covalently bind with high regio and chemoselectivity to azide-bearing biomolecules with highly stable reactants in aqueous media. This reaction has been used for modifying antibodies and peptides with high selectivity and little alteration of their pharmacokinetic properties. However, this reaction suffers from slow rates due to the coupling process, which displays a second-order rate constant around $0.0020 \text{ M}^{-1}\text{s}^{-1}$. Therefore, the Staudinger-Bertozzi ligation must proceed at high enough concentrations to complete the reaction in a short time for visualization purposes; this attribute can be problematic for fluorescence imaging, because an excess of the probe reagent would be difficult to remove and would result in a high background signal.⁴⁶ Phosphine reagents are also susceptible to oxidation by air or metabolic enzymes, which could decrease the concentration of active phosphine present in biological systems and be detrimental to final pre-targeting reactions.⁴⁵



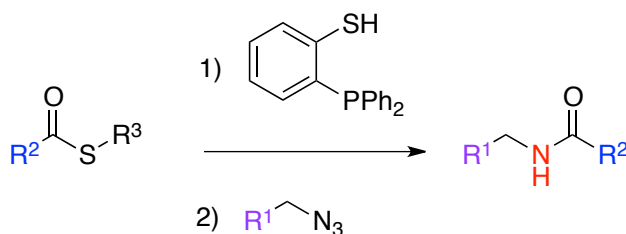
Scheme 1-3: Staudinger ligation of a 2-(diphenylphosphoryl)benzoic ester derivatives with an alkyl azide

To minimize unwanted oxidation and improve the Staudinger-Bertozzi ligation reaction, protection of the phosphine in the form of borane adduct and subsequent removal of the boron protecting group by using 1,4-diazabicyclo[2.2.2]octane (DABCO) can be accomplished (Scheme 1-4).⁴⁷



Scheme 1-4: Synthesis of borane protected phosphine and subsequent coupling to acetylalanine and deprotection with DABCO

The Staudinger ligation has been applied to the modification of glycans in living cells within cell surfaces⁴⁸, proteomic analysis of glycosylation^{49,50} and new metabolic functionality for recombinant proteins.⁵¹ Raines and colleagues have combined the Staudinger reaction and native chemical ligation (NCL). They have shown that phosphinobenzenethiol can serve as an intermediate to link thioester and azide to produce an amide-linked product (Scheme 1-5).^{52,53} This concept could overcome the limitation of native chemical ligation, which requires cysteine at the ligation juncture. This modified Staudinger ligation has been applied to the attachment of proteins and small molecules onto glass slides.^{54,55}

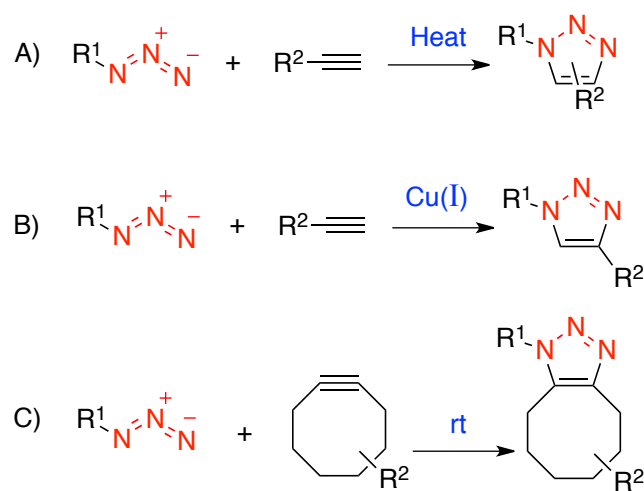


Scheme 1-5: Amide bond formation with a modified Staudinger ligation

1.2.3.2 Cu-catalyzed [3+2] azide-alkyne cycloaddition (CuAAC)

In 1967, Huisgen and co-workers described the [3+2] cycloaddition between azides and terminal alkynes to provide stable triazole adducts.⁵⁶ This process required elevated

temperatures, high pressures and activated alkynes that are not compatible with living systems (Scheme 1-6 (A)). Later, Sharpless⁵⁷ and Meldal⁵⁸ demonstrated that the rate of cycloaddition between azides and alkynes can be accelerated by 10⁶ fold using catalytic amounts of Cu(I) (Scheme 1-6 (B)). This copper catalyzed azide–alkyne cycloaddition (CuAAC) or “click” reaction, proceeds readily in physiological environments and provides 1,4–disubstituted triazoles with nearly complete regioselectivity. Over the past few decades, CuAAC has been used in protein modification,⁵⁹ DNA and RNA modification,⁶⁰ and glycobiology.⁶¹ Unfortunately, Cu(I) salts are toxic to living systems as they catalyze the atmospheric oxygen to produce reactive oxygen species causing cell death.⁶² Recently, the addition of certain copper–binding ligands increased the rate of CuAAC reaction and significantly lowered the toxic effects.^{62–64} Although recent improvement in CuAAC can solve the Cu(I) toxicity, bioorthogonal labeling without the need of a metal catalyst is more straightforward.



Scheme 1-6: (A) The thermal 1,3–dipolar cycloaddition of azides (B) The Cu(I)–catalyzed formal azide–alkyne cycloaddition (C) The strain–promoted cycloaddition between azides and cyclooctynes

1.2.3.3 Strain–promoted alkyne–azide cycloaddition (SPAAC)

Krebs and Wittig reported studies on the strain–promoted alkyne–azide cycloaddition (SPAAC) reaction in 1961, where a cyclooctyne and phenyl azide gave a single triazole

product.⁶⁵ In 2004, Bertozzi and co-workers exploited an alternative catalyst-free [3+2] cycloaddition of alkynes and azides exploiting primarily the ring-strain of cyclooctyne (Scheme 1-6 (C)).⁶⁶ Alkynes within an eight-membered ring contain a ring strain of ~18 kcal/mol. Most of the molecular strain of cyclooctyne is released in the transition state upon [3+2] cycloaddition with an azide.⁶⁷ In this way, the reaction can occur under physiological conditions and without requiring the presence of a catalyst.⁶⁵ This strain-promoted azide-alkyne cycloaddition (SPAAC) has been used to tag biomolecules *in vitro* without observable toxic effects.⁶⁸⁻⁷⁰ The reaction rate however is low. The second-order rate constant for the reaction of a derivatized cyclooctyne with benzyl azide in aqueous CD₃CN is 0.0012 M⁻¹s⁻¹ whereas the same rate constant for the Staudinger ligation is 0.0025 M⁻¹s⁻¹.^{45,66} Modifications of cyclooctyne using electron withdrawing groups like monofluorinated cyclooctyne (MOFO) and difluorinated cyclooctyne DIFO have been reported to increase the reaction rate (Figure 1-4).⁷¹ Other examples include dibenzocyclooctyne (DIBO)⁷² and biarylazacyclooctynone (BARAC)⁷³, which contain cyclooctyne cores fused to benzene rings providing increase in strain energy and accelerating the cycloaddition reaction with azides (Figure 1-4).

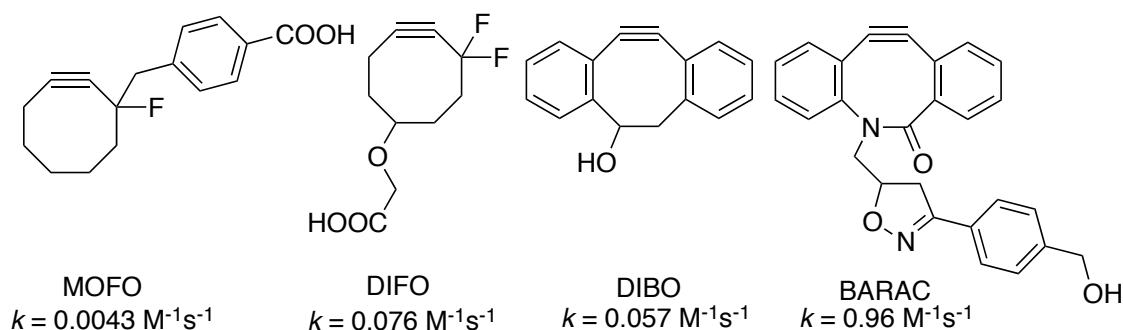


Figure 1-4: Cyclooctynes synthesized for Cu-free click chemistry in living cells

1.2.4 Diels-Alder cycloadditions

In 2008 Fox and co-workers developed a second major class of bioorthogonal cycloadditions (Diels-Alder ligations) between strained alkenes and tetrazines.⁷⁴ It was shown that the reaction of trans-cyclooctene (TCO) with electron-deficient tetrazines has

a relatively fast reaction rate compared to other bioorthogonal reactions in aqueous media. Rate constants of these second order reactions range from 10^3 to $10^6 \text{ M}^{-1} \text{ s}^{-1}$ and are considered to be the fastest bioorthogonal transformations.^{75,76} Another advantage of these reactions is the straightforward synthesis of the starting materials. Due to the higher reactivity of the TCO–tetrazine reaction, this ligation has been applied in a variety of biological studies in living cells and animal imaging.⁷⁷⁻⁸¹ Different tetrazines and cycloalkynes have been developed to improve inverse electron–demand Diels–Alder reaction (IED–DA) rate. Hilderbrand and co-workers described the use of norbornene (NB) and electron deficient tetrazines (Table 1-1).⁷⁷

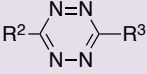
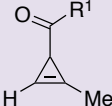
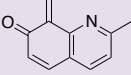
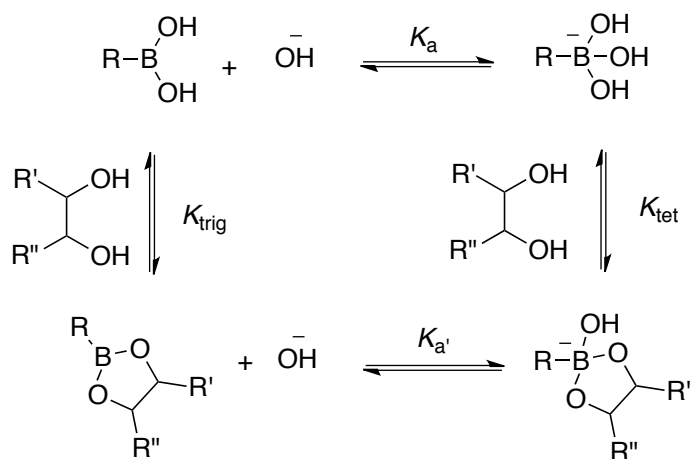
Reaction type	Name	Reactant 1 Diene	Reactant 2 Dienophile	Comment	References
Inverse Electron–demand Diels–Alder reaction (IED–DA)	TCO			TCO can isomerize over time	Blackman ⁷⁴ 2008
	NB			norbornene and functionalized cyclopropene are stable	Deveraj ⁷⁸ 2008
	Cyclopropene			Yang ⁸³ 2012 Patterson ⁸² 2012	
Hetero–Diels–Alder	Vinyl thioether (VT)			Quinone methide generated in situ	Li ⁸⁴ 2013

Table 1-1: Click Diels–Alder cycloadditions⁸⁵

Another possibility is the use of cyclopropenes as strained alkenes to react with various tetrazines.^{82,83} The small size of cyclopropenes shows advantages over TCO in cellular environment but have considerably lower rate constants compared to TCO. In 2013, Li and co-workers reported click hetero–Diels–Alder cycloaddition of *o*-quinolinone quinone methide (oQQM) and vinyl thioether (VT). This reaction is highly selective and efficient in physiological conditions. Vinyl thioethers are small and stable *in vivo* and are considered to be suitable bioorthogonal chemical reporters, which effectively coupled to various biomolecules (Table 1-1).⁸⁴

1.3 Chemoselective sensors of saccharides using simple boronic acids

Arylboronic acids have been employed in the construction of receptors for saccharide sensors.⁸⁶⁻⁸⁸ Phenylboronic acid was first synthesized by Michaelis and Becker in 1880,⁸⁹ however the first binding studies of diols (or saccharides) were published in 1954 by Kuivila,⁸⁹ in which he found that addition of boronic acids can solubilize a saturated solution of mannitol, leading to the postulation of cyclic boronic ester formation. The ability of borates to form complexes with polyhydroxyl compounds was revealed after this experiment. Quantitative evaluation of the interactions between boronic acids and saccharides were first reported by Lorand and Edwards in 1959.⁹⁰ They showed that the conjugate base of phenylboronic acid preferred a tetrahedral structure rather than trigonal structure. The interaction of boronic acid with diol is highly pH dependent, as we can see in the thermodynamic cycle in Scheme 1-7.



Scheme 1-7: Thermodynamic cycle of boronic acid interaction with cis-1,2-diols

Studies of boronic acids reaction with diols have confirmed that they become more acidic, in boronate ester formation $pK_{a'}$ is lower than pK_a by 2–3 units; however, in some examples involving weak diol binding, $pK_{a'}$ was found to be slightly higher.⁹¹ In addition, the formation of stable anionic forms of tetrahedral boronate esters (K_{tet}) is generally higher than neutral trigonal boronate esters (K_{trig}) base in the $K_a K_{\text{tet}} = K_{a'} K_{\text{trig}}$ equation. In this way, a higher pH favors diol binding to form stable anionic boronic acid. However,

based on the experiment, the optimal binding pH is not always higher than the pK_a of the boronic acid, and the pK_a values of both the boronic acid and the diol should be considered.⁹²

For the biological applications of boronic acid sensors, reversibility, quick response, stability at physiological pH and lack of toxicity are imperative. Boronic acid sensors have been improved by the addition of electron-withdrawing substituents to the boronic acid moiety or by the utilization of B–N interaction.⁹³⁻⁹⁶ The first boronic acid based saccharide sensor was prepared by Yoon and Czarnik in 1992 (Probe 1, Figure 1-5), and showed fluorescence quenching after reaction with saccharide.⁹⁷ D–Glucose selectivity was achieved in 1994 by James and Shinkai (Probe 2, Figure 1-5). In probe 2, the neighboring group participation of the amine group provides an electron-rich center for photo-induced electron transfer (PET). Titration of probe 2 in aqueous media gives rise a very high fluorescence “switch-on” factor on saccharide binding. The increased acidity of the boronic acid moiety strengthens the boron-nitrogen bond and effectively suppresses the PET process.⁹⁸

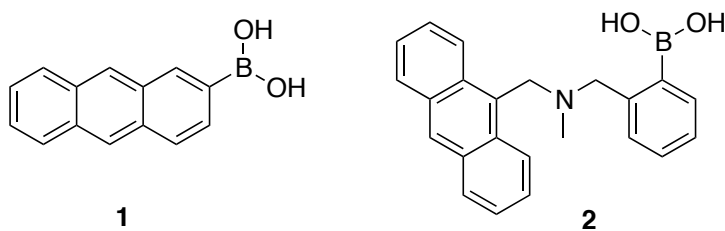
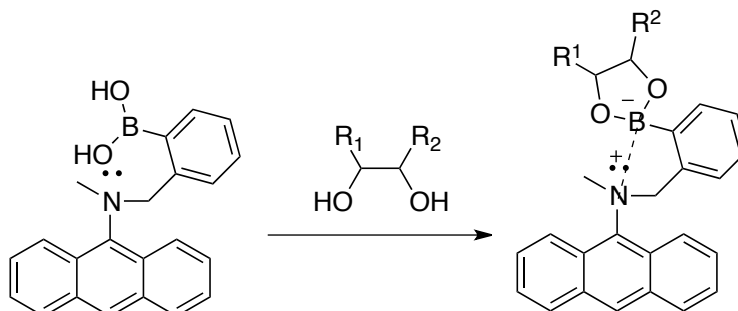


Figure 1-5: Boronic acid sensors

This work was followed by asymmetric saccharide discrimination. By addition of the second benzylic amine group to the anthracene scaffold, higher selectivity of the probe towards glucose was observed in comparison to other monosaccharides. This simple probe can be applied as a chemosensor for diagnosing glucose in high blood pressure (Probe 4, Figure 1-6).⁹⁸ In probe 2, the lone pair of electrons on nitrogen is observed to quench the fluorescence of the anthracene moiety. Following ester formation with diols, however, the Lewis acidity of the boron atom increases. This increase in acidity strengthens the B–N bond interaction, resulting in the decrease of availability of nitrogen

lone pair electrons for PET with a consequent increase of fluorescence intensity (Scheme 1-8).^{93,98,99}



Scheme 1-8: B–N bond interaction after boronic ester formation

Wulff and co-workers began to utilize diboronic acids as sugar receptors in the late 1980s.¹⁰⁰ By 1991, Tsukagoshi and Shinkai reported the possibility of using diboronic acid sensor as a multivalent saccharide binding site.¹⁰¹ Although the sensor displays a high binding constant to glucose, it is not a good sensor since it lacks chromophores to aid absorption of visible light (Probe **3**, Figure 1-6). This discovery was followed by the first glucose–selective diboronic acid–based PET sensor in 1994 (Probe **2**). CH– π interaction between the hydrocarbon skeleton of glucose and the anthracene core of probe **4** contributes to the high affinity between the boronic acid and diols of the glucose (Figure 1-6).⁹⁸

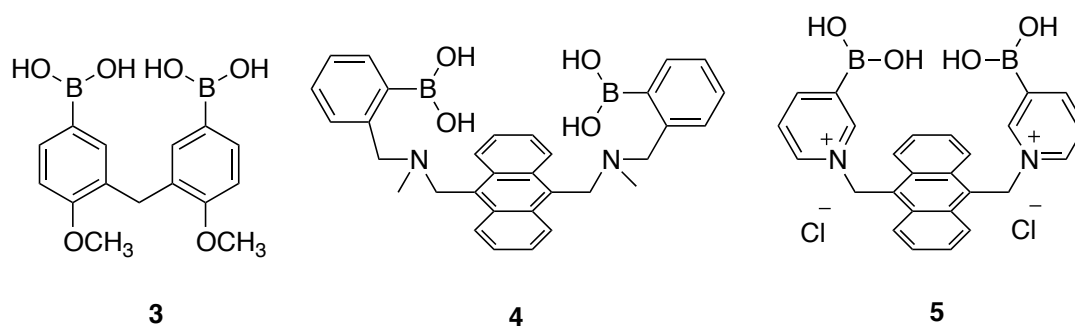


Figure 1-6: Diboronic acids sensors

The pyridinium analogue of probe **4** (Probe **5**, Figure 1-6) was reported by Norrild and co-workers. Positively charged pyridinium cations increase water solubility of the probe and acidity of the boron center and allowed its use at physiological pH.¹⁰²

Flexible diboronic acid sensors adopt different conformations depending whether a 1:1 cyclic or a 1:2 acyclic complex is formed and generate the complex with high selectivity. A tweezer-like receptor contains two pyrenes, which cause a long wavelength of excimer emission (Figure 1-7).

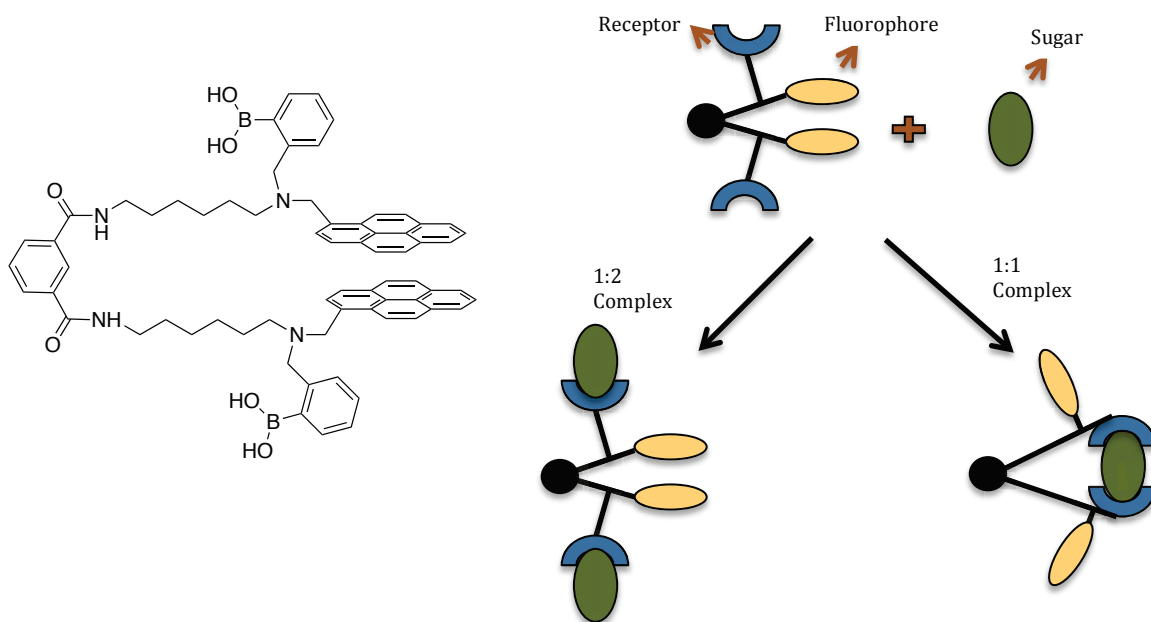


Figure 1-7: Flexible diboronic acid tweezer sensors

Quenching of the excimer emission occurs after binding of the carbohydrate, which forces a separation of the pyrene units. Fructose forms a 1:2 boronate and could not interrupt the stacking of pyrene, therefore the excimer emission remains intact, however binding to glucose, galactose or mannose forms 1:1 boronate which forces the pyrene moieties to split apart and to quench the excimer emission. The binding constants follow the order of D-glucose >> D-galactose > D-mannose. Although D-fructose forms a complex with higher stability constant with the tweezer (complex 1:2), it fails to open the tweezer and change the fluorescence intensity.¹⁰³ By screening a large library of diverse benzoboroxoles, Hall and co-workers successfully developed a receptor that selectively targets the tumor-associated carbohydrate antigen Thomsen-Friedenreich disaccharide Gal- β -1,3-GalNAc, (Figure 1-8).¹⁰⁴ Their design of the receptor was performed by using combinatorial strategy, which is well suited for identifying receptors for structurally

complicated substrates such as oligosaccharides.¹⁰⁵ In contrast to normal boronic acids, the benzoboroxole moiety has the capability of binding to glycopyranosides efficiently at neutral pH in water.¹⁰⁶ The bis(boroxole) library of 400 receptors contained a variety in spacer R¹ (out of 20 amino acid residues) and the capping group R² (out of 20 carboxylic acids).¹⁰⁴

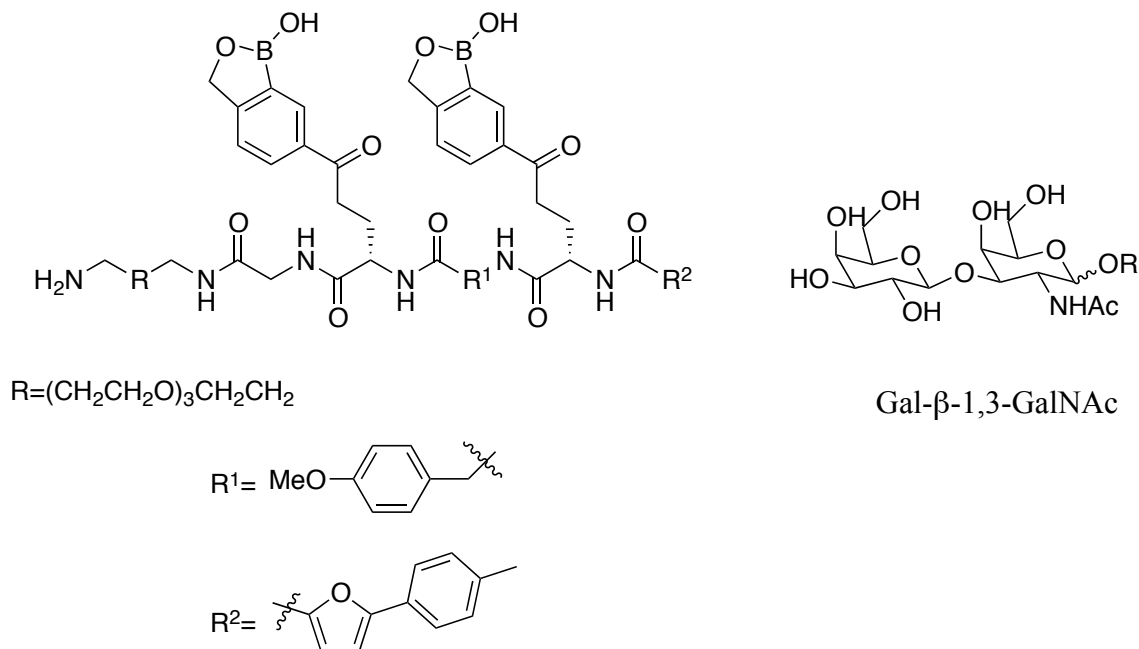


Figure 1-8: Structure of benzoboroxole library and Gal-β-1,3-GalNAc

The variable groups R¹ and R² contained suitable functional groups that help for additional hydrogen bonding, hydrophobic CH-π interactions with the nonpolar part of saccharides, with a purpose of better selectivity action. The identified receptor was highly selective for the targeted Gal-β-1,3-GalNAc oligosaccharide as the binding constant was in the same order of diboronic acid–glucose interactions ($1.1 \times 10^3 \text{ M}^{-1}$).¹⁰⁴

A ratiometric fluorescent chemosensor based on an amphiphilic monoboronic acid was developed that contains a hydrophobic pyrene fluorophore linked *via* a cationic pyridinium (Figure 1-9).¹⁰⁷

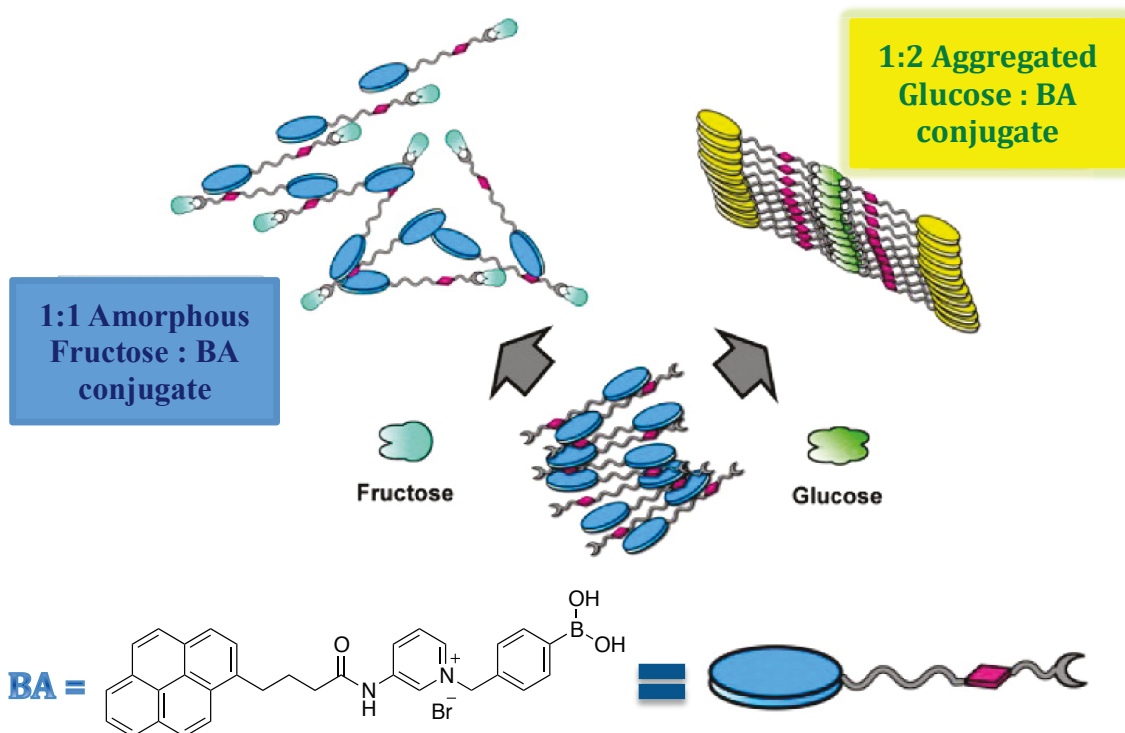


Figure 1-9: Different aggregation behavior of boronic acid probe with fructose and glucose. Reprinted with permission from *J. Am. Chem. Soc.*, 2013, 135, 1700–1703. Copyright 2013 American Chemical Society.

This sensor is highly selective and sensitive for glucose and causes very large fluorescent responses in aqueous environment. At basic pH, this probe exhibits only pyrene monomer fluorescence at 390 nm, but after binding to glucose, pyrene excimer emission increases to 510 nm. However, fructose shows only little enhancement of fluorescence. This suggested that aggregation of the probe is promoted by glucose but not fructose. Also, the hydrodynamic diameter of the probe increases dramatically from *ca.* 500 to 2000 nm, when glucose is added and reduces to *ca.* 200 nm when fructose is added. These studies indicate that 1:2 glucose–probe binding not only increases aggregation but also provides well–ordered aggregated structure and strong excimer emission (Figure 1-9).¹⁰⁷

The sialic acid (SA)–phenylboronic acid (PBA) recognition has been used in bioconjugation studies, as it is simple, fast, efficient, and biocompatible. Recently, this

system has been successfully used to label virus surface by modifying quantum dots (QDs) with phenyl boronic acid (PBA) (Figure 1-10). Quantum dots (QDs) are semiconductor nanoparticles that exhibit high fluorescence emission. They have strong size dependency, which facilitate their ability to show different emission wavelength upon binding to other molecules.¹⁰⁸ Available methods of bioconjugation, such as azide and cyclooctyne are irreversible and require transforming active functional groups. Therefore, utilization of a reversible method allows recycling and reusing viruses for subsequent studies. Labeling by boronic acids is a mild, reliable and reversible method and also maintains infectivity and ability of virus and the fluorescence properties of QDs. The QDs-PBA showed a strong fluorescence and after binding to virus (VSV), producing QDs-VSV that is capable of being imaged with fluorescence spectroscopy.¹⁰⁸

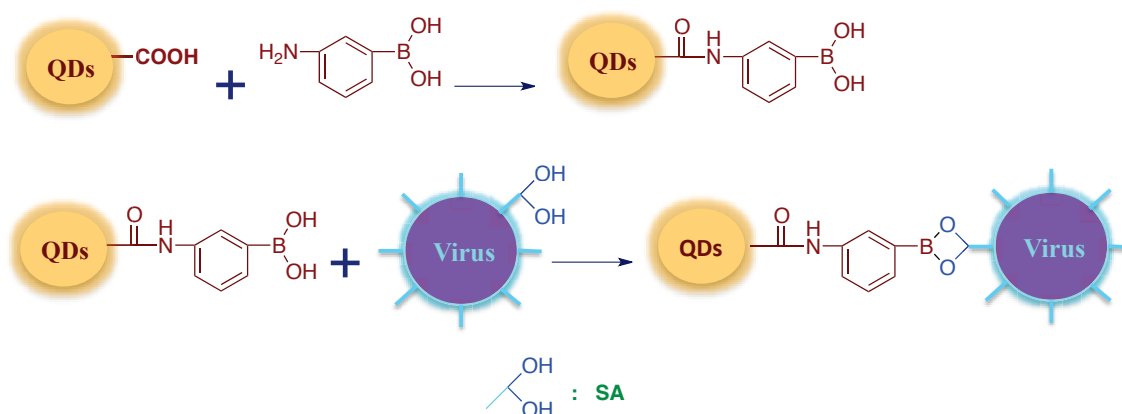


Figure 1-10: Recognition of sialic acid on virus surface by modifying quantum dots with phenyl boronic acid

1.4 Boronic acid sensors for selective recognition of proteins

The application of certain mono- and bis-boronic acid sensors had been limited to sensing sugars and other simple 1,2 and 1,3 cis-diols. In 2009, Schepartz and co-workers reported that these systems could be applied to the sensing of peptide sequences, which contain a linear tetraserine motif.²⁸ Based on their observation, bisboronic acids bind monosaccharides containing one diol with mixed stoichiometry and two diol with 1:1 stoichiometry. It was rationalized that peptide motifs with two pairs of cis-diols can show fluorescent response to bisboronic acid fluorophores (Figure 1-3). A new technique for

reversible protein modification was published in 2012 by Gois and co-workers.¹⁰⁹ It was shown that small boronic acid molecules can modify the lysine of *N*-terminal protein based on the formation of stable iminoboronates.¹⁰⁹ Forming imines can selectively modify lysine residue of proteins; however, reaction between lysine and carbonyl derivatives are reversible and a second reductive step is needed to provide stable conjugation.^{110,111} Formation of stable imines would provide a selective, and potentially reversible modification on *N*-terminal lysine residues. Bioconjugation techniques that allow a selective and reversible modification of the protein are currently highly promising tools as delivery systems, like antibody–drug conjugate, to deliver cytotoxic drugs to cancer cells.¹¹² It was shown that 2–formylbenzeneboronic acid reacts with amine to form a stable iminoboronate due to a well-known dative N–B interaction in aqueous media (Figure 1-11). More importantly, these modifications were also shown to be reversible as lysine can be unconjugated upon addition of glutathione, dopamine, or fructose. These molecules probably induce hydrolysis of the iminoboronate by interruption of the B–N bond.¹¹³

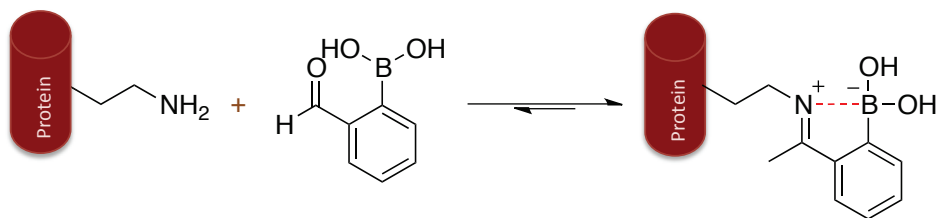


Figure 1-11: Stable iminoboronate with reversible linkage

Gois and co-workers also developed new reagents for bioconjugation based on the iminoboronate, which can selectively target cancer cells. They prepared fluorescent 2–acetylbenzeneboronic acid derivatives that can conjugate *via* a B–N linkage with lysozyme and N-(2–aminoethyl) folic acid and selectively recognize human non-small lung cancer cells (NCI-H460) due to their over–expression of folic acid receptors (Figure 1-12).¹¹⁴

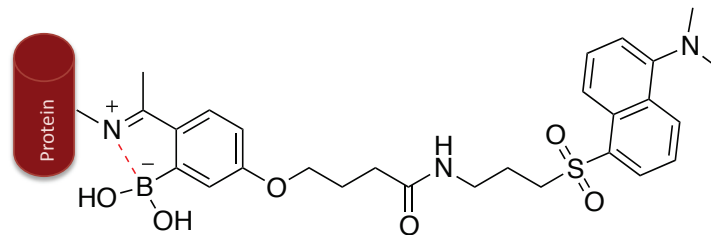


Figure 1-12: Iminoboronate probe for labeling cancer cells

1.5 Thesis Objective

Boronic acids have been known to form a high affinity complex with 1,2-dihydroxyl functionalities *via* reversible boronate ester formation. Since 1994, mono- and bis-boronic acids have been employed as fluorescence probes for saccharides. However, little effort was devoted to the development of boronic acid sensor molecules for analyzing target proteins in live cells, which is vitally important to understanding their molecular roles in both native biological processes and disease. In 2009, Schepartz and co-workers employed a rhodamine-derived bisboronic acid sensor (RhoBo), which was previously reported as a sensor for saccharides (Scheme 1-3). RhoBo is able to selectively label tetraserine (SSPGSS) with high affinity, selectivity and large fluorescent response over other diserine and tetraserine peptide sequences in the presence of other biologically relevant diols such as monosaccharides and disaccharides. They also showed the ability of RhoBo to permeate cells *via* crossing saccharide-rich plasma membrane for intracellular protein imaging.²⁸ The goal of this thesis work is to create a smaller and simpler arylboronic acid reporter, with potentially four covalent, reversible points of attachment, which can bind to a small peptide tag in a sequence specific manner with high affinity. This kind of short, noninvasive peptide could then be genetically fused to the protein of interest for bioconjugation purposes or for *in vivo* probing. Also, lysine side chain in proteins is involved in many post-translational modifications, and the formation of stable imines in aqueous media has been applied as a direct, selective and potentially reversible strategy to modify the lysine residues and N-terminal proteins.¹⁰⁹ Based on literature precedent, we designed a small, functionalized boronic acid that potentially binds to two or three serine residues of a peptide and form a stable boronate ester. A

ketone unit in the molecule would be able to form a stable imine with a lysine side chain *via* cooperative boronate–imine complexation. For these purposes, peptide libraries were synthesized and reacted with the designed molecules to investigate their binding affinity. Dye displacement assay and UV spectroscopy were applied to test their binding affinity. Unfortunately, I could not observe strong binding between the designed molecules and peptides, which will be presented in Chapter 2. Continuing our goal, we then designed Michael acceptor derivatives of boronic acids to show site-specific interaction of the molecule with cysteine containing peptides. I successfully showed that interaction of the designed boronic acid with a N-terminal serine could increase the rate of nucleophilic addition of cysteine to Michael acceptor and this work will be described in Chapter 3.

1.6 References

- (1) Nienhaus, G. U. (2008) The green fluorescent protein: a key tool to study chemical processes in living cells. *Angew. Chem., Int. Ed.* *47*, 8992–8994.
- (2) Prescher, J. A., and Bertozzi, C. R. (2005) Chemistry in living systems. *Nat. Chem. Biol.* *1*, 13–21.
- (3) Kremers, G. J., Gilbert, S. G., and Cranfill, P. J. (2011) Fluorescent proteins at a glance. *J. Cell Sci.* *124*, 157–160.
- (4) Lisenbee, C. S., Karnik, S. K., and Trelease, R. N. (2003) Overexpression and mislocalization of a tail–anchored GFP redefines the identity of peroxisomal ER. *Traffic.* *4*, 491–501.
- (5) Marguet, D., Spiliotis, E. T., Pentcheva, T., and Lebowitz, M. (1999) Lateral diffusion of GFP–tagged H2L molecules and of GFP–TAP1 reports on the assembly and retention of these molecules in the endoplasmic reticulum. *Immunity.* *11*, 231–240.
- (6) Watanabe, S., Mizukami, S., and Hori, Y. (2010) Multicolor protein labeling in living cells using mutant β –lactamase–tag technology. *Bioconjugate Chem.* *21*, 2320–2326.
- (7) Carroll, L., Evans, H. L., and Aboagye, E. O. (2013) Bioorthogonal chemistry for pre–targeted molecular imaging–progress and prospects. *Org. Biomol. Chem.* *11*, 5772–5781.
- (8) Debets, M. F., Hest, J. C. M., and Rutjes, F. P. J. T. (2013) Bioorthogonal labelling of biomolecules: new functional handles and ligation methods. *Org. Biomol. Chem.* *11*,

6439–6455.

(9) Agarwal, P., Kudirka, R., Albers, A. E., Barfield, R. M., de Hart, G. W., Drake, P. M., Jones, L. C., and Rabuka, D. (2013) Hydrazino–Pictet–Spengler ligation as a biocompatible method for the generation of stable protein conjugates. *Bioconjugate Chem.* 24, 846–851.

(10) Kalia, J., and Raines, R. T. (2008) Hydrolytic stability of hydrazones and oximes. *Angew. Chem., Int. Ed.* 120, 7633–7636.

(11) Cornish, V. W., Hahn, K. M., and Schultz, P. G. (1996) Site–specific protein modification using a ketone handle. *J. Am. Chem. Soc.* 118, 8150–8151.

(12) Lelle, M., and Peneva, K. (2014) An amino acid–based heterofunctional cross–linking reagent. *Amino Acids.* 46, 1243–1251.

(13) Jencks, W. P. (1994) Reaction mechanisms, catalysis, and movement. *Protein Science.* 3, 2459–2464.

(14) Vepřek, P., and Ježek, J. (1999) Peptide and glycopeptide dendrimers. Part II. *J. Pept. Sci.* 5, 203–220.

(15) Wang, L., Zhang, Z., Brock, A., and Schultz, P. G. (2003) Addition of the keto functional group to the genetic code of *Escherichia coli*. *Proc. Nat. Acad. Sci. U.S.A.* 100, 56–61.

(16) Mahal, L. K., Yarema, K. J., and Bertozzi, C. R. (1997) Engineering chemical reactivity on cell surfaces through oligosaccharide biosynthesis. *Science.* 276, 1125–1128.

(17) Agarwal, P., Weijden, J. V., Sletten, E. M., Rabuka, D., and Bertozzi, C. R. (2013) A Pictet–Spengler ligation for protein chemical modification. *Proc. Nat. Acad. Sci. U.S.A.* 110, 46–51.

(18) Tanaka, F., Fuller, R., Asawapornmongkol, L., Warsinke, A., and Gobuty, S. (2007) Development of a small peptide tag for covalent labeling of proteins. *Bioconjugate Chem.* 18, 1318–1324.

(19) Gaietta, G., Deerinck, T. J., Adams, S. R., Bouwer, J., Tour, O., Laird, D. W., Sosinsky, G. E., Tsien, R. Y., and Ellisman, M. H. (2002) Multicolor and electron microscopic imaging of connexin trafficking. *Science.* 296, 503–507.

-
- (20) Griffin, B. A., Adams, S. R. J., and Tsien, R. Y. (1998) Specific covalent labeling of recombinant protein molecules inside live cells. *Science*. 281, 269–272.
- (21) Zürn, A., Klenk, C., Zabel, U., Reiner, S., Lohse, M. J., and Hoffmann, C. (2010) Site-specific, orthogonal labeling of proteins in intact cells with two small biarsenical fluorophores. *Bioconjugate chem.* 21, 853–859.
- (22) Guignet, E. G., Hovius, R., and Vogel, H. (2004) Reversible site-selective labeling of membrane proteins in live cells. *Nature Biotechnol.* 22, 440–444.
- (23) Bhagawati, M., Lata, S., Tampé, R., and Piehler, J. (2010) Native laser lithography of His-tagged proteins by uncaging of multivalent chelators. *J. Am. Chem. Soc.* 132, 5932–5933.
- (24) Marks, K. M., Rosinov, M., and Nolan, G. P. (2004) *In vivo* targeting of organic calcium sensors *via* genetically selected peptides. *Chem. Biol.* 11, 347–356.
- (25) Franz, K. J., Nitz, M., and Imperiali, B. (2003) Lanthanide-binding tags as versatile protein coexpression probes. *ChemBioChem.* 4, 265–271.
- (26) Sculimbrene B. R., and Imperiali, B. (2006) Lanthanide-Binding Tags as Luminescent Probes for Studying Protein Interactions. *J. Am. Chem. Soc.* 128, 7346–52.
- (27) Giriat I., and Muir, T. W. (2003) Protein semi-synthesis in living cells. *J. Am. Chem. Soc.* 125, 7180–7181.
- (28) Halo, T. L., Appelbaum, J., Hobert, E. M., Balkin, D. M., and Schepartz, A. (2009) Selective recognition of protein tetraserine motifs with a cell-permeable, pro-fluorescent bis-boronic acid. *J. Am. Chem. Soc.* 131, 438–439.
- (29) Griffin, R. J (1994) The medicinal chemistry of the azido group. *Prog. Med. Chem.* 31, 121–232.
- (30) Oyelere, A. K., Chen, P. C., and Yao, L. P. (2006) Heterogeneous diazo-transfer reaction: a facile unmasking of azide groups on amine-functionalized insoluble supports for solid-phase synthesis. *J. Org. Chem.* 71, 9791–9796.
- (31) Kiick, K. L., Saxon, E., and Tirrell, D. A. (2002) Incorporation of azides into recombinant proteins for chemoselective modification by the Staudinger ligation. *Proc. Nat. Acad. Sci. U.S.A.* 99, 19–24.
- (32) Xiao, J., and Tolbert, T. J. (2009) Synthesis of N-terminally linked protein dimers

and trimers by a combined native chemical ligation–CuAAC click chemistry strategy. *Org. Lett.* *11*, 4144–4147.

(33) Ngo, J. T., and Tirrell, D. A. (2011) Noncanonical amino acids in the interrogation of cellular protein synthesis. *Acc. Chem. Res.* *44*, 677–685.

(34) Dieterich, D. C., Hodas, J. J. L., Gouzer, G., Shadrin, I. Y., Ngo, J. T., Triller, A., Tirrell, D. A., and Schuman, E. M. (2010) In situ visualization and dynamics of newly synthesized proteins in rat hippocampal neurons. *Nature Neuroscience.* *13*, 897–905.

(35) Agard, N. J., and Bertozzi, C. R. (2009) Chemical approaches to perturb, profile, and perceive glycans. *Acc. Chem. Res.* *42*, 788–797.

(36) Laughlin, S. T., Baskin, J. M., Amacher, L. S., and Bertozzi, C. R. (2008) *In vivo* imaging of membrane-associated glycans in developing zebrafish. *Science.* *320*, 664–667.

(37) Kostiuk, M. A., Corvi, M. M., Keller, B. O., Plummer, G., Prescher, J. A., Hangauer, M. J., Bertozzi, C. R., Rajaiah, G., Falck, J. R., and Berthiaume, L. G. (2008) Identification of palmitoylated mitochondrial proteins using a bio-orthogonal azido-palmitate analogue. *FASEB J.* *22*, 721–732.

(38) Heal, W. P., Jovanovic, B., Bessin, S., and Wright, M. H. (2011) Bioorthogonal chemical tagging of protein cholesterylation in living cells. *Chem Commun.* *47*, 4081–4083.

(39) Salic, A., and Mitchison, T. J. (2008) A chemical method for fast and sensitive detection of DNA synthesis *in vivo*. *Proc. Nat. Acad. Sci. U.S.A.* *105*, 415–2420.

(40) Martin, B. R., Wang, C., Adibekian, A., Tully, S. E., and Cravatt, B. F. (2012) Global profiling of dynamic protein palmitoylation. *Nature Methods.* *9*, 84–89.

(41) Schieber, C., Bestetti, A., Lim, J. P., Ryan, A. D., Nguyen, T. L., Eldridge, R., White, A. R., Gleeson, P. A., Donnelly, P. S., Williams, S. J., and Mulvaney, P. (2012) Conjugation of transferrin to azide-modified CdSe/ZnS core-shell quantum dots using cyclooctyne click chemistry. *Angew. Chem., Int. Ed. Engl.* *51*, 10523–10527.

(42) Köhn, M., and Breinbauer, R. (2004) The Staudinger ligation—a gift to chemical biology. *Angew. Chem., Int. Ed.* *43*, 3106–16.

(43) Gololobov, Y. G., Zhmurova, I. N., and Kasukhin, L. F. (1981) Sixty years of

Staudinger reaction. *Tetrahedron*. 37, 3437–472.

(44) Saxon, E., and Bertozzi, C. R. (2000) Cell surface engineering by a modified Staudinger reaction. *Science*. 287, 2007–2010.

(45) Fiona L Lin, Helen M Hoyt, Herman van Halbeek, Robert G Bergman, A., Carolyn R Bertozzi. (2005) Mechanistic investigation of the Staudinger ligation. *J. Am. Chem. Soc.* 127, 2686–2695.

(46) Sletten, E. M., and Bertozzi, C. R. (2011) From mechanism to mouse: a tale of two bioorthogonal reactions. *Acc. Chem. Res.* 44, 666–676.

(47) Carroll, L., Boldon, S., Bejot, R., Moore, J. E., Declerck, J., and Gouverneur, V. (2011) The traceless Staudinger ligation for indirect ¹⁸F–radiolabelling. *Org. Biomol. Chem.* 9, 136–140.

(48) Saxon, E., and Bertozzi, C. R. (2000) Cell surface engineering by a modified Staudinger reaction. *Science*. 287, 2007–2010.

(49) Hang, H. C., Yu, C., Kato, D. L., and Bertozzi, C. R. (2003) A metabolic labeling approach toward proteomic analysis of mucin–type O–linked glycosylation. *Proc. Nat. Acad. Sci. U.S.A.* 100, 14846–14851.

(50) Vocadlo, D. J., Hang, H. C., Kim, E. J., Hanover, J. A., and Bertozzi, C. R. (2003) A chemical approach for identifying O–GlcNAc–modified proteins in cells. *Proc. Nat. Acad. Sci. U.S.A.* 100, 9116–9121.

(51) Sarah J Luchansky, Sulabha Argade, Bradley K Hayes, A., Carolyn R Bertozzi. (2004) Metabolic functionalization of recombinant glycoproteins. *Biochemistry*. 43, 12358–12366.

(52) Bradley L Nilsson, Laura L Kiessling, A., Ronald T Raines. (2000) Staudinger Ligation: a peptide from a thioester and azide. *Org. Lett.* 2, 1939–1941.

(53) Saxon, E., Armstrong, J. I., and Bertozzi, C. R. (2000) A “traceless” Staudinger ligation for the chemoselective synthesis of amide bonds. *Org. Lett.* 2, 2141–2143.

(54) Matthew B Soellner, Kimberly A Dickson, Bradley L Nilsson, A., Ronald T Raines. (2003) Site–specific protein immobilization by Staudinger ligation. *J. Am. Chem. Soc.* 125, 11790–11791.

(55) Köhn, M., Wacker, R., Peters, C., Schröder, H., Soulère, L., Breinbauer, R.,

Niemeyer, C. M., and Waldmann, H. (2003) Staudinger ligation: a new immobilization strategy for the preparation of small-molecule arrays. *Angew. Chem., Int. Ed.* *42*, 5830–5834.

(56) Huisgen, R., Adelsberger, K., Aufderhaar, E., Knupfer, H., and Wallbillich, G. N. (1967) Unterschiedliche reaktivitäten substituierter nitrilimine. *Monatshefte für Chemie.* *98*, 1618–1650.

(57) Agnew, H. D., Rohde, R. D., Millward, S. W., Nag, A., Yeo, W. S., Hein, J. E., Pitram, S. M., Tariq, A. A., Burns, V. M., Krom, R. J., Fokin, V. V., Sharpless, K. B., and Heath, J. R. (2009) Iterative in situ click chemistry creates antibody-like protein-capture agents. *Angew. Chem., Int. Ed.* *48*, 4944–4948.

(58) Christian W Tornøe, Caspar Christensen, A., and Meldal, M. (2002) Peptidotriazoles on solid phase: [1,2,3]-triazoles by regiospecific copper(I)-catalyzed 1,3-dipolar cycloadditions of terminal alkynes to azides. *J. Org. Chem.* *67*, 3057–3064.

(59) Hao, Z., Hong, S., Chen, X., and Chen, P. R. (2011) Introducing bioorthogonal functionalities into proteins in living cells. *Acc. Chem. Res.* *44*, 742–51.

(60) El-Sagheer, A. H., and Brown, T. (2012) Click nucleic acid ligation: applications in biology and nanotechnology. *Acc. Chem. Res.* *45*, 1258–1267.

(61) Zhang, X., and Zhang, Y. (2013) Applications of azide-based bioorthogonal click chemistry in glycobiology. *Molecules.* *18*, 7145–7159.

(62) Hong, V., Steinmetz, N. F., and Manchester, M. (2010) Labeling live cells by copper-catalyzed alkyne-azide click chemistry. *Bioconjugate Chem.* *21*, 1912–1916.

(63) Hong, V., Presolski, S. I., Ma, C., and Finn, M. G. (2009) Analysis and optimization of copper-catalyzed azide-alkyne cycloaddition for bioconjugation. *Angew. Chem., Int. Ed.* *48*, 9879–9883.

(64) Amo, D. S., Wang, W., Jiang, H., Besanceney, C., Yan, A. C., Levy, M., Liu, Y., Marlow, F. L., and Wu, P. (2010) Biocompatible copper(I) catalysts for *in vivo* imaging of glycans. *J. Am. Chem. Soc.* *132*, 16893–16899.

(65) Wittig, G., and Krebs, A. (1961) On the existence of low-membered cycloalkynes. *Chem. Ber.* *94*, 3260–3275.

-
- (66) Nicholas J Agard, Jennifer A Prescher, A., and Bertozzi, C. R. (2004) A strain-promoted [3 + 2] azide-alkyne cycloaddition for covalent modification of biomolecules in living systems. *J. Am. Chem. Soc.* *126*, 15046–15047.
- (67) Turner, R. B., Jarrett, A. D., and Goebel, P. (1973) Heats of hydrogenation. IX. Cyclic acetylenes and some miscellaneous olefins. *J. Am. Chem. Soc.* *95*, 790–792.
- (68) Ning, X., Guo, J., Wolfert, M. A., and Boons, G. J. (2008) Visualizing metabolically labeled glycoconjugates of living cells by copper-free and fast Huisgen cycloadditions. *Angew. Chem., Int. Ed.* *47*, 2253–2255.
- (69) Baskin, J. M., Prescher, J. A., and Laughlin, S. T. (2007) Copper-free click chemistry for dynamic *in vivo* imaging. *Proc. Nat. Acad. Sci. U.S.A.* *104*, 16793–16797.
- (70) Agard, N. J., Prescher, J. A., and Bertozzi, C. R. (2004) A strain-promoted [3+ 2] azide-alkyne cycloaddition for covalent modification of biomolecules in living systems. *J. Am. Chem. Soc.* *126*, 15046–15047.
- (71) Ning, X., Temming, R. P., Dommerholt, J., Guo, J., Ania, D. B., Debets, M. F., Wolfert, M. A., Boons, G. J., and van Delft, F. L. (2010) Protein modification by strain-promoted alkyne-nitrone cycloaddition. *Angew. Chem., Int. Ed.* *49*, 3065–3068.
- (72) Marks, S. I., Kang, S. J., Jones, T. B., Landmark, J. K., and Cleland, J. A. (2011) Strain-promoted “click” chemistry for terminal labeling of DNA. *Bioconjugate Chem.* *22*, 1259–1263.
- (73) Jewett, J. C., Sletten, E. M., and Bertozzi, C. R. (2010) Rapid Cu-free click chemistry with readily synthesized biarylazacyclooctynones. *J. Am. Chem. Soc.* *132*, 3688–3690.
- (74) Blackman, M. L., Royzen, M., and Fox, J. M. (2008) Tetrazine ligation: fast bioconjugation based on inverse-electron-demand Diels-Alder reactivity. *J. Am. Chem. Soc.* *130*, 13518–13519.
- (75) Selvaraj, R., and Fox, J. M. (2013) Trans-cyclooctene—a stable, voracious dienophile for bioorthogonal labeling. *Curr. Opin. Chem. Biol.* *17*, 753–760.
- (76) Bach, R. D. (2009) Ring strain energy in the cyclooctyl system. The effect of strain energy on [3 + 2] cycloaddition reactions with azides. *J. Am. Chem. Soc.* *131*, 5233–5243.

-
- (77) Rossin, R., Bosch, S. M., and Hoeve, W. T. (2013) Highly Reactive trans-cyclooctene tags with improved stability for Diels–Alder chemistry in living systems. *Bioconjugate chem.* *24*, 1210–1217.
- (78) Devaraj, N. K., Thurber, G. M., Keliher, E. J., Marinelli, B., and Weissleder, R. (2012) Reactive polymer enables efficient *in vivo* bioorthogonal chemistry. *Proc. Nat. Acad. Sci. U.S.A.* *109*, 4762–4767.
- (79) Rossin, R., Verkerk, P. R., van den Bosch, S. M., Vulders, R. C. M., Verel, I., Lub, J., and Robillard, M. S. (2010) *In vivo* chemistry for pretargeted tumor imaging in live mice. *Angew. Chem., Int. Ed.* *49*, 3375–3378.
- (80) Budin, G., Chung, H. J., Lee, H., and Weissleder, R. (2012) A magnetic Gram stain for bacterial detection. *Angew. Chem., Int. Ed.* *51*, 7752–7755.
- (81) Devaraj, N. K., Weissleder, R., and Hilderbrand, S. A. (2008) Tetrazine–based cycloadditions: application to pretargeted live cell imaging. *Bioconjugate Chem.* *19*, 2297–2299.
- (82) Patterson, D. M., Nazarova, L. A., and Xie, B. (2012) Functionalized cyclopropenes as bioorthogonal chemical reporters. *J. Am. Chem. Soc.* *134*, 18638–18643.
- (83) Cole, C. M., Yang, J., Šečkutè, J., and Devaraj, N. K. (2013) Fluorescent live-cell imaging of metabolically incorporated unnatural cyclopropene–mannosamine derivatives. *ChemBioChem.* *14*, 205–208.
- (84) Li, Q., Dong, T., Liu, X., and Lei, X. (2013) A bioorthogonal ligation enabled by click cycloaddition of *o*-quinolinone quinone methide and vinyl thioether. *J. Am. Chem. Soc.* *135*, 4996–4999.
- (85) Patterson, D. M., Nazarova, L. A., and Prescher, J. A. (2014) Finding the right Bioorthogonal chemistry. *ACS. Chem. Biol.* *9*, 592–605.
- (86) Jelinek, R., and Kolusheva, S. (2004) Carbohydrate biosensors. *Chem. Rev.* *104*, 5987–6015.
- (87) Cao, H., and Heagy, M. D. (2004) Fluorescent chemosensors for carbohydrates: A decade's worth of bright spies for saccharides in review. *J. Fluoresc.* *14*, 569–584.
- (88) James, T. D., Linnane, P., and Shinkai, S. (1996) Fluorescent saccharide receptors: a sweet solution to the design, assembly and evaluation of boronic acid derived PET

sensors. *Chem. Commun.* 281–288.

(89) Hall, D. G. (2012) Boronic Acids: Preparation and applications in organic synthesis, medicine and materials.

(90) Lorand, J. P., and Edwards, J. O. (1959) Polyol Complexes and structure of the benzenboronate ion. *J. Org. Chem.* 24, 769–774.

(91) Springsteen, G., and Wang, B. (2002) A detailed examination of boronic acid–diol complexation. *Tetrahedron.* 58, 5291–5300.

(92) Yan, J., Springsteen, G., Deeter, S., and Wang, B. (2004) The relationship among pKa, pH, and binding constants in the interactions between boronic acids and diols—it is not as simple as it appears. *Tetrahedron.* 60, 11205–11209.

(93) James, T. D., Sandanayake, K. R. A. S., and Shinkai, S. (1994) Novel photoinduced electron–transfer sensor for saccharides based on the interaction of boronic acid and amine. *J. Am. Chem. Soc.* 117, 8982–8987.

(94) Tong, A. J., Yamauchi, A., Hayashita, T., and Zhang, Z. Y. (2001) Boronic acid fluorophore/ β -cyclodextrin complex sensors for selective sugar recognition in water. *Anal. Chem.* 73, 1530–1536.

(95) Larkin, J. D., Fossey, J. S., James, T. D., Brooks, B. R., and Bock, C. W. (2010) A computational investigation of the nitrogen–boron interaction in *o*-(N,N-dialkylaminomethyl)arylboronate systems. *J. Phys. Chem.* 114, 12531–12539.

(96) Collins, B. E., Metola, P., and Anslyn, E. V. (2013) On the rate of boronate ester formation in ortho-aminomethyl-functionalised phenyl boronic acids. *Supramol Chem.* 25, 79–86.

(97) Cao, H., and Heagy, M. D. (2004) Fluorescent chemosensors for carbohydrates: a decade's worth of bright spies for saccharides in review. *J. Fluoresc.* 14, 569–584.

(98) James, T. D., Sandanayake, K. R. A. S., and Shinkai, S. (1994) A glucose-selective molecular fluorescence sensor. *Angew. Chem., Int. Ed.* 33, 2207–2209.

(99) James, T. D., Sandanayake, K. R. A. S., and Shinkai, S. (1995) Chiral discrimination of monosaccharides using a fluorescent molecular sensor. *Nature.* 374, 345–347.

(100) Wulff, G. (1995) Molecular imprinting in cross-linked materials with the aid of molecular templates—a way towards artificial antibodies. *Angew. Chem., Int. Ed.* 34,

1812–1832.

(101) Tsukagoshi, K., and Shinkai, S. (1991) Specific complexation with mono- and disaccharides that can be detected by circular dichroism. *J. Org. Chem.* *56*, 4089–4091.

(102) Eggert, H., Frederiksen, J., Morin, A. C., and Norrild, C. J. (1999) A new glucose-selective fluorescent bisboronic acid. First report of strong α -furanose complexation in aqueous solution at physiological pH. *J. Org. Chem.* *64*, 3846–3852.

(103) Liu, Y., Deng, C., Tang, L., Qin, A., and Hu, R. (2010) Specific detection of D-glucose by a tetraphenylethene-based fluorescent sensor. *J. Am. Chem. Soc.* *133*, 660–663.

(104) Pal, A., Bérubé, M., and Hall, D. G. (2010) Design, synthesis, and screening of a library of peptidyl bis(boroxoles) as oligosaccharide receptors in water: identification of a receptor for the tumor marker TF-antigen disaccharide. *Angew. Chem., Int. Ed.* *49*, 1492–1495.

(105) Stones, D., Manku, S., and Lu, X. (2004) Modular solid-phase synthetic approach to optimize structural and electronic properties of oligoboronic acid receptors and sensors for the aqueous recognition. *Chem. Eur. J.* *10*, 92–100.

(106) Bérubé, M., Dowlut, M., and Hall, D. G. (2008) Benzoboroxoles as efficient glycopyranoside-binding agents in physiological conditions: structure and selectivity of complex formation. *J. Org. Chem.* *73*, 6471–6479.

(107) Huang, Y. J., Ouyang, W. J., Wu, X., Li, Z., Fossey, J. S., James, T. D., and Jiang, Y. B. (2013) Glucose sensing *via* aggregation and the use of “knock-out” binding to improve selectivity. *J. Am. Chem. Soc.* *135*, 1700–1703.

(108) Huang, L. L., Jin, Y. J., Zhao, D., Yu, C., Hao, J., and Xie, H. Y. (2014) A fast and biocompatible living virus labeling method based on sialic acid-phenylboronic acid recognition system. *Anal. Bioanal. Chem.* *406*, 2687–2693.

(109) Cal, P. M. S. D., Vicente, J. B., Pires, E., Coelho, A. V., Veiros, L. F., Cordeiro, C., and Gois, P. M. P. (2012) Iminoboronates: a new strategy for reversible protein modification. *J. Am. Chem. Soc.* *134*, 10299–10305.

(110) McFarland J. M., and Francis, M. B. (2005) Reductive alkylation of proteins using iridium catalyzed transfer hydrogenation. *J. Am. Chem. Soc.* *127*, 13490–13491.

-
- (111) Raindlová, V., Pohl, R., and Hocek, M. (2012) Synthesis of aldehyde-linked nucleotides and DNA and their bioconjugations with lysine and peptides through reductive amination. *Chem. Eur. J.* *18*, 4080–4087.
- (112) Smith, M. E. B., Schumacher, F. F., Ryan, C. P., Tedaldi, L. M., Papaioannou, D., Waksman, G., Caddick, S., and Baker, J. R. (2010) Protein modification, bioconjugation, and disulfide bridging using bromomaleimides. *J. Am. Chem. Soc.* *132*, 1960–1965.
- (113) Zhu, L., Shabbir, S. H., Gray, M., and Lynch, V. M. (2006) A structural investigation of the N-B interaction in an *o*-(N, N-dialkylaminomethyl) arylboronate system. *J. Am. Chem. Soc.* *128*, 1222–1232.
- (114) Cal, P. M. S. D., Frade, R. F. M., Chudasama, V., Cordeiro, C., Caddick, S., and Gois, P. M. P. (2014) Targeting cancer cells with folic acid–iminoboronate fluorescent conjugates. *Chem. Commun.* *50*, 5261–5263.

Chapter 2

Design and Synthesis of Small Aryl Boronic Acid Reporters with Potentially Four Covalent, Reversible Points of Attachment to Peptides

2.1 Introduction

Proteins with their numerous side-chain functionalities and diverse biological activity are very important and it is essential to understand their molecular roles in biological systems. As discussed in the introduction chapter, boronic acid sensors are traditionally limited to sensing sugars and other simple cis-1,2- and 1,3-diols. However, boronic acids have been utilized as reversible, selective and non-toxic sensors for protein modification. In 2009, the first example of a new class of nontoxic, boronic acid-based fluorophores was reported to label a tetraserine peptide with high affinity and selectivity as a selective small-molecule tag for proteins within living cells (Figure 1-3, Chapter 1).¹ Specifically, a rhodamine-derived bisboronic acid sensor (RhoBo) was used to selectively label a tetraserine peptide tag. The RhoBo sensor is able to bind to two diols in the SSPGSS peptide tag with a 1:1 stoichiometric ratio. Titrations of the RhoBo sensor with peptides containing two or four serines with shorter or longer intervening sequences, however, could not provide any detectable fluorescent changes. To the best of my knowledge, only the RhoBo sensor was reported in the construction of boronic acid-based sensors applicable in bio-orthogonal chemistry *via* a selective bond formation with a designed peptide.¹ In 2012, the reversible and selective modification on N-terminal lysine residues was reported using a small boronic acid molecule. It was shown that the well-known dative N-B interaction can be applied to form a stable iminoboronate (Figure 1-10, Chapter 1).² Later, these stable iminoboronates were utilized for selective recognition of cancer cells over-expressing folic acid receptors (Figure 1-11, Chapter 1).³ There are critical issues to the development of a labeling compound with high affinity and high specificity. The binding motifs should recognize the unique structural features of the target molecules, and a detectable signal should be produced upon binding. In this

chapter, boronic acids were chosen as a binding motif with potentially four covalent, reversible points of attachment, which could selectively bind to a small peptide tag in a sequence specific manner with high affinity. Therefore, our goal was to design a small monoarylboronic acid and also a peptide tag with two or more serines and a lysine. Boronate ester formation between serines and the boronic acid part of the molecule was believed to potentially increase the selectivity and stability of imine formation between the lysine and ketone part of the molecule.

2.2 Design and synthesis of small monoboronic acid probes

Small monoboronic acids that could potentially provide four covalent, reversible points of attachment to the peptide tags were designed with a view to increase their selectivity and affinity towards a specific peptide sequence. The initial attempt was to synthesize a boronic acid with a functional group that could increase the affinity towards the peptide sequence. Therefore, the ketone functional group was first considered for its ability to form Schiff bases (Figure 2-1).

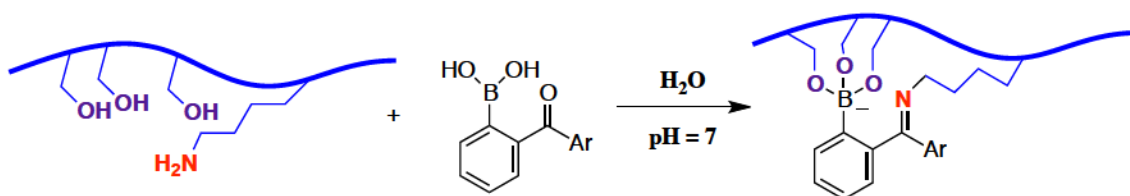


Figure 2-1: A designed boronic acid with potentially four covalent bonds with a peptide tag

Three different compounds with a boronic acid positioned at ortho-, meta- and para-positions on a benzophenone framework were designed in order to investigate the optimal spacing between the boronate ester and the imine unit (Figure 2-2). We proposed that boronate ester formation with the hydroxyl groups of serines in the designed peptide, which will be discussed in the next section, could facilitate the imine formation of a ketone with the amine of a lysine on the corresponding peptide.

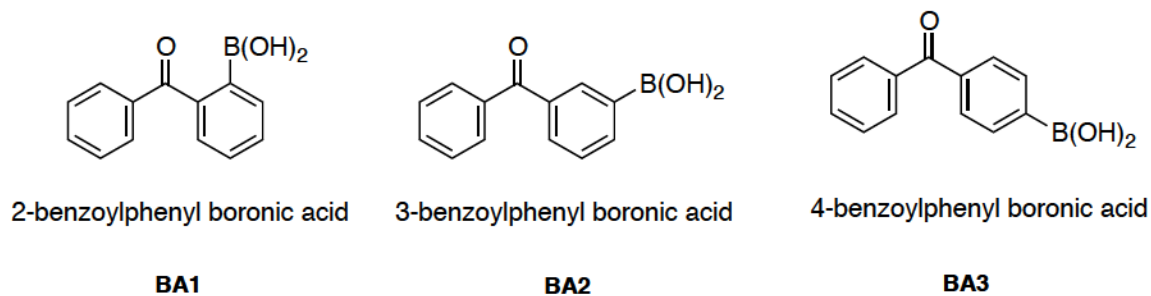
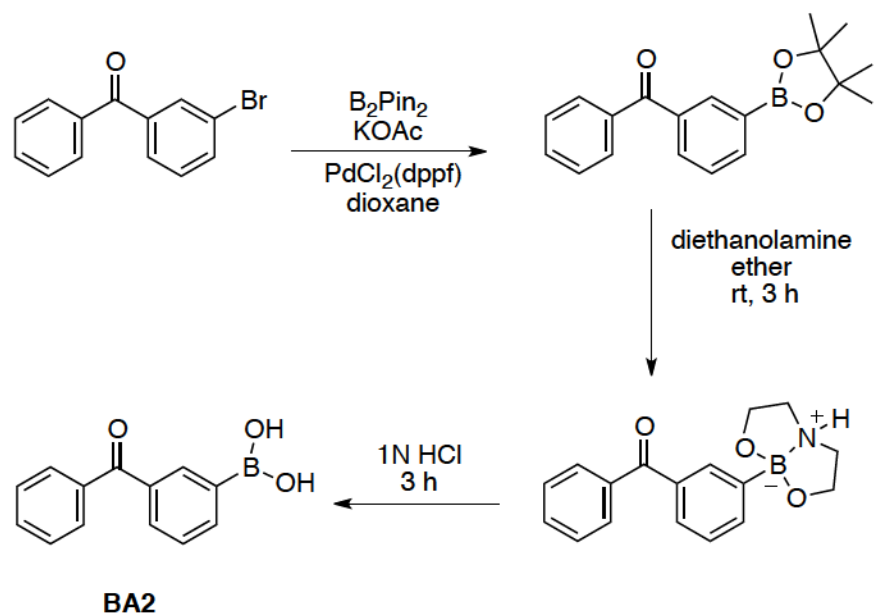


Figure 2-2: Boronic acid functionalized benzophenone derivatives

These three boronic acids were synthesized based on the Miyaura borylation reaction, which enables the synthesis of boronates by cross-coupling of bis(pinacolato)diboron (B_2Pin_2) with aryl halides in the presence of a palladium catalyst (Scheme 2-1).⁴

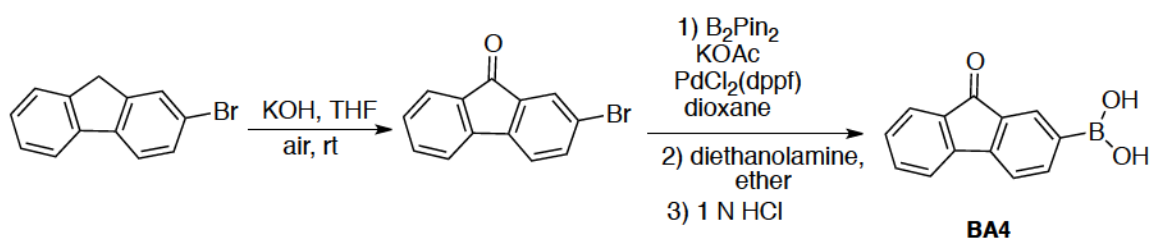


Scheme 2-1: Synthesis of 3-benzoylphenyl boronic acid (BA2)

A two-step procedure for deprotection of the pinacolyl boronate esters *via* transesterification with diethanolamine followed by hydrolysis was successfully performed to obtain the free boronic acid without further purification (Scheme 2-1).⁵

Later, binding of all three synthesized boronic acids towards a selection of chosen peptides was evaluated *via* two methods, ARS colorimetric assay and UV

spectrophotometry. Following these results, 9-fluorenone cores, which exhibit prominent emissions of fluorescence, were considered to be a better option in determining the binding affinity between the boronic acids and peptides by fluorescence spectroscopy.⁶ Therefore, 9-fluorenone-2-boronic acid (BA4) was synthesized by oxidation of 2-bromofluorene, Miyaura borylation reaction and a final deprotection was achieved as shown in Scheme 2-2.



Scheme 2-2: Synthesis of 9-fluorenone-2-boronic acid (BA4)

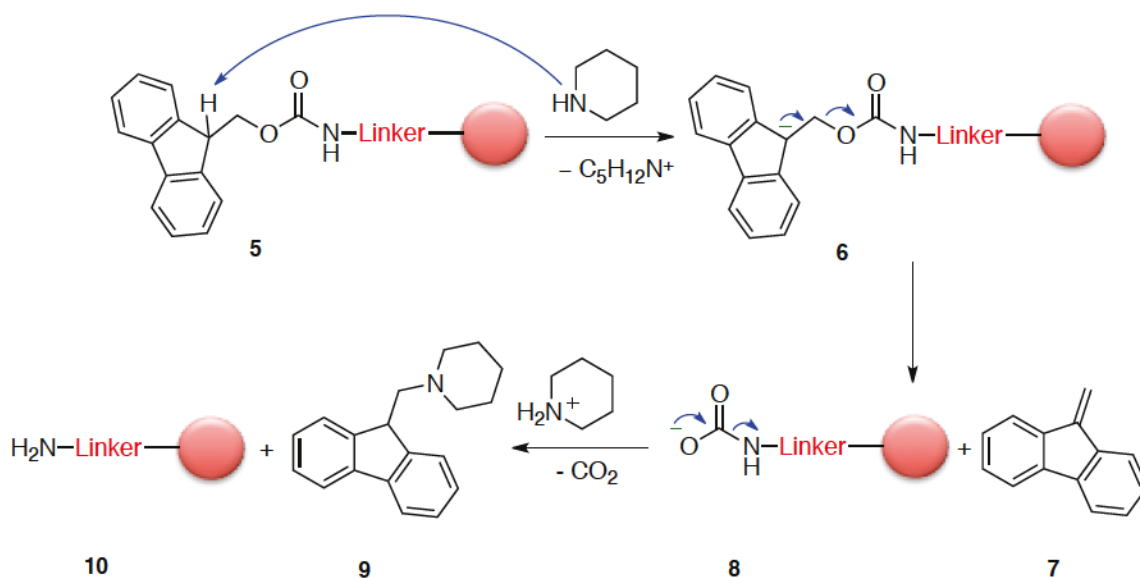
The binding ability of 9-fluorenone-2-boronic acid towards peptides was tested by fluorescence spectroscopy, mass spectrometry and with the ARS colorimetric assay (See Sections 2.4 and 2.5).

2.3 Design of a peptide array

Our plan was to find a small, high affinity receptor peptide domain composed entirely of natural amino acids. In this way, the boronic acid probe could bind selectively to the designed peptide with high affinity. As illustrated in Figure 2-1, the designed small peptide tag could be introduced genetically to the protein of interest to provide a unique binding site that could be selectively recognized by the small probe, the designed boronic acid. The small probe that contains both boronic acid and ketone functionalities is able to bind up to four amino acids in a peptide. The ideal peptide sequence would contain serines, which could bind to the boronic acid and form the boronate ester. With an optimal spacing between serines and lysine in the peptide, the boronate ester could stabilize the imine based on the well-known dative N-B interaction. We considered that various small intervening sequences in the peptides would help to orient the hydroxyl and amine side chains to effectively bind the boronic acid probe. An array of short peptides

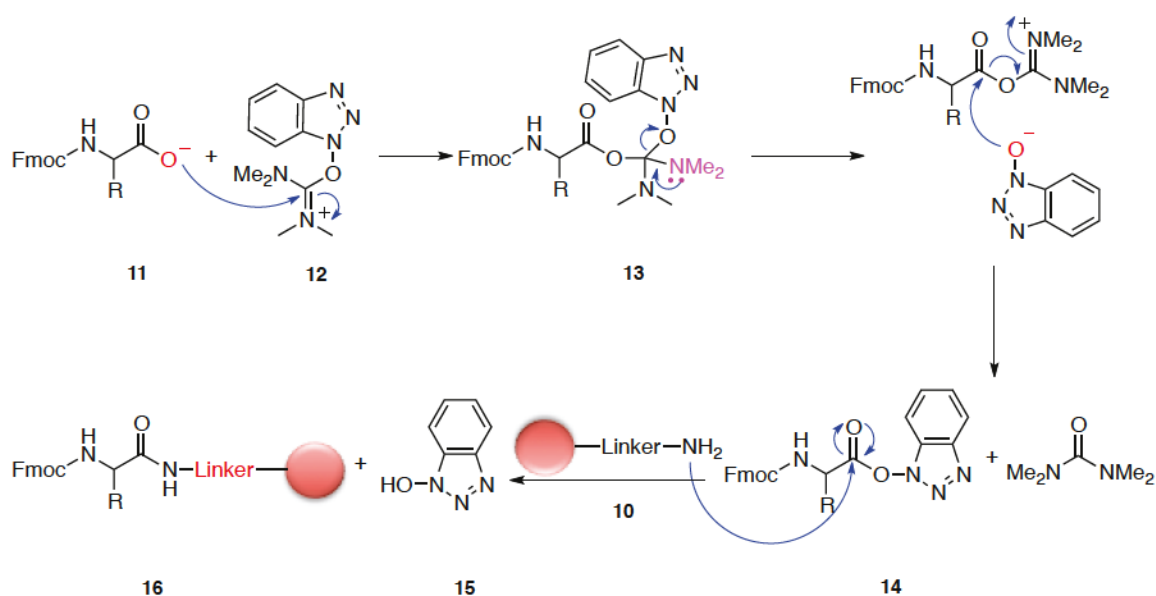
sequence was constructed and their binding ability with the probes would be subsequently evaluated. Thus, a series of peptides that contained either proline or glycine amino acids as the intervening sequence between serine and lysine residues were synthesized (Table 2-1).

All peptides were synthesized by solid phase peptide synthesis (SPPS) on Rink amide resin following the Fmoc protocol. The general process for solid phase peptide synthesis on the Rink amide resin begins with the deprotection of the Fmoc group using piperidine (Scheme 2-3). Piperidine serves as a base to deprotonate **5**, which then decomposes to **7** and **8**. The carbamic acid intermediate, **8**, loses carbon dioxide, forming the free amine, **10**. The piperidine is added onto the produced 9-methylene fluorene, **7** to form **9** as a byproduct.



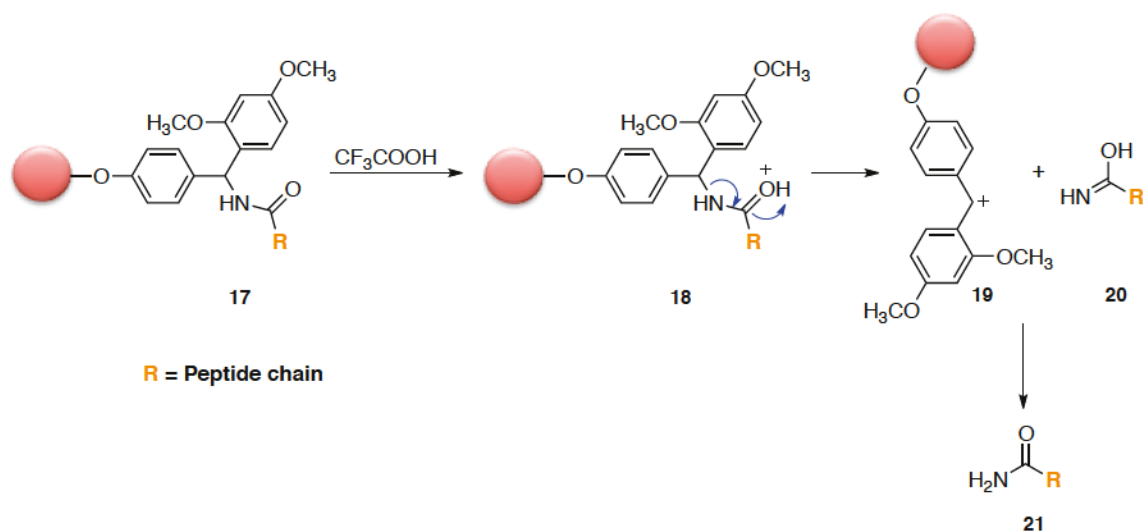
Scheme 2-3: Mechanism for Fmoc deprotection in SPPS

The first Fmoc protected amino acid is allowed to couple with the resin once the free amine linker is formed by using HBTU as a coupling reagent. The mechanism of coupling amino acid with HBTU is shown in Scheme 2-4. The coupling reagent, HBTU (**12**), is attacked by the carboxylate anion of amino acid, **11**, which forms ester intermediate **13**, which becomes the active ester **14**. Then, the latter is attacked by the amine group on the resin and forms the coupling product **16** and triazole **15**.



Scheme 2-4: Mechanism for coupling amino acids in SPPS

Once the amino acid is attached to the resin, the resin is filtered and washed to remove byproducts and excess reagents. Next, the Fmoc protecting group is removed by repeating the piperidine process and the resin is again washed to remove byproducts and excess reagents. Another amino acid is then coupled to the attached amino acid. This is followed by another washing procedure, which leaves the resin-peptide ready for the next coupling cycle. The cycle is repeated until the peptide sequence is completed. Then typically, all the protecting groups are removed and the resin is washed. Concentrated trifluoroacetic acid (TFA) is the common reagent used to perform the final cleavage of the peptide from the resin together with the removal of the side chain protecting groups. During the reaction, highly reactive carbocations produce and can cause a problem with sensitive amino acids such as Cys, Met, Ser, Thr, Trp, Tyr.⁷ So, it is necessary to trap them to avoid undesired reactions, and the addition of scavengers to the cleavage solution is essential. Therefore, a mixed solution of TFA/H₂O/phenol/TIPS [85:5:5:5 (v/v/v/v)] was used for the peptide cleavage. The mechanism of peptide cleavage from the Rink amide resin is shown in Scheme 2-5, which starts with the protonation of compound 17. Later, decomposition of compound 17 forms the stable carbocation 19 and product 20, which tautomerizes to the peptide 21 (Scheme 2-5).



Scheme 2-5: Mechanism of peptide cleavage from resin with TFA

I started with synthesizing a series of peptides including, peptide 1: Ac-KSGSSGG-NH₂, peptide 2: Ac-KSPSSGG-NH₂, peptide 3: Ac-KSGGSSGG-NH₂, and peptide 4: AcKGGSSSSGG-NH₂, which contained an intervening sequence whereas the fifth peptide did not contain an intervening sequence, peptide 5: Ac-KSSSSSPG-NH₂ (Table 2-1). We were not certain if these intervening sequences would provide optimal spacing between the hydroxyls and the amine. To solve this issue, a hairpin-prone intervening sequence was installed in the peptide. Proline and glycine show relatively high preferences for forming a β -turn.¹ Therefore, peptide 8: AcWKAPGSSSG and peptide 9: AcWKPGSSSG were synthesized in reference to this preference.

In the field of structural biology, the role of tryptophan zippers (trpzips) in peptides has been applied for the study of secondary structures in proteins.^{8,9} Trpzips contain only 16 to 20 amino acids in length, which forms a highly stable β -hairpin structure stabilized by tryptophan-tryptophan cross-strand pairing interactions in aqueous solution. A highly folded and preorganized structure of peptides can minimize the entropic force they need to form the essential conformation to bind to the target with higher affinity.⁷ It could be anticipated that the application of trpzip to synthesize a peptide can maximize adopting a β -hairpin structure in the peptide and possibly increase the binding affinity between the boronic acid and the peptide. Thus, peptide 8: KWTWSSGKWTWS, which contained

serines and lysine in the intervening sequences, was designed and synthesized. Additionally, negative control peptides included peptide 6: Ac-KAGSGAG-NH₂ with only one serine and lysine, and peptide 7: Ac-ASGGSSGG-NH₂ without lysine, were synthesized so as to determine the effect of each amino acid in the peptide array.

Label	Peptide Sequence	Molecular Formula	Calculated Mass	Measured Mass by HPLC-MS	Identity
Peptide 1	Ac-KSGSSGG-NH ₂	C ₂₃ H ₄₁ N ₉ O ₁₁	619.29	620.3	(M+H) ⁺
Peptide 2	Ac-KSPSSGG-NH ₂	C ₂₆ H ₄₅ N ₉ O ₁₁	659.32	660.7	(M+H) ⁺
Peptide 3	Ac-KSGSSGG-NH ₂	C ₂₅ H ₄₄ N ₁₀ O ₁₂	676.31	677.1	(M+H) ⁺
Peptide 4	AcKGGSSSGG-NH ₂	C ₂₅ H ₄₄ N ₁₀ O ₁₂	676.31	677.7	(M+H) ⁺
Peptide 5	Ac-KSSSSSPG-NH ₂	C ₃₀ H ₃₇ N ₉ O ₁₂	776.37	777.3	(M+H) ⁺
Peptide 6	Ac-KAGSGAG-NH ₂	C ₂₄ H ₄₂ N ₈ O ₉	587.31	588.3	(M+H) ⁺
Peptide 7	Ac-ASGGSSGG-NH ₂	C ₂₂ H ₃₇ N ₉ O ₁₂	619.26	620.2	(M+H) ⁺
Peptide 8	AcWKAPGSSSG-NH ₂	C ₂₄ H ₄₂ N ₈ O ₉	916.42	916.8	(M) ⁺
Peptide 9	AcWKPGSSSG-NH ₂	C ₂₂ H ₃₇ N ₉ O ₁₂	845.39	845.7	(M) ⁺
Peptide 10	KWTWSSGKWTWS	C ₇₅ H ₉₉ N ₁₉ O ₁₆	1538.7	1539.5	(M+H) ⁺
Peptide 11	AKAAASAASAA-NH ₂	C ₄₀ H ₇₁ N ₁₅ O ₁₅	887.4	888.4	(M+H) ⁺

Amino acid abbreviation: A: Alanine, G: Glycine, K: Lysine, S: Serine, P: Proline, T: Threonine, W: Tryptophan

Table 2-1: Calculated and observed mass of peptides 1-11

To support the design of peptide 11: AKAAASAASAA-NH₂, molecular modeling was performed by Dr. Sylvain Bernard. The calculation level used for the modelisation was the semi empirical program AM1 method¹⁰ in the Facio molecular builder¹¹. To execute the energy minimization process (the actual modeling), the Firefly modeling program¹² was performed with a high level of calculation (ab initio) in a protic solvent (water) and room temperature. Molecular modeling studies showed that peptide 11 can form an alpha helix conformation, and two serines could position towards 9-fluorenone-2-boronic acid, and likely induce the desired ester bond formation with the boronic acid. Also, imine formation between the amine of lysine and the ketone part of the probe molecule is probable (Figure 2-3).

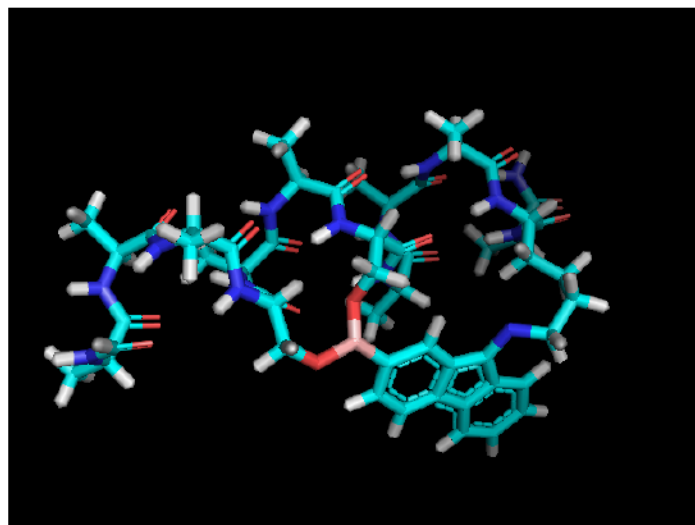
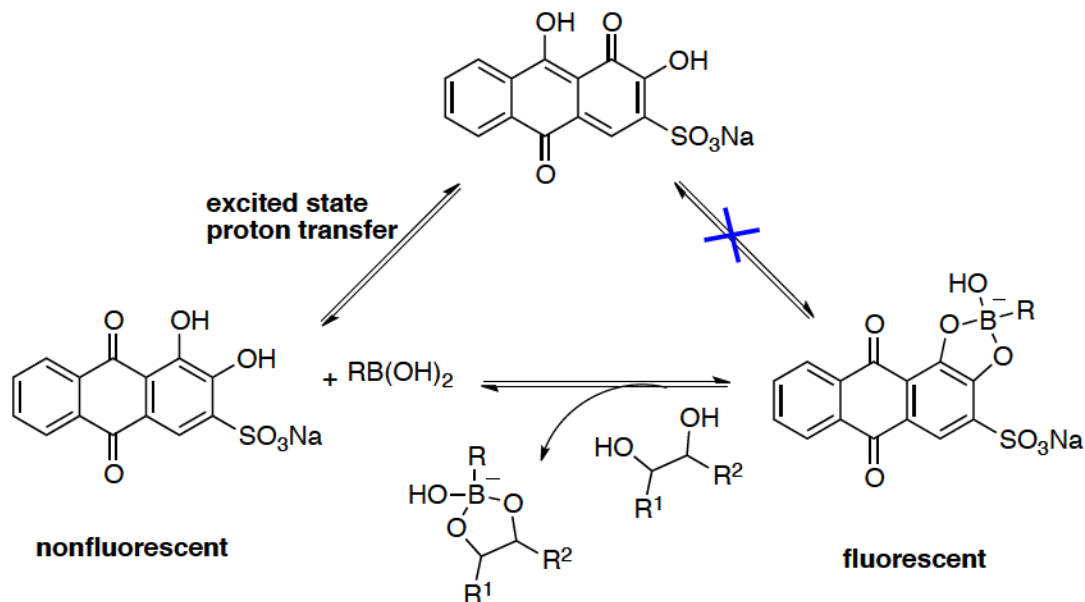


Figure 2-3: Molecular modeling for interaction of peptide 11 and 9-fluorenone-2-boronic acid (4)

D-Glucamine, an aminopolyol model was purchased and used as a positive control due to its expected, high affinity to the probes. After manually synthesizing all the peptides, they were analyzed by HPLC-MS and MALDI-TOF to assess their purity and identity. Some of them were purified by reverse-phase HPLC. The results for the binding behavior of boronic acids to these designed peptides will be discussed in detail in the following sections.

2.4 Alizarin Red S (ARS) as a competitive assay for the complexation of boronic acids

The Alizarin Red S (ARS) competitive dye displacement assay has been developed by Wang and coworkers.¹³ It has been used for studying carbohydrate-boronic acid interactions quantitatively and qualitatively. ARS is intrinsically not fluorescent because of its excited state induced by proton transfer from one of the catechol dihydroxyl groups to the ketone oxygen (Scheme 2-6).⁹ Binding of a boronic acid to the catechol diol of ARS removes the quenching effect of active protons and therefore abolishes the fluorescence quenching. Thus, it can show dramatic changes in the fluorescence intensity and color from pink to yellow upon binding to non-fluorescent boronic acids.

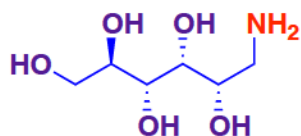


Scheme 2-6: Alizarin Red S binding with a boronic acid

In other words, formation of the ARS-boronic acid complex provides an obvious change in the color of the solution, thus the emitted fluorescence or absorption can be easily measured. Upon addition of a competing diol like a sugar to the complex, the ARS-boronic acid equilibrium is disturbed, which can be used to measure the strength of the boronic acid-diol association. The result of perturbing the reporter-boronic acid equilibrium will provide a change in the color and fluorescence intensity. The color changes in a three-component system can be used for the determination of binding affinity between boronic acid and diols. Alizarin Red S assay was reported as a quick and colorful determination method to monitor the binding affinity of boronic acids to a saccharide in aqueous solution at pH 7.4.⁹ The addition of boronic acid to a pink ARS solution produces a complex, causing a color change from pink to yellow, which serves as the background. By adding saccharide, which is ten times more concentrated than the boronic acid, a second equilibrium is created and the boronic acid binds competitively to the saccharide and releases the free ARS. Free ARS leads to a red color solution due to the formation of a boronic acid-saccharide complex. This signifies that a higher binding affinity between a boronic acid and a carbohydrate molecule increases the intensity of the resulting red solution.

Based on this knowledge, I considered that replacing the saccharide with a peptide might lead to the same response. In the case of strong binding between a peptide and a boronic acid, free ARS could be released and the color of the solution is expected to change from yellow to pink. Here, our aim was to compare the relative affinities of designed boronic acids toward different peptides by using the qualitative ARS method. Competitive studies were run in a similar manner to the ARS-boronic acid for saccharide studies. Solution A was prepared by 50 mL of 10^{-3} M stock solution of ARS solution in 0.10 M sodium phosphate monobasic buffer. It was diluted 10 times with 0.10 M sodium phosphate monobasic buffer in a 500 mL volumetric flask and was brought to pH 7.4 with 1N NaOH. Solution B was prepared by dissolving the boronic acids (0.10 mmol) in solution A in a 1 mL volumetric flask to give 0.02 M solution of the boronic acids. Because of the lower solubility of the boronic acids in water, 30% THF: H₂O solution was employed. The pH was adjusted to 7.4 with 1N NaOH. Colorimetric assays were done with solution B for each boronic acid. The solutions of peptides **1-7** (0.5 M) and D-glucamine (0.5 M) were added to 0.5 mL of the control solution B to compare the changes in the color. The competitive ARS colorimetric assay was achieved with D-glucamine instead of saccharide, and showed significant color change to red after the addition of D-glucamine to all ARS-boronic acids complexes (Figure 2-4). Fructose was also tested in the same conditions, which showed a lower affinity compared to D-glucamine as the solution changed only to a pale pink color (Figure 2-5). Therefore, D-glucamine was considered as a suitable positive control for all boronic acids. The general procedure for colorimetric assays was applied for all boronic acids with peptides and D-glucamine. By adding D-glucamine as a positive response, changing the color into red was observed after binding to all boronic acids. In the case of boronic acid (**BA1**), no color change was observed with peptides in comparison to D-glucamine. As shown in Figure 2-6, the solution in all vials retained a yellow color similar to the boronic acid/ARS complex after addition of peptides. In the case of boronic acid (**BA2**), the color of the solution did not change as a pale yellow color can be seen in all vials (Figure 2-7). For the boronic acid (**BA3**), no color change was observed which indicated the absence of binding; again all vials remained in a yellow color (Figure 2-8). In the case of boronic acid (**BA4**) (Figure 2-9), yellow colored solutions indicated no binding to the model peptides (vials B–H), which

was opposite to D-glucamine where the color was changed to red (vial A). As a result according to the ARS assay, there was no indication of binding between the four boronic acids and peptides 1-7.



D-Glucamine
(Positive control)



Figure 2-4: Solutions of ARS (10^{-4} M in 0.10 M phosphate buffer) and A) phenylboronic acid with D-glucamine B) boronic acid (BA1) with D-glucamine C) boronic acid (BA2) with D-glucamine D) boronic acid (BA3) with D-glucamine and E) boronic acid (BA4) with D-glucamine

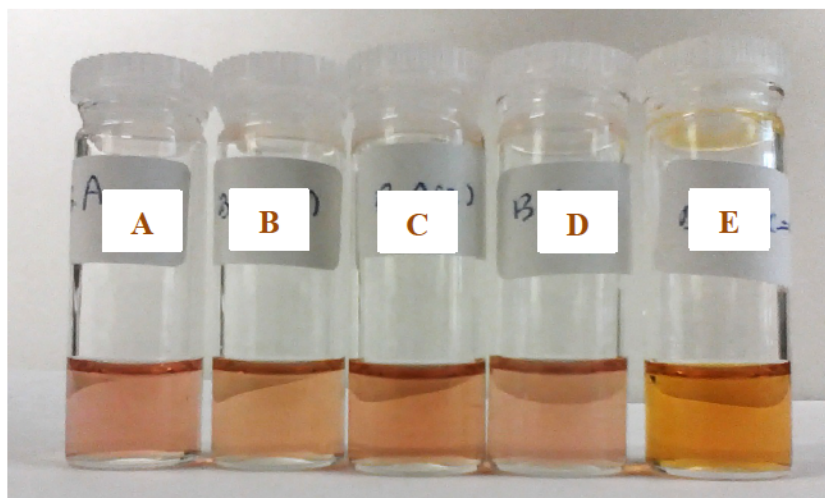


Figure 2-5: Solutions of ARS (10^{-4} M in 0.1 M phosphate buffer) and A) phenylboronic acid with fructose B) boronic acid (BA1) with fructose C) boronic acid (BA2) with fructose D) boronic acid (BA3) with fructose and E) boronic acid (BA4) with fructose



Figure 2-6: Solutions of ARS (10^{-4} M in 0.1 M phosphate buffer) and boronic acid (BA1) (0.02 M) containing: A, 0.5 M peptide 1; B, 0.5 M peptide 2; C, 0.5 M peptide 3; D, 0.5 M peptide 4; E, 0.5 M peptide 5; F, 0.5 M peptide 6; G, 0.5 M peptide 7



Figure 2-7: Solutions of ARS (10^{-4} M in 0.1 M phosphate buffer) and boronic acid (BA2) (0.02 M) containing: A, 0.5 M peptide 1; B, 0.5 M peptide 2; C, 0.5 M peptide 3; D, 0.5 M peptide 4; E, 0.5 M peptide 5; F, 0.5 M peptide 6; G, 0.5 M peptide 7

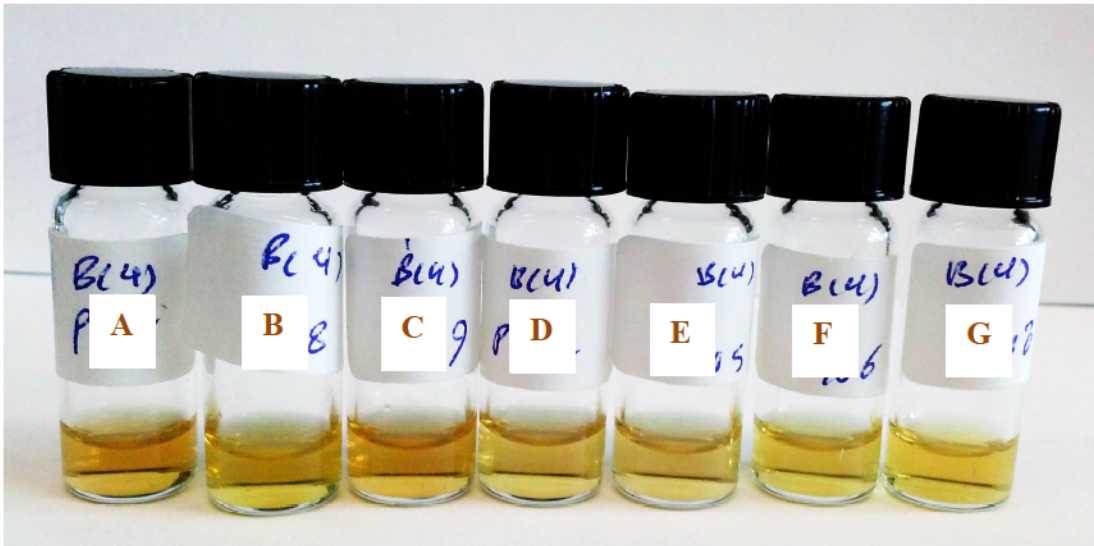


Figure 2-8: Solutions of ARS (10^{-4} M in 0.1 M phosphate buffer) and boronic acid (BA3) (0.02 M) containing: A, 0.5 M peptide 1; B, 0.5 M peptide 2; C, 0.5 M peptide 3; D, 0.5 M peptide 4; E, 0.5 M peptide 5; F, 0.5 M peptide 6; G, 0.5 M peptide 7



Figure 2-9: Solutions of ARS (10^{-4} M in 0.1 M phosphate buffer) and boronic acid (BA4) (0.02 M) containing: A, 0.5 M D-glucamine; B, 0.5 M peptide 1; C, 0.5 M peptide 2; D, 0.5 M peptide 3; E, 0.5 M peptide 4; F, 0.5 M peptide 5; G, 0.5 M peptide 6; H, 0.5 M peptide 7; I, no peptide

2.5 Other methods for the determination of binding affinity between boronic acids and peptides

Although the results obtained from the ARS competitive assay were unsuccessful, we tried to confirm the complexation experiment with other methods, including: fluorescence spectroscopy, UV spectrophotometry, and HPLC-MS analysis. Designed boronic acids and peptides were chosen to test their binding.

2.5.1 Binding studies with UV spectrophotometry

All boronic acids were analyzed to determine their binding affinity to peptides **1-7** *via* UV-Vis spectrophotometry (Figures 2-10 to 2-13). Boronic acid can exhibit absorption spectral changes upon binding to a diol depending on the binding affinity, which can be monitored by UV spectrophotometry. Peptide GGSS-NH₂ and peptide SPGS-NH₂ were synthesized to monitor interaction between serine and the boronic acids. Interactions of all boronic acids with peptides **1-7** and peptide GGSS-NH₂ and peptide Ac-SPGS-NH₂ were quantified by UV-Vis spectrophotometry at 292 nm. Boronic acids (0.05 mM) combined with the peptides **1-7** (0.05 mM), peptide Ac-SPGS-NH₂ (0.05 mM), and peptide GGSS-NH₂ (0.05 mM) in 30:70% THF: 0.10 M sodium phosphate monosic buffer and brought to pH 7.4 with 1N NaOH. Also, 9-fluorenone-2-boronic acid (0.025 mM) was used to measure UV changes in interaction with peptide **1-7** (0.025 mM). As a control, D-glucamine and fructose were added in same stoichiometry to the boronic acids. Then, 2 mL of the mixture was transferred into a cuvette for absorbance measurement.

As shown in the following figures, there were no significant absorbance changes after the addition of peptides **1-7**, peptide GGSS-NH₂ and peptide Ac-SPGS-NH₂, fructose and D-glucamine.

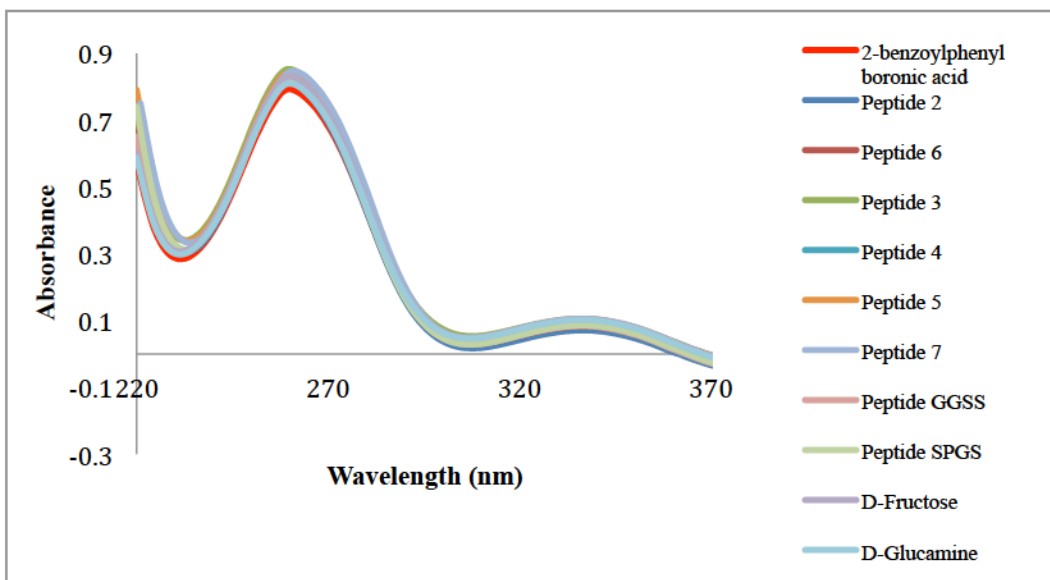


Figure 2-10: UV absorbance of 2-benzoylphenyl boronic acid (BA1) in pH = 7 with peptides 1-7, peptide GGSS-NH₂ and peptide Ac-SPGS-NH₂, fructose and D-glucamine

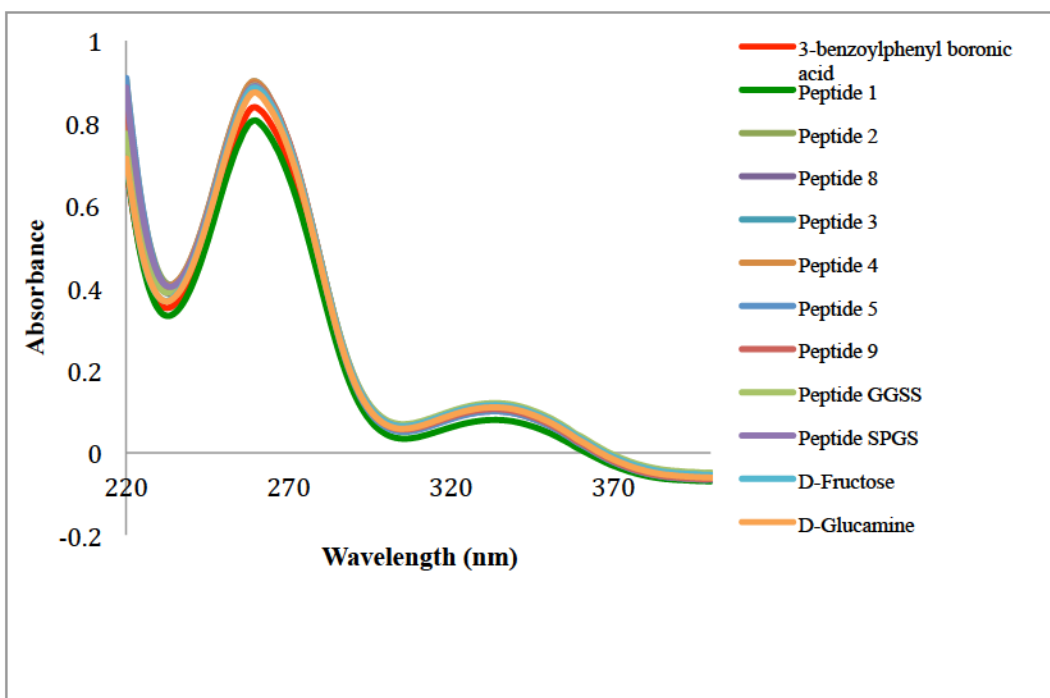


Figure 2-11: UV absorbance of 3-benzoylphenyl boronic acid (BA2) in pH = 7 with peptides 1-7, peptide GGSS-NH₂ and peptide Ac-SPGS-NH₂, fructose and D-glucamine

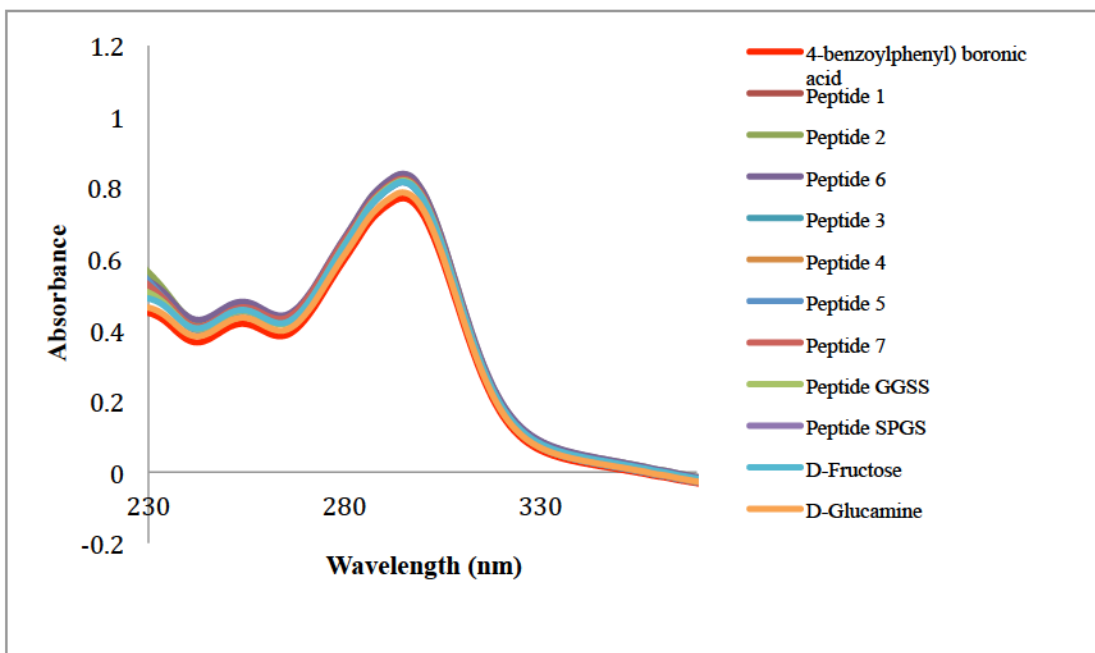


Figure 2-12: UV absorbance of 4-benzoylphenyl boronic acid (BA3) in pH = 7 with peptides 1-7, peptide GGSS-NH₂ and peptide Ac-SPGS-NH₂, fructose and D-glucamine

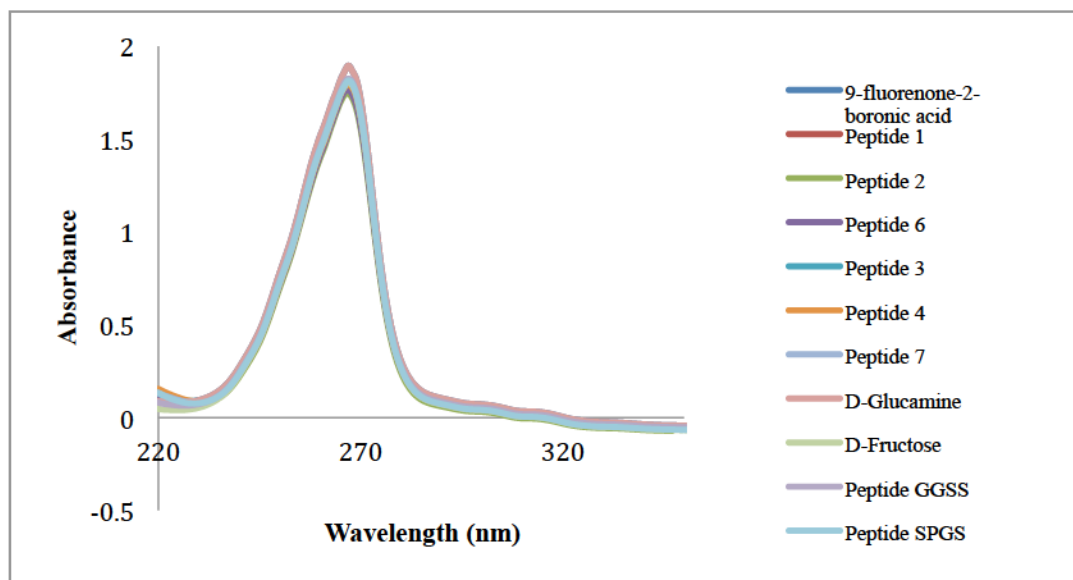


Figure 2-13: UV absorbance of 9-fluorenone-2-boronic acid (BA4) in pH = 7 with peptides 1-7, peptide GGSS-NH₂ and peptide Ac-SPGS-NH₂ fructose and D-glucamine

Even though D-glucamine was chosen as a positive control, it didn't result in any significant changes in UV absorbance. This result was unexpected because of the high affinity of D-glucamine to boronic acids, which should have created a dramatic change in the UV absorbance. This result might be explained in a way that the change in the UV absorbance was undetectable due to its small value. Therefore, it can be concluded that UV spectrophotometry could not give information on peptide complexation.

2.5.2 Binding studies with fluorescence spectroscopy

Then, 9-fluorenone-2-boronic acid was employed to probe its binding to peptides **1-7** via fluorescence spectroscopy. Changes in fluorescent intensity were monitored to find evidence of boronic acid complexation to the peptides. Peptides **1-7** (10 mM) were added to 9-fluorenone-2-boronic acid (10 mM) in 30:70% THF: 0.10 M sodium phosphate monobasic buffer and brought to pH 7.4 with 1N NaOH. After 0.5 h, changes in the fluorescence intensity were monitored to find evidence of boronic acid affinity towards peptides (Figure 2-14).

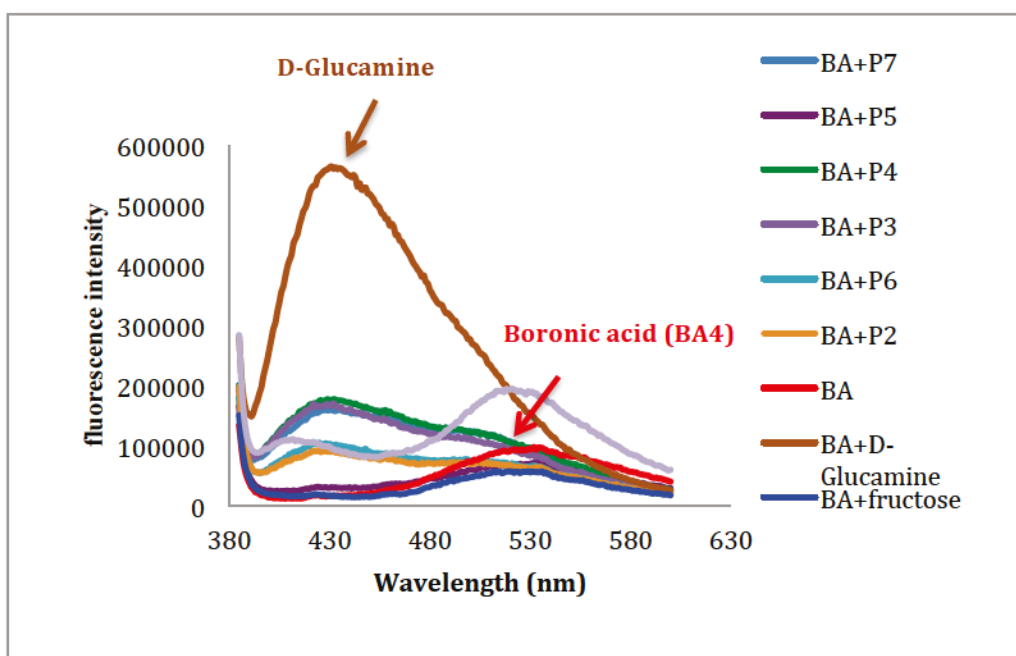


Figure 2-14: Fluorescence response of 9-fluorenone-2-boronic acid (BA4) towards peptides

As we can see in the Figure 2-14, the addition of the peptides did not appear to set up a second strong equilibrium between the boronic acids and serine-rich peptides with or without lysine moiety as no significant changes in the fluorescence intensity was observed.

In Figure 2-14, the red line is related to 9-fluorenone-2-boronic acid. Fructose, denoted with a blue color, decreases the fluorescence intensity, and peptide 5 also shows some activity similar to fructose. A dramatic increase in the fluorescence intensity is observed in the presence of the D-glucamine, as a positive control, as shown by the brown line. The absence of significant fluorescence intensity changes in other peptides does not necessarily imply an absence of binding; however, when we compare these shifts with the fluorescence intensity of pure peptides, the peaks suggest that there are no strong changes in the fluorescence of 9-fluorenone-2-boronic acid with the peptides. As shown in Figure 2-15, a red line is related to 9-fluorenone-2-boronic acid, a purple line is related to peptide 3 and a blue line is related to the mixture of both. There was no significant fluorescence intensity change upon addition of peptide 3 to 9-fluorenone-2-boronic acid.

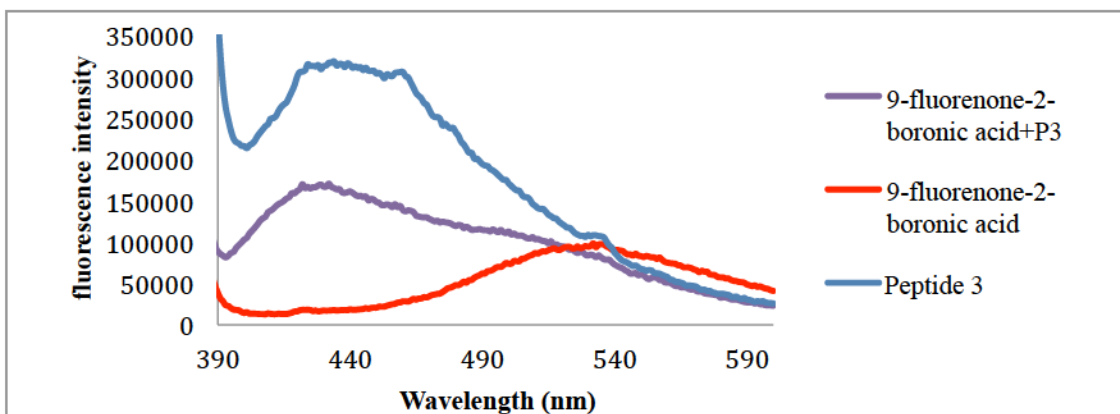


Figure 2-15: Fluorescent response of 9-fluorenone-2-boronic acid towards peptide 3

Based on a molecular modeling study with the same method, as done with the peptide 11, which was performed by Dr. Sylvain Bernard, we anticipated that serines of peptide Ac-SGPS-NH₂ should be able to bind to 9-fluorenone-2-boronic acid. To this end, Alizarin Red S (10⁻⁴ M) was evaluated as a reagent for the fluorometric determination of a

possible complexation between 9-fluorenone-2-boronic acid (10^{-3} M) with peptide Ac-SGPS-NH₂ (10^{-2} M) at pH = 7 and aqueous solution of 0.10 M phosphate buffer. In order to determine the suitability of ARS for the determination of the binding between a boronic acid and the peptide in a three-component system, I used D-glucamine (10^{-2} M) as a model compound, which previously demonstrated a high binding affinity in the colorimetric assay. When D-glucamine was added to the mixture of 9-fluorenone-2-boronic acid and ARS, a fluorescent change was observed (Figure 2-16). However, peptide Ac-SGPS-NH₂ (10^{-2} M) showed no significant changes in its fluorescence intensity. This result was also confirmed by the ARS colorimetric assay, where the solution did not change color and indicated an absence of significant binding. However, as shown in Figure 2-17, upon mixing D-glucamine to the ARS/9-fluorenone-2-boronic acid complex, the solution exhibited a color change from yellow to red.

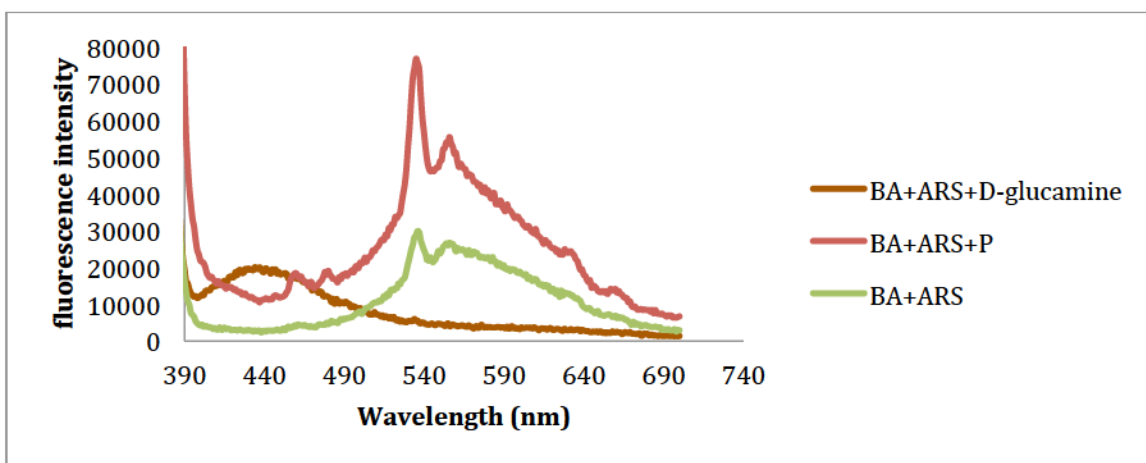


Figure 2-16: Fluorescent response of ARS (10^{-4}) to A) 9-fluorenone-2-boronic acid (10^{-3}) and peptide Ac-SGPS-NH₂(10^{-2}) B) 9-fluorenone-2-boronic acid (10^{-3}) and C) D-glucamine (10^{-2})

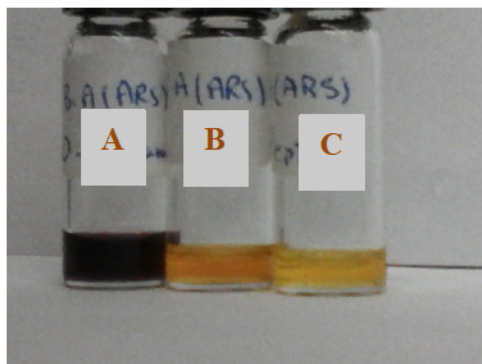


Figure 2-17: Vials of ARS (10^{-4} M in 0.1 M phosphate buffer) and boronic acid (BA4) (0.02 M) containing: A, 0.5 M D-glucamine; B, no peptide; C, peptide Ac-SGPS-NH₂

2.5.3 Binding studies by HPLC-MS analysis

Later, monitoring by HPLC was performed for the reaction of 9-fluorenone-2-boronic acid and peptides **8-11** as an attempt to detect the product formation. 9-fluorenone-2-boronic acid (10 mM, respectively) was stirred with the peptide **8-11** (10 mM) in ammonium acetate buffer (50,0 mM, pH 7.0) at room temperature. Reactions of the boronic acid and peptides were monitored by HPLC-ESI-MS overnight; HPLC data showed no products had been formed. More data was obtained by using MALDI spectroscopy. The analysis indicated that there was no additional peak corresponding to the peptide-boronic acid complex.

2.6 Summary

In this chapter, the interactions between small boronic acid probe molecules and short peptide motifs were studied for the purpose of protein labeling. Boronic acids with a ketone functional group, which have a potential to form four covalent bonds were designed and synthesized. Our hypothesis was that imine formation with a lysine residue could provide a complex further stabilized by boronate ester formation. To achieve this objective, peptides with different intervening sequences between serines and lysine were designed and synthesized. A hairpin-prone intervening sequence was designed to increase the possibility of interactions, and also a sequence with alpha helix conformation was

synthesized as molecular modeling showed a probable interaction between 9-fluorenone-2-boronic acid and the corresponding peptide. D-Glucamine was used as a positive control because of its demonstrated high binding affinity towards boronic acids. The ARS colorimetric assay and other methods were applied to detect complexation between boronic acids towards peptides. Unfortunately, no complex formation was observed between the two species based on the ARS colorimetric assay, UV spectrophotometry, fluorescence spectroscopy, HPLC and mass spectrometric analysis.

2.7 Future work

We investigated the application of a boronic acid receptor that could potentially recognize peptide structures with high selectivity and affinity. Although we synthesized four different small boronic acid derivatives, other modifications could be tested in the future. A boronic acid sensor could be designed in a way to turn into an instantaneous indication if fluorescently active molecule binds to the peptide *in vivo*. Other methods of modification could involve designing a ketone part of the molecule with increased reactivity such as difluoromethyl ketone, which would form a more stable imine. Also, a more rigid library of boronic acid molecules could be synthesized, where the position of the ketone varies in distance to the boronic acid. Also, a peptide library technique can be applied to rapidly synthesize hundreds of peptides to find if a boronic acid substrate can attach to a peptide with high affinity.

2.8 Experimental

2.8.1 General information

All reagents used for the synthesis of boronic acids were purchased from Sigma-Aldrich or Combi-Blocks and used without further purification. Unless otherwise stated, all reactions were performed under a nitrogen atmosphere using flame-dried glassware. THF and toluene were obtained from a MBraun MB SPS solvent system prior to use. Anhydrous 1,4-dioxane was purchased from Sigma-Aldrich, 99.8%, and it was deoxygenated with dry nitrogen for one hour before use. All peptides were synthesized

manually using Fmoc-protected amino acids and Rink Amide resin from Novabiochem. Thin layer chromatography (TLC) was performed on Merck Silica Gel 60 F254 plates and was visualized with UV light and KMnO_4 stain. NMR spectra were recorded on Varian INOVA-400 or INOVA-500 MHz instruments. The residual solvent protons (^1H) or the solvent carbons (^{13}C) were used as internal standards. ^1H NMR data is presented as follows: chemical shift in ppm (δ) downfield from tetramethylsilane (multiplicity, coupling constant, integration). The following abbreviations are used in reporting NMR data: s, singlet; br s, broad singlet; d, doublet; t, triplet; dd, doublet of doublets; m, multiplet. High-resolution mass spectra were recorded by the University of Alberta mass spectrometry services laboratory using either electron impact (EI) or electrospray ionization (ESI) techniques. Infrared spectra were obtained on a Nicolet Magna-IR instrument with frequencies expressed in cm^{-1} , with the range of wavenumber $650\text{--}4000\text{ cm}^{-1}$ in microscope-FTIR, by using crystalized samples or dissolving in dichloromethane. Peptide analysis and purification were determined using Agilent 1100 HPLC-MS (UV-Vis fluorescence detector). Peptides with molecular weight more than 1000 were acquired with an AB Sciex Voyager Elite MALDI. A Hewlett Packard 8453 UV-Vis spectrophotometer was used for all absorption studies. A Photon Technology International (PTI) MP1 fluorescence system was used for all fluorescence studies.

2.8.2 General procedure for the preparation of aryl boronic acids using the Miyaura reaction⁴

To a suspension of bromobenzophenone (3.0 mmol), KOAc (3.0 mmol) and B_2pin_2 (3.2 mmol) in 1,4-dioxane (10 mL) at room temperature was added PdCl_2dppf (0.05 mmol). The reaction mixture was stirred at $80\text{ }^\circ\text{C}$ for 12 hours, then allowed to cooled down. Then the reaction mixture was filtered through Celite and the solvent was evaporated under reduced pressure. The residue was purified by silica gel column chromatography to give benzoylphenylboronic pinacol ester in pure form. Then, to the solution of benzoylphenyl boronic pinacol ester (2.2 mmol) in diethyl ether (100 mL) was added a 2-propanol solution (20 mL) of diethanolamine (5.5 mmol). The solution was stirred for 3 h at room temperature. A precipitate was separated by filtration, washed with diethyl ether

and dried *in vacuo*. Then, the suspension of the colourless powder in 1 N HCl (100 mL) was stirred for 3 h at room temperature. The precipitate was then separated by filtration, washed with water and dried *in vacuo* to provide the boronic acid without further purification.

2.8.3 Synthesis of 2-benzoylphenyl boronic acid (BA1)

Application of the general procedure to 2-bromobenzophenone (BA1) in Figure 2-2, (784 mg, 3.00 mmol), KOAc (294 mg, 3.00 mmol), B₂pin₂ (915 mg, 3.20 mmol) and PdCl₂dppf (40 mg, 0.05 mmol) in 1,4-dioxane (10 mL) afforded 2-benzoylphenyl boronate ester, which was purified by silica gel column chromatography (hexane/EtOAc = 8:2). Then 2-benzoylphenyl boronate ester was hydrolyzed by using diethanolamine method to form 2-benzoylphenyl boronic acid as an ivory solid (441 mg, 65%).

¹H NMR (500 MHz, CD₃OD) δ 7.4-7.5 (m, 2H), 7.58 (m, 1H), 7.64-7.89 (m, 6H)

¹³C NMR (125 MHz, DMSO-*d*₆) δ 197.5, 141.9, 137.3, 132.8, 132.4, 130.3, 129.7, 128.6, 128.3, 127.8 (The boron-bound carbon was not detected due to quadrupolar relaxation)

¹¹B NMR (128 MHz, CD₃OD) 28.4

IR (Microscope, cm⁻¹) 3057.1, 1668.6, 1596.2, 1449.4

HRMS (EI) for C₁₃H₁₁BO₃: calcd. 226.0801; found 226. 0798

M.P. 196-198 °C

2.8.4 Synthesis of 3-benzoylphenyl boronic acid (BA2)

Application of the general procedure to 3-bromobenzophenone (BA2) in Figure 2-2, (784 mg, 3.00 mmol), KOAc (294 mg 3.00 mmol), B₂pin₂ (915 mg 3.20 mmol) and PdCl₂dppf (40 mg, 0.05 mmol) in 1,4-dioxane (10 mL) afforded 3-benzoylphenyl boronate ester, which was purified by silica gel column chromatography (hexane/EtOAc = 8:2). Then 3-benzoylphenyl boronate ester was hydrolyzed by using diethanolamine method to form 3-benzoylphenyl boronic acid as an ivory solid (576 mg, 85%).

¹H NMR (500 MHz, CDCl₃) δ 7.96 (m, 1H), 7.81 (m, 2H), 7.74 (m, 2H), 7.63 (m, 1H), 7.52 (m, 2H), 7.39 (m, 1 H)

¹³C NMR (125 MHz, DMSO-*d*₆) δ 196.0, 138.1, 137.2, 137.0, 134.0, 132.7, 129.6, 128.8, 128.5, 128.4 (The boron-bound carbon was not detected due to quadrupolar relaxation)

¹¹B NMR (128 MHz, CD₃OD) 29.5

IR (Microscope, cm⁻¹) 3058.63, 1666.6, 1596.5, 1520.4, 1491.2

HRMS (EI) for C₁₃H₁₁BO₃: calcd. 226.0801; found 226.0795

M.P. 200-202 °C

2.8.5 Synthesis of 4-benzoylphenyl boronic acid (BA3)

Application of the general procedure to 4-bromobenzophenone in Figure 2-2, (BA3) (784 mg, 3.00 mmol), KOAc (294 mg 3.00 mmol), B₂pin₂ (915 mg 3.20 mmol) and PdCl₂dppf (40 mg, 0.05 mmol) in 1,4-dioxane (10 mL) afforded 4-benzoylphenyl boronate ester, which was purified by silica gel column chromatography (hexane/EtOAc = 8:2). Then 4-benzoylphenyl boronate ester was hydrolyzed by using diethanolamine method to form 4-benzoylphenyl boronic acid as a white solid (542 mg, 80%).

¹H NMR (500 MHz, DMSO-*d*₆) δ 8.29 (br s, 2H), 7.88 (m, 2H), 7.65 (m, 5H); 7.48 (m, 2H)

¹³C NMR (100 MHz, DMSO-*d*₆) δ 197.5, 141.9, 137.3, 132.8, 132.4, 130.3, 129.7, 128.6, 128.3, 127.8 (The boron-bound carbon was not detected due to quadrupolar relaxation)

¹¹B NMR (128 MHz, CDCl₃) 27.27

IR (Microscope, cm⁻¹) 3438.7, 1657.4, 1598.5, 1503.8, 1447.1, 1401.3

HRMS (EI) for C₁₃H₁₁BO₃: calcd. 226.0801; found 226.0801

M.P. 204-206 °C

2.8.6 Synthesis of 2-bromo-9-fluorenone

Into a 100 mL flask in open air, charged 2-bromofluorene (1.25 g, 5.00 mmol), KOH (0.280 g, 5.00 mmol) and THF (5 mL) stirred at room temperature. The reaction mixture

was filtered to remove KOH and the filtrate was concentrated to obtain the crude product. The crude product was washed with water, dried over anhydrous sodium sulfate filtered and evaporated. Then, it was purified by recrystallization from ethanol to afford 2-bromo-9-fluorenone as a yellow solid (1.264 g, 95%).

¹H NMR (400 MHz, CDCl₃) δ 7.78 (s, 1H), 7.68 (m, 1H), 7.62 (dd, *J* = 7.8, 1.8 Hz, 1H), 7.51-7.54 (m, 2H), 7.4 (d, *J* = 7.8, 1H), 7.33 (m, 1H)

¹³C NMR (100 MHz, DMSO-*d*₆) δ 197.4, 143.6, 143.0, 137.1, 135.8, 135.0, 133.7, 129.4, 127.6, 124.6, 122.9, 121.7, 120.4

IR (Microscope, cm⁻¹) 2988, 2935, 1667, 1638, 1527, 1500

HRMS (EI) for C₁₃H₇BrO: calcd. 259.9660; found 259.9660

M.P. 146–148 °C

2.8.7 Synthesis of 9-fluorenone-2-boronic acid (BA4)

Application of the general procedure to 2-bromo-9-fluorenone in Figure 2-2, (BA4) (672 mg, 3.00 mmol), KOAc (294 mg 3.00 mmol), B₂pin₂ (915 mg 3.20 mmol) and PdCl₂dppf (40 mg, 0.05 mmol) in 1,4-dioxane (10 mL) afforded 9-fluorenone-2-boronic acid, which was purified by silica gel column chromatography (hexane/EtOAc = 8:2). Then 9-fluorenone-2-boronate ester was hydrolyzed by using diethanolamine method to form 2-benzoylphenyl boronic acid as a yellow solid (504 mg, 75% yield).

¹H NMR (500 MHz, CD₃OD) δ 7.96 (br s, 1H), 7.84 (br s, 1H), 7.58-7.68 (m, 3H), 7.54 (m, 1H), 7.32 (m, 1H)

¹³C NMR (125 MHz, DMSO-*d*₆) δ 193.4, 145.4, 143.7, 141.4, 135.2, 133.6, 132.4, 129.6, 129.2, 123.8, 121.3, 120.2 (The boron-bound carbon was not detected due to quadrupolar relaxation)

¹¹B NMR (128 MHz, CD₃OD) 28.6

IR (Microscope, cm⁻¹) 3344, 1701, 1613, 1638, 1601, 1576

HRMS (EI) for C₁₃H₉BO₃: calcd. 224.0645; found 224.0640

M.P. 290 °C decomposed

2.8.8 Peptides 1-10: Synthesis and characterization

Standard Fmoc-SPPS was performed manually in a 25 mL polypropylene tubes equipped with a frit, solid phase synthesis reaction vessel (Figure 2-18). Rink amide resin on 0.69 mmol scale (0.69 mmol/g loading) was used to provide peptides **1-11**. Following the resin was swelled in DCM (10 mL, 0.5 h) and treatment with 10 mL of 25% piperidine-DMF for 20 min to remove the Fmoc protecting group and to activate the resin. After this step had completed, the resin beads were rinsed thoroughly twice in the sequence of methanol, dichloromethane, DMF to flush out left over reagents and by-products. Next, to the activated resin, the Fmoc-amino acid (2.76 mmol, 4.0 eq), the two coupling reagents, HBTU (2.69 mmol, 3.9 eq) and DIPEA (5.5 mmol, 8.0 eq), were added into the reaction vessel and dissolved in 10 mL DMF to start the first coupling reaction. The deprotection-washing-coupling-washing cycle was repeated several times until the desired peptide chain was synthesized. The acetylation reaction was performed before the final cleavage; a 12 ml solution of acetic anhydride/pyridine/DMF (2:4:6) was transferred to the peptidyl resin and was reacted at room temperature (2×60 min). The resin was drained, washed with DMF (12×1 min), isopropanol (6×1 min), and hexane (6×1 min), and dried *in vacuo* for 2 h.

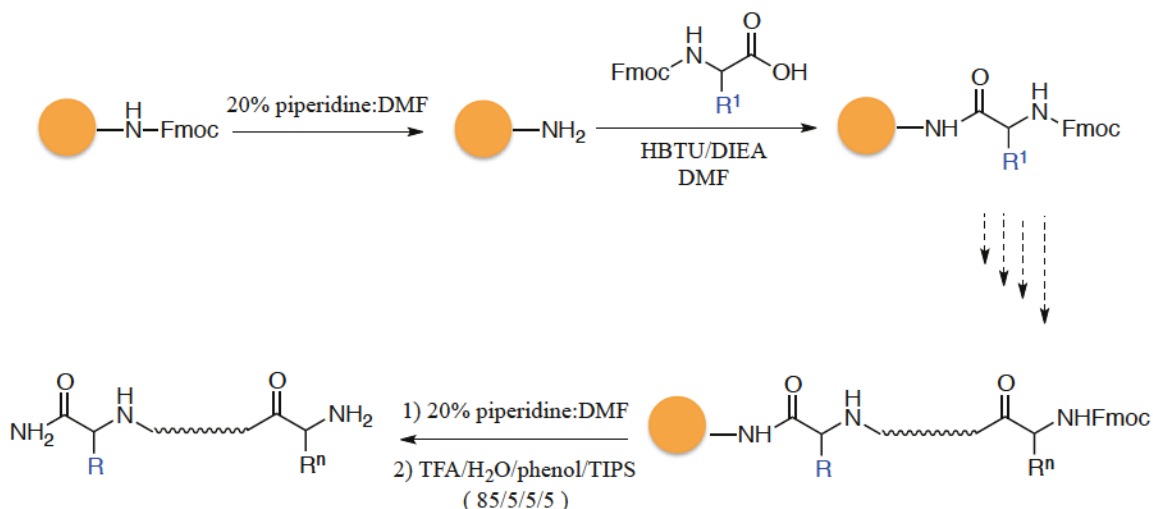


Figure 2-18: General strategy for SPPS on Rink Amide resin

2.8.9 Resin cleavage with TFA

The dried resin was treated with TFA/H₂O/phenol/TIPS (10 mL, 85/5/5/5 (v/v/v/v)) for 2 h to cleave the peptide. The cleavage mixture was filtered from the resin, and precipitated in ice-cold diethyl ether for 20 min. The precipitate was next centrifuged (2000 g, 5 min) at 4 °C, washed three times with cold diethyl ether, dried under vacuum. The aqueous layer was flash-frozen and dried in a lyophilizer and analyzed using analytical HPLC and MALDI-TOF to assess purity and verify identity. Peptides **1-7** with 85-95% purity used for colorimetric assay without further purification. The peptides **8-11** were purified by reverse-phase HPLC. Molecular formulas, calculated masses, and measured (m/z) ratios of polypeptides as determined by HPLC (80-90% purity) and MALDI (positive mode) is presented in Table 2-1 and Appendix 2.

2.9 References

- (1) Halo, T. L., Appelbaum, J., Hobert, E. M., Balkin, D. M., and Schepartz, A. (2009) Selective recognition of protein tetraserine motifs with a cell-permeable, pro-fluorescent bis-boronic acid. *J. Am. Chem. Soc.* *131*, 438–439.
- (2) Cal, P. M. S. D., Vicente, J. B., Pires, E., Coelho, A. V., Veiros, L. F., Cordeiro, C., and Gois, P. M. P. (2012) Iminoboronates: a new strategy for reversible protein modification. *J. Am. Chem. Soc.* *134*, 10299–10305.
- (3) Cal, P. M. S. D., Frade, R. F. M., Chudasama, V., Cordeiro, C., Caddick, S., and Gois, P. M. P. (2014) Targeting cancer cells with folic acid–iminoboronate fluorescent conjugates. *Chem. Commun.* *50*, 5261–5263.
- (4) Zheng, H., Lejkowski, M., and Hall, G. D. (2011) Mild and selective boronic acid catalyzed 1,3-transposition of allylic alcohols and Meyer-Schuster rearrangement of propargylic alcohols. *Chem. Sci.* *2*, 1305-1310.
- (5) Wada, T., Muckerman, T. J., Fujitab, E., Tanaka, K. (2011) Substituents dependent capability of bis (ruthenium-dioxolene-terpyridine) complexes toward water oxidation. *Dalton Trans.* *40*, 2225-2233.

-
- (6) Adeogun, A. I., Odozi, N. W., Obiegbedi N. O., and Bello O. S. (2008) Solvents effect on $n \rightarrow \pi^*$ and $\pi \rightarrow \pi^*$ transition of 9-fluorenone. *Afr. J. Biotechnol.* 7, 2736-2738.
- (7) Cleavage, deprotection, and isolation of peptides after Fmoc synthesis. *Applied Biosystems*.
- (8) Cochran, A. G., Skelton, N. J., and Starovasnik, M. A. (2001) Tryptophan zippers: stable, monomeric β -hairpins. *Proc. Nat. Acad. Sci.* 98, 5578–5583.
- (9) Cheng, Z., Campbell, E. R. (2009) An engineered tryptophan zipper type peptide as a molecular recognition scaffold. *J. Pept. Sci.* 15, 523–532.
- (10) Dewar, J. S. M., Zoebisch, G. E., Healy, F. E., and Stewart, J. P. J. (1985) Development and use of quantum mechanical molecular models. 76. AM1: a new general purpose quantum mechanical molecular model. *J. Am. Chem. Soc.* 107, 3902–3909.
- (11) Suenaga, M. (2005) Facio: new computational chemistry environment for PC GAMESS. *J. Comput. Chem. Jpn.* 4, 25-32.
- (12) Schmidt, W. M., Baldridge, K. K., Boatz, A. J., Elbert, T. S., Gordon, S. M., Jensen, H. J., Koseki, S., Matsunaga, N., Nguyen, A. H., Su, S., Windus, L. T., Dupuis, M., and Montgomery A. J. (1993) General atomic and molecular electronic structure system. *J. Comput. Chem.* 14, 1347-1363.
- (13) Springsteen, G., and Wang, B. (2002) A detailed examination of boronic acid–diol complexation. *Tetrahedron.* 58, 5291–5300.

Chapter 3

Design and Synthesis of Boronic Acids Containing Michael Acceptor Units for Selective Labeling of Proteins

3.1 Introduction

Chemical modification of proteins is a rapidly developing area in chemical biology. Selective installation of biochemical probes has led to a better understanding of natural protein modification and function.¹ A unique chemical reaction is required to selectively modify the protein of choice. Selective modification is much more likely to be successful for expressed proteins, involving site-directed mutagenesis. One of the most common ways to achieve site-selective protein modification is to alkylate newly introduced cysteine residues.² This reactivity is in part due to the high nucleophilicity of the thiolate anion, as cysteine partially exists in the deprotonated thiolate form. The relatively low natural abundance of cysteine makes the introduction of a single cysteine *via* site-directed mutagenesis and subsequent chemical modification a very effective method to access modified proteins.² The unique reactivity of cysteine has been known as the most widely used method for selective chemical tagging of proteins. The development of new applications and reactions involving cysteine has brought it to widespread use in selective protein modification. Reaction of the sulfhydryl group in cysteine has been performed with a variety of electrophiles such as haloacetyl groups, maleimides, disulfides, sulfamidate, α,β -unsaturated esters, iodoacetamides, vinyl sulfones, and acrylamides, as they can be linked to new functionalities through disulfide formation with activated thiol reagents.^{1,3} These reactions can be performed in water at a neutral pH, which supplies a great amount of reactive thiolate species. In some cases, a catalyst is added to the reaction system to promote the reaction as an example in some Michael additions.⁴ Moreover, excellent selectivity can be reached in thiol-based ligations since thiolates are better nucleophiles than amines, which exist mainly in the protonated ammonium salt form at

neutral pH. Formation of thioether and disulfide bonds, however, are not completely bioorthogonal chemoselective ligation reactions, since many free thiol groups e.g, glutathione are present in biological systems and generally can only be used when competing sulfhydryl groups are not present.³ The work that will be described in this chapter aims to promote non-catalytic site-specific Michael additions in an aqueous environment. Small boronic acid molecules containing a Michael acceptor were designed, in which the boronic acid region was used to increase site-specificity towards the thiol-Michael addition reactions. Small peptides with serine and cysteine were designed and synthesized with the purpose of boronate ester formation between serine and the boronic acid part of the molecule. Formation of the boronate ester could increase the rate and site specificity of covalent reactions between cysteine and the Michael acceptor part of the probe molecule.

3.2 Design and synthesis of functionalized boronic acids

We began this project by synthesizing boronic acid molecules containing a Michael acceptor unit. We hypothesized that cysteine residue of the designed peptide could be coupled with Michael acceptor unit. Moreover, boronic acid part could incorporate into the reaction by temporary intramolecular interaction as a way to increase the rate of the reaction. So proximity of boronic acid and serine would be a key to design the molecules. For this purpose, we started with the design and synthesis of simple boronic acids (BA5 and BA6), analogues of chalcone (Figure 3-1).

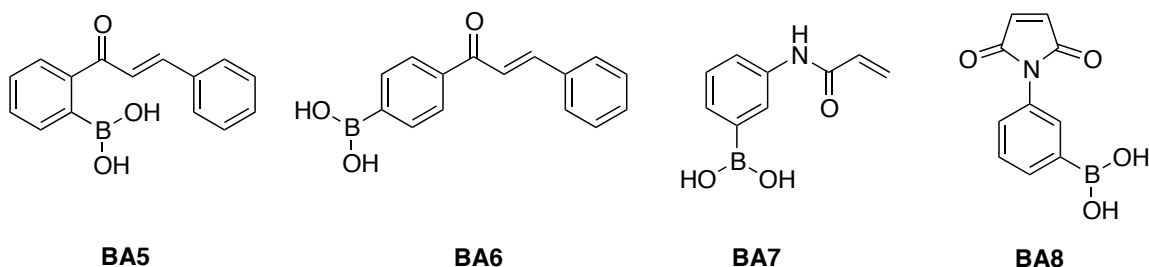
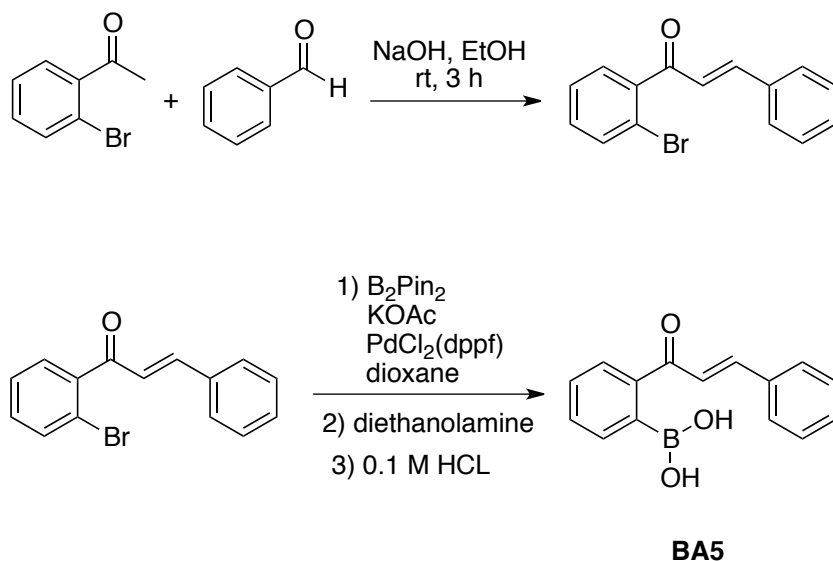


Figure 3-1: Proposed boronic acids functionalized with a Michael acceptor

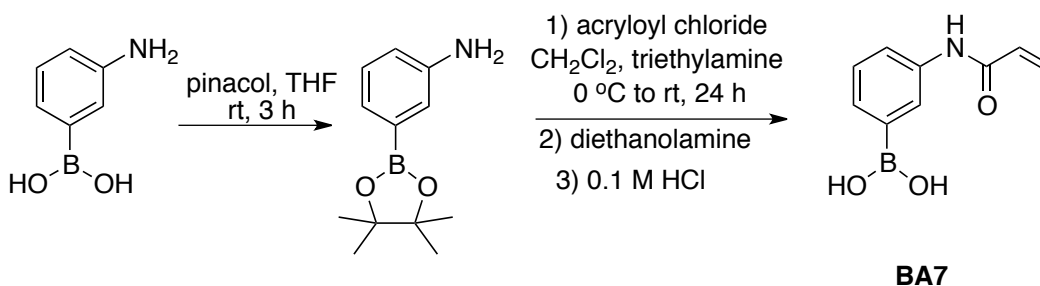
Boronic esters of BA5 and BA6 were obtained by Miyaura borylation reaction on (*E*)-2-bromo chalcone and (*E*)-4-bromo chalcone, which were then hydrolyzed to provide the

corresponding boronic acids. These chalcones were synthesized under base-promoted Claisen–Schmidt condensation from appropriately substituted bromo-acetophenone and the aldehyde (Scheme 3-1).⁵



Scheme 3-1: Preparation of (*E*)-2-boronic acid-chalcone (BA5)

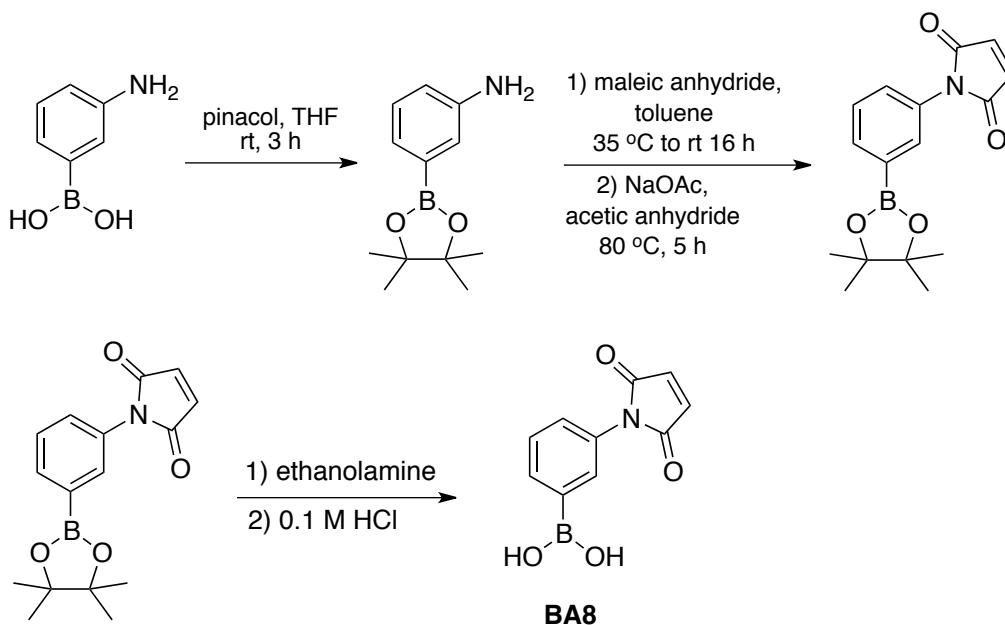
Later, 3-acrylamidophenyl boronic acid (AAPBA) was synthesized, which was previously reported in polymer chemistry as a sugar sensitive probe.⁶ To synthesize AAPBA, 3-aminophenylboronic acid pinacol ester was submitted to an acylation with acryloyl chloride in the presence of triethylamine to provide 3-acrylamidophenylboronic acid pinacol ester, which was then hydrolyzed to provide the desired product (Scheme 3-2).



Scheme 3-2: Synthesis of 3-acrylamidophenylboronic acid (BA7)

Reactivity of the three synthesized boronic acids towards the designed peptides was monitored by using HPLC-MS. Unfortunately, there were no products observed which could be identified as the Michael addition of cysteine to the α,β -unsaturated part of the molecule. We concluded that, in these cases, a catalyst in the form of a base should be added to the reaction system to promote the Michael addition. However, we were hoping to find a Michael addition that does not require any heat or catalyst. The efficient, fast and highly selective Michael addition reaction between maleimide and thiol moieties has been used extensively in biological applications.⁷ The nucleophilic addition of thiols to maleimide does not require any heat or catalyst, and simple stirring of the two reactants at room temperature is often sufficient to achieve complete conversion. Some examples of the use of the maleimide-thiol Michael addition include protein crosslinking,⁸ disulfide bridge replacement,³ surface functionalization⁹ and fluorescent labeling of peptides and proteins.¹⁰ To attain our objective we attempted bioconjugation using cysteine-specific maleimide chemistry, which can be achieved at room temperature and neutral pH, and proceed to completion within a few hours. Thus, we synthesized 3-maleimidophenylboronic acid (**BA8**) as shown in Figure 3-1. First, 3-aminophenylboronic acid pinacol ester was prepared and reacted with maleic anhydride in toluene, and the precipitate was filtrated and dried in vacuum and then reacted with sodium acetate in the presence of acetic anhydride. After preparing 3-maleimidophenylboronic ester, it was hydrolyzed to provide the desired boronic acid (Scheme 3-3).

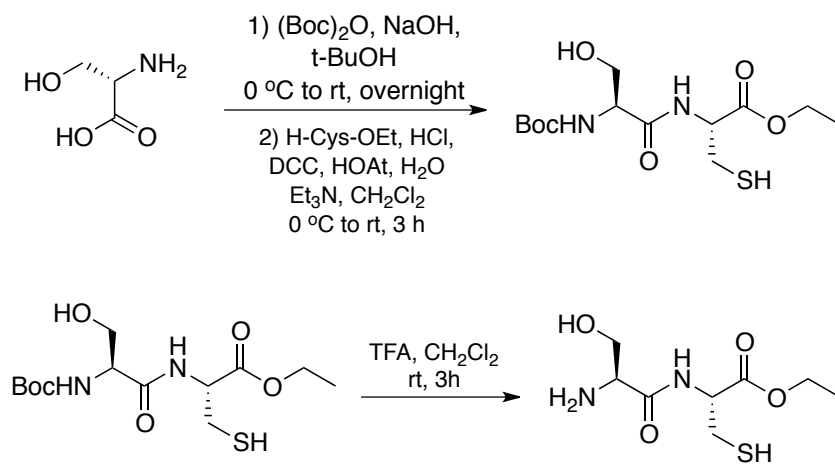
Reaction of 3-maleimidophenylboronic acid with the designed peptide containing serine and cysteine was tested and monitored by using ¹H NMR. Analysis has shown the desired product after five minutes of reaction time. In addition, HPLC-MS confirmed the formation of desired product. With these positive results, we moved on to examine the effect of the boronic acid functionality in the molecule as a method to increase the rate of the reaction for the purpose of increasing selectivity. To address this objective, we used ¹H NMR spectroscopy for kinetic studies, which will be further discussed in Section 3.4.



Scheme 3-3: Preparation of 3-maleimidophenylboronic acid (BA8)

3.3 Design of peptide array

To create the peptide array, we started with the synthesis of peptides **1** and **2**, which included cysteine and serine residues (Figure 3-2). Then, boronic acid reactivity was tested against these two peptides. Peptide **1** was synthesized by manual solid phase peptide synthesis (SPPS) and peptide **2** was synthesized by coupling Boc-L-serine and H-Cys-OEt in the presence of coupling agent DCC/HOAt. Then the Boc protection product was removed by using TFA to deliver peptide **2** (Scheme 3-4).



Scheme 3-4: Synthesis of peptide 2

Peptides **1** and **2** were allowed to react with the all boronic acids in 30 % CD₃CN: H₂O solution with pH = 7, these reactions were monitored by HPLC-MS and showed that 3-maleimidophenylboronic acid can provide a covalent bond between cysteine of the peptide and the Michael acceptor. After confirmation that only 3-maleimidophenylboronic acid was reactive, we followed our studies by synthesizing more peptides to identify different positions of serine and cysteine that could bind with higher affinity to the boronic acid. We chose peptides **3-5** and synthesized them by using SPPS (Figure 3-2).

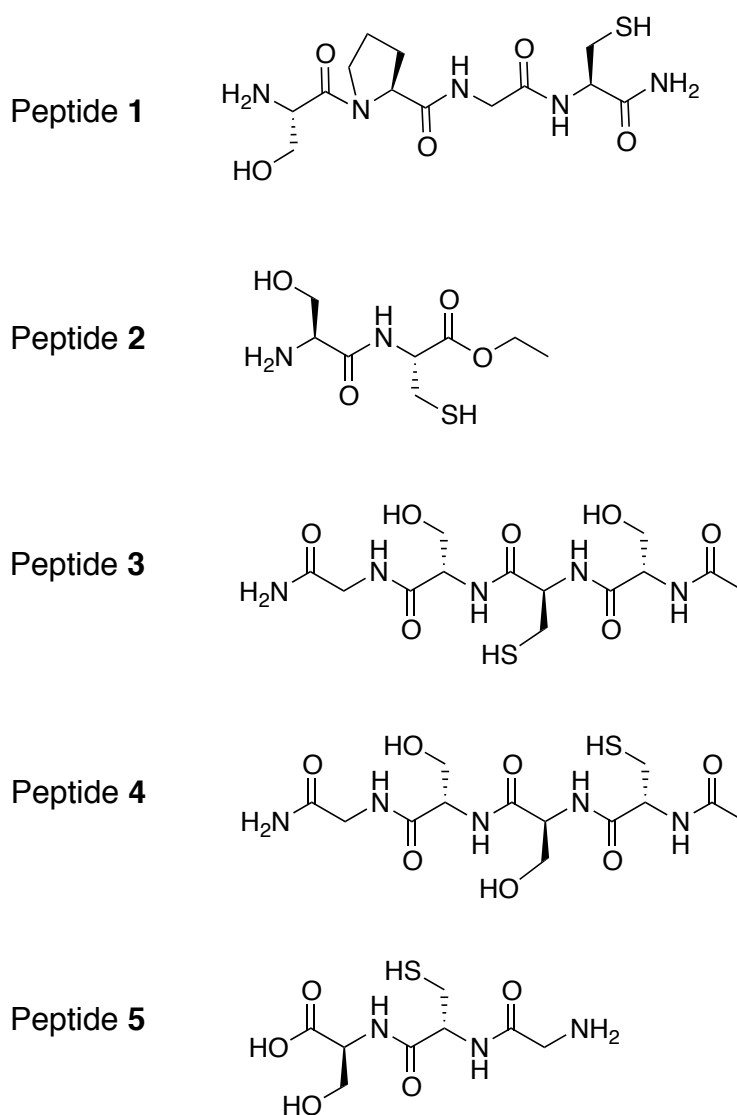


Figure 3-2: Library of peptides 1-5

Reaction kinetic analysis was performed to monitor the addition of these peptides with 3-maleimidophenylboronic acid by ^1H NMR and the data was used to calculate the rate constant. Data showed that reaction of 3-maleimidophenylboronic acid and peptide **2** has a rate constant that is two times higher than the reaction of control maleimide molecule devoid of a boronic acid with peptide **2**, which be discussed below.

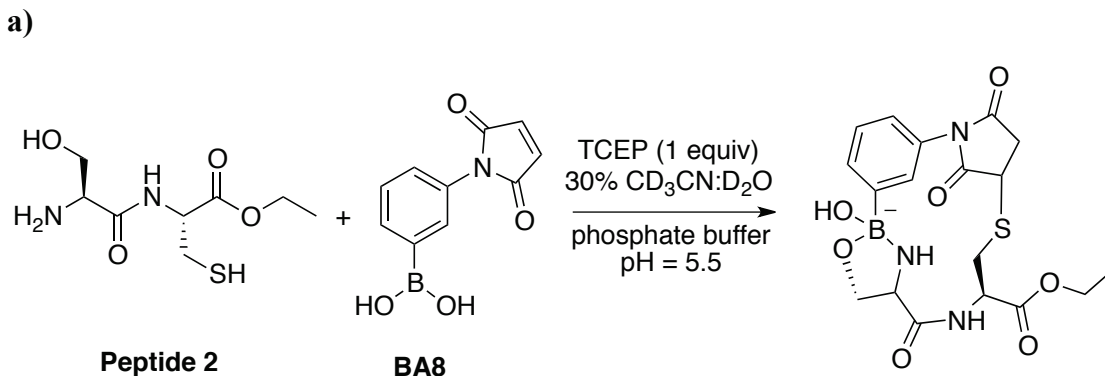
All boronic acids (0.1 mM) were reacted with peptide **2** (0.1 mM) in aqueous solution of 30 % acetonitrile: H_2O and pH was adjusted to 7.4 by ammonium acetate. After incubation overnight, reaction samples were injected into HPLC to observe product formation. Only 3-maleimidophenylboronic acid formed the desired product by covalent attachment of cysteine to the maleimide part of the molecule. As a result, this data showed that boronic acids (BA5, BA6 and BA7) do not demonstrate the expected reactivity based on the Michael addition reaction in aqueous environment without using a catalyst, so we switched to monitoring the reactivity of 3-maleimidophenylboronic acid by ^1H NMR.

3.4 ^1H NMR kinetic analysis

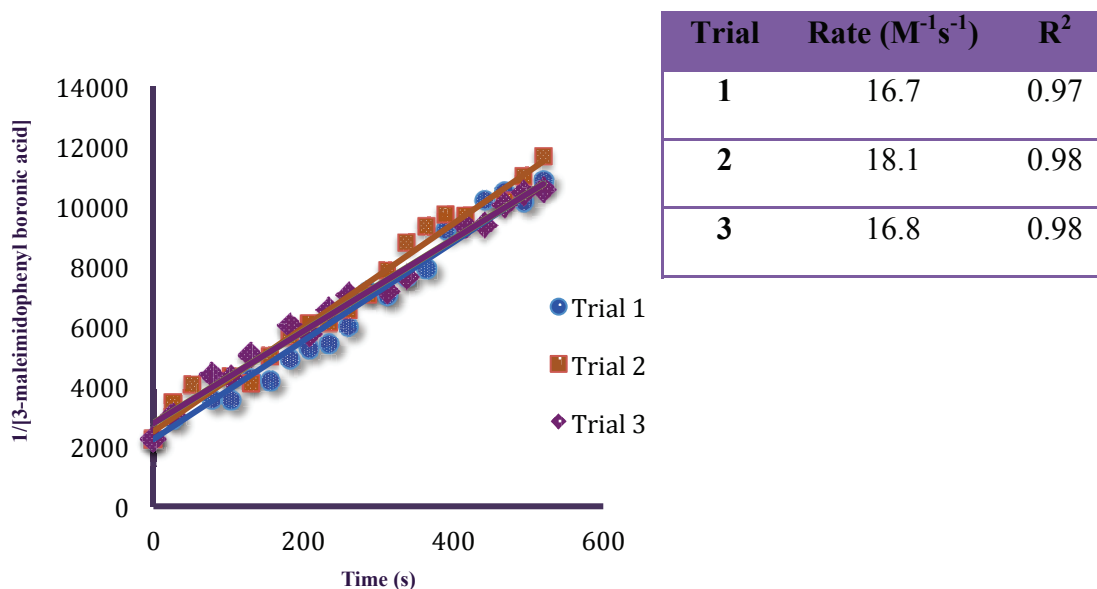
Kinetic data for the reactions between 3-maleimidophenylboronic acid and all peptides were obtained by ^1H NMR at room temperature. As a control, N-phenylmaleimide was synthesized and reacted with all peptides to compare the effect of a boronic acid on the reaction rate. 1,4-Dinitrobenzene was chosen as an internal standard, which in ^1H NMR shows a singlet related to four protons at 8.2 ppm without overlapping the boronic acid proton peaks. The singlet peak at around 7.2 ppm, which is related to two maleimide protons, will be eliminated upon reaction with cysteine. Proton integration corresponding to the internal standard was applied to ensure the correct relative concentrations of each solution. First, we tried to evaluate kinetic experiments by ^1H NMR at pH = 7 (phosphate buffer applied), as the optimal pH for this reaction is between pH 6.8 - 7.5. However, high rate of the both reactions directed us to drop the pH to 5.5, which allowed us to decrease the rate of Michael addition to maleimide. In this way, the reaction solution was scanned once every 46 seconds over 20 minutes to provide ^1H NMR data. Second order

rate constants were calculated by plotting $1/[\text{boronic acid}]$ or $1/[\text{maleimide}]$ as a function of time. The slope of the resulting line is the rate constant. Details of the experiment will be discussed in the experimental section. The reaction rate of 3-maleimidophenylboronic acid with peptide **2** and N-phenylmaleimide with peptide **2** at pH = 5.5 was measured and compared (Figure 3-3 and 3-4). This data showed enhanced reaction rate for 3-maleimidophenylboronic acid, which was two times higher than with N-phenylmaleimide. We concluded that it is most likely related to a temporary intramolecularly effect of the boronic acid with both hydroxyl group of serine and terminal amine. Subsequently, the reactions of 3-maleimidophenylboronic acid with peptides **1**, **3**, **4**, and **5** were tested. After data was plotted for peptide **1**, second order rate constants were calculated and the control molecule, N-phenylmaleimide showed a higher reaction rate compared to 3-maleimidophenylboronic acid (Figures 3-5 and 3-6). The lower rate for 3-maleimidophenylboronic acid is likely linked to distortion of the optimal distance between the boronic acid and Michael acceptor fragment; therefore, interaction of boronic acid with the terminal serine caused a decrease in the Michael addition reaction rate.

In the case of peptide **3**, the rate constant for 3-maleimidophenylboronic acid was slightly higher than N-phenylmaleimide (Figures 3-7 and 3-8), which could be related to interaction of serine to the boronic acid. However, in this case serine interaction with boronic acid is not as effective as the terminal serine probably because of lack of proximity. Peptide **4** showed a response similar to peptide **3**, which has slightly more activity towards 3-maleimidophenylboronic acid (Figures 3-9 and 3-10). This distinction shows that internal serines show less activity in comparison to the terminal serine, as in terminal serine amine group are involved to form five-member ring boronic ester. For peptide **5**, which replaces the N-terminus serine with a C-terminus serine, the same reactivity was observed for both the boronic acid functionalized molecule and the control molecule (Figure 3-11 and 3-12). These results suggest that serines in C-terminus do not interact efficiently with a boronic acid. We concluded that peptide **2** with a N-terminal serine has a higher reaction rate and can be further optimized as a small peptide tag because of its higher selectivity towards 3-maleimidophenylboronic acid.

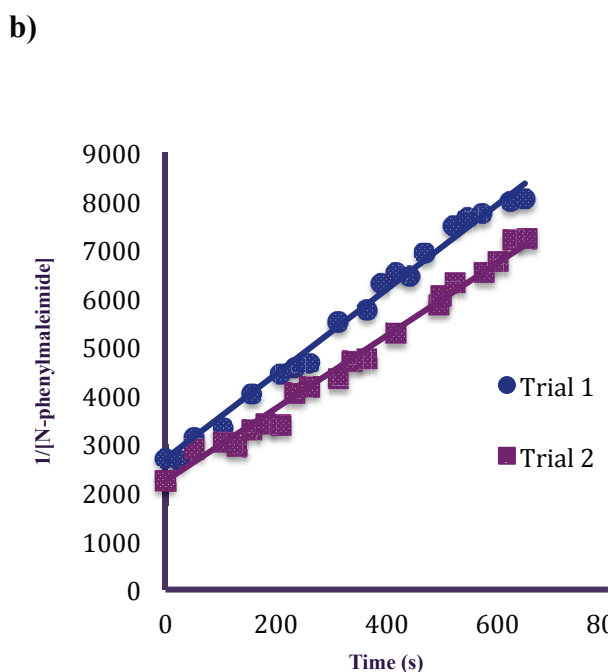
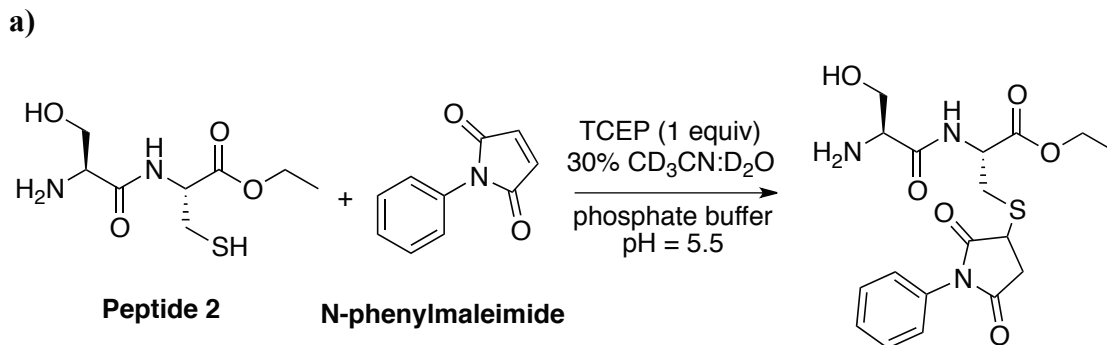


b) c)



Average second order rate constant: $17.2 \pm 0.9 \text{ M}^{-1}\text{s}^{-1}$

Figure 3-3: a) The reaction between 3-maleimidophenylboronic acid and peptide **2** was monitored at $\sim 0.5 \text{ mM}$ concentrations in 30 % $\text{CD}_3\text{CN}:\text{D}_2\text{O}$ by ^1H NMR at room temperature. b) The second-order rate constant was calculated by plotting $1/[\text{3-maleimidophenylboronic acid}]$ as a function of time. The slope of the resulting line is the rate constant. Data is plotted to within 76% and 82% conversion to the product. c) Calculated second-order rate constants for each trial; average $k = 17.2 \pm 0.9 \text{ M}^{-1} \text{ s}^{-1}$

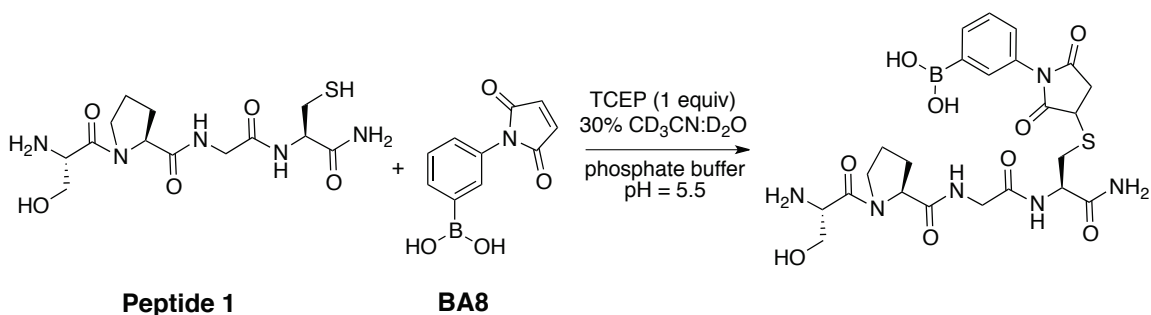


c)

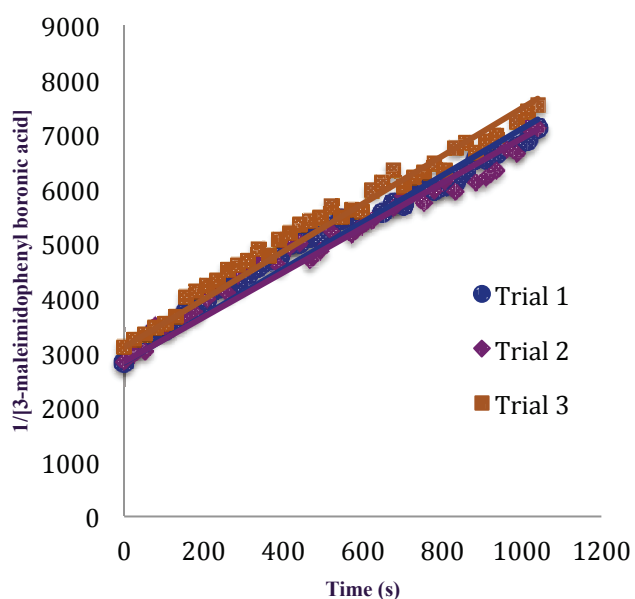
Trial	Rate ($\text{M}^{-1}\text{s}^{-1}$)	R^2
1	8.7	0.99
2	7.5	0.99

Average second order rate constant: $8.1 \pm 0.6 \text{ M}^{-1}\text{s}^{-1}$

Figure 3-4: **a)** The reaction between N-phenylmaleimide and peptide **2** was monitored at $\sim 0.5 \text{ mM}$ concentrations in 30 % $\text{CD}_3\text{CN}:\text{D}_2\text{O}$ by ^1H NMR at room temperature. **b)** The second-order rate constant was calculated by plotting $1/[\text{N-phenylmaleimide}]$ as a function of time. The slope of the resulting line is the rate constant. Data is plotted to within 67% and 71% conversion to the product. **c)** Calculated second-order rate constants for each trial; average $k = 8.1 \pm 0.6 \text{ M}^{-1} \text{ s}^{-1}$



b)

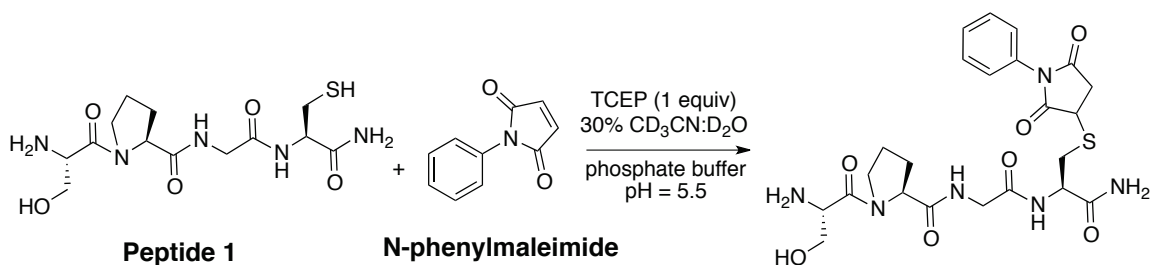


c)

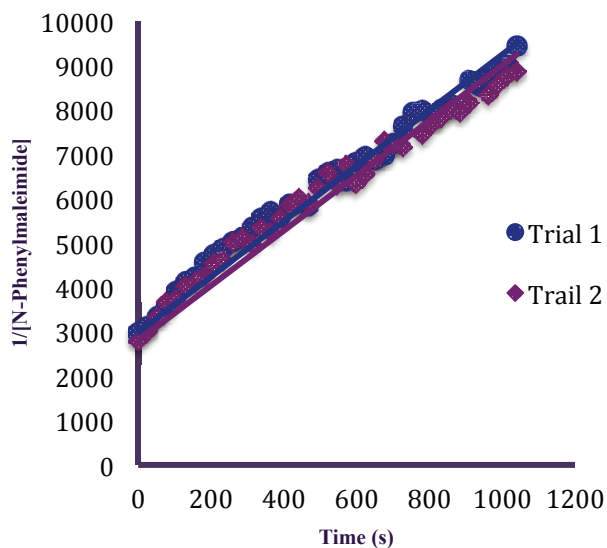
Trial	Rate ($M^{-1}s^{-1}$)	R^2
1	4.3	0.96
2	4.1	0.96
3	4.4	0.98

Average second order rate constant: $4.2 \pm 0.2 M^{-1}s^{-1}$

Figure 3-5: a) The reaction between 3-maleimidophenylboronic acid and peptide **1** was monitored at ~ 0.5 mM concentrations in 30 % $CD_3CN:D_2O$ by 1H NMR at room temperature. b) The second-order rate constant was calculated by plotting $1/[3\text{-maleimidophenylboronic acid}]$ as a function of time. The slope of the resulting line is the rate constant. Data is plotted to within 62% and 67% conversion to the product. c) Calculated second-order rate constants for each trial; average $k = 4.2 \pm 0.2 M^{-1} s^{-1}$



b)

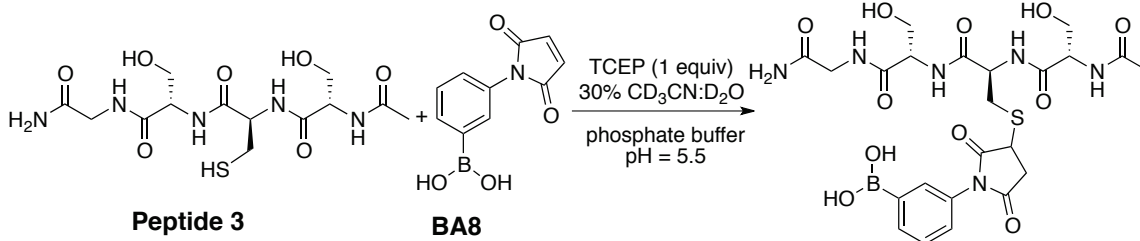


c)

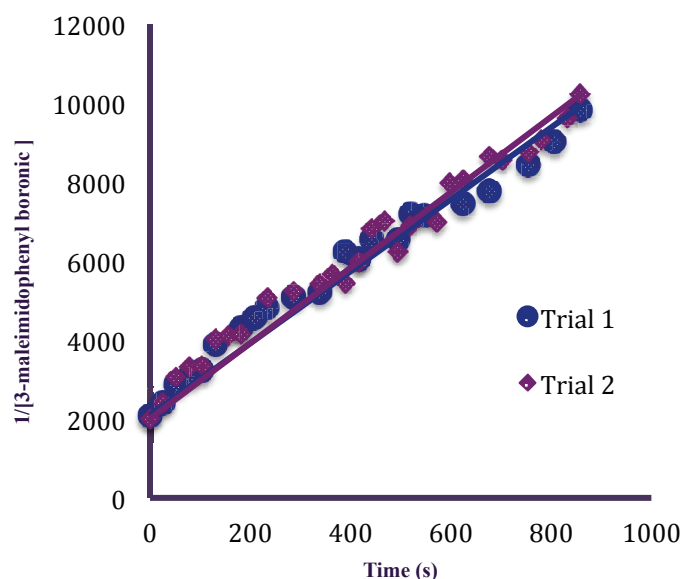
Trial	Rate (M ⁻¹ s ⁻¹)	R ²
1	6.3	0.98
2	6.2	0.96

Average second order rate constant: $6.2 \pm 0.1 \text{ M}^{-1}\text{s}^{-1}$

Figure 3-6: a) The reaction between N-phenylmaleimide and peptide **1** was monitored at $\sim 0.5 \text{ mM}$ concentrations in 30 % CD₃CN: D₂O by ¹H NMR at room temperature. b) The second-order rate constant was calculated by plotting $1/[\text{N-phenylmaleimide}]$ as a function of time. The slope of the resulting line is the rate constant. Data is plotted to within 62% and 67% conversion to the product. c) Calculated second-order rate constants for each trial; average $k = 6.2 \pm 0.1 \text{ M}^{-1} \text{ s}^{-1}$



b)

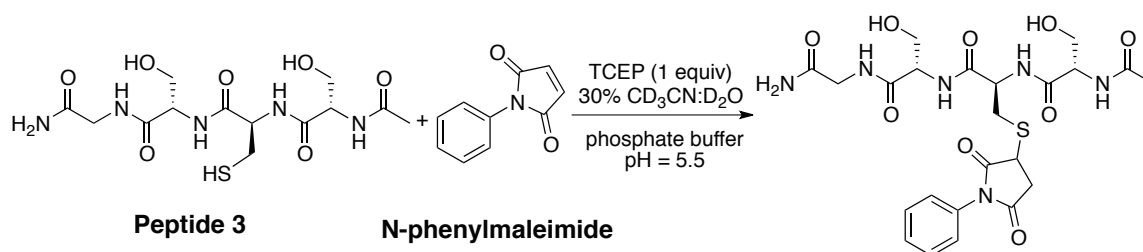


c)

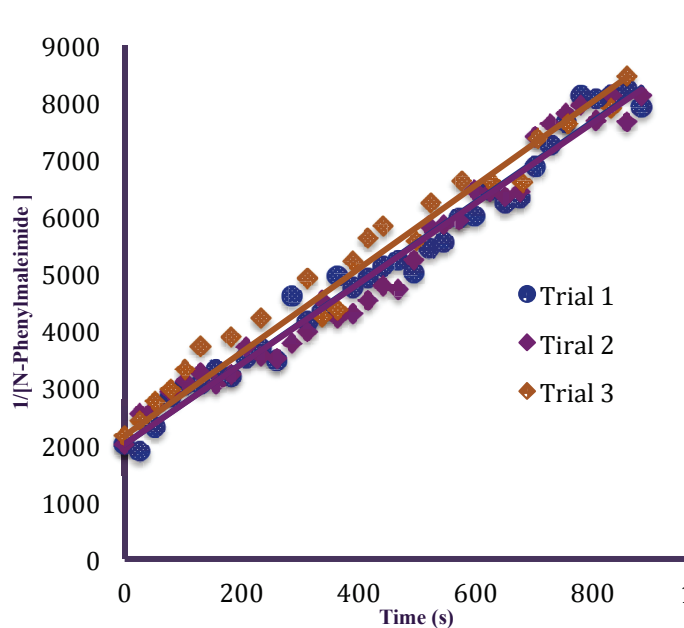
Trial	Rate ($\text{M}^{-1}\text{s}^{-1}$)	R^2
1	9.1	0.97
2	9.6	0.97

Average second order rate constant: $9.4 \pm 0.2 \text{ M}^{-1}\text{s}^{-1}$

Figure 3-7: a) The reaction between 3-maleimidophenylboronic acid and peptide **3** was monitored at $\sim 0.5 \text{ mM}$ concentrations in 30 % $\text{CD}_3\text{CN}:\text{D}_2\text{O}$ by ^1H NMR at room temperature. b) The second-order rate constant was calculated by plotting $1/[\text{3-maleimidophenylboronic acid}]$ as a function of time. The slope of the resulting line is the rate constant. Data is plotted to within 79% and 80% conversion to the product. c) Calculated second-order rate constants for each trial; average $k = 9.4 \pm 0.2 \text{ M}^{-1}\text{s}^{-1}$



b)

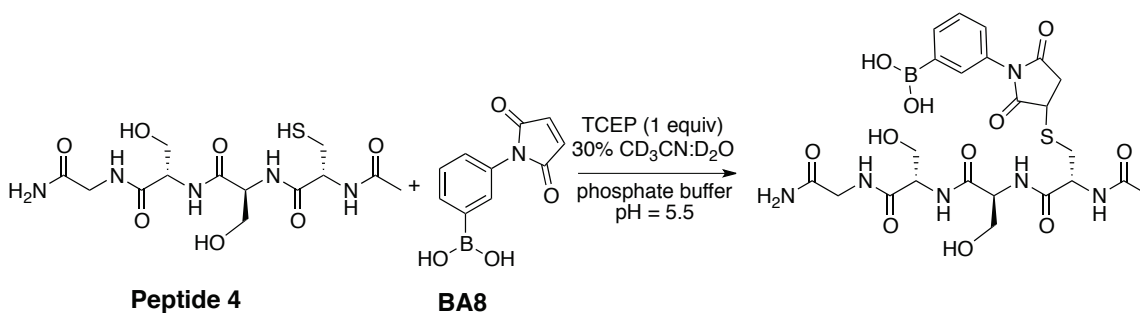


c)

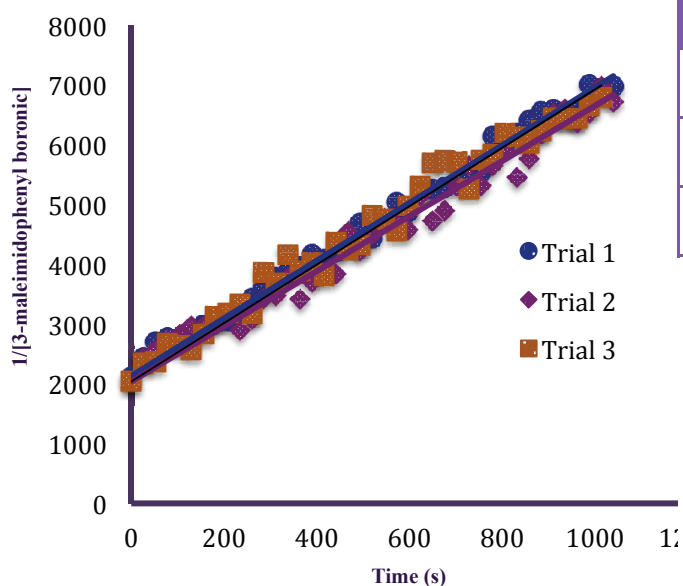
Trial	Rate ($M^{-1}s^{-1}$)	R^2
1	7.1	0.98
2	7.0	0.97
3	7.3	0.97

Average second order rate constant: $7.1 \pm 0.2 M^{-1}s^{-1}$

Figure 3-8: a) The reaction between N-phenylmaleimide and peptide **3** was monitored at ~ 0.5 mM concentrations in 30 % $CD_3CN:D_2O$ by 1H NMR at room temperature. **b)** The second-order rate constant was calculated by plotting $1/[N\text{-phenylmaleimide}]$ as a function of time. The slope of the resulting line is the rate constant. Data is plotted to within 74% and 79% conversion to the product. **c)** Calculated second-order rate constants for each trial; average $k = 7.1 \pm 0.2 M^{-1} s^{-1}$



b)

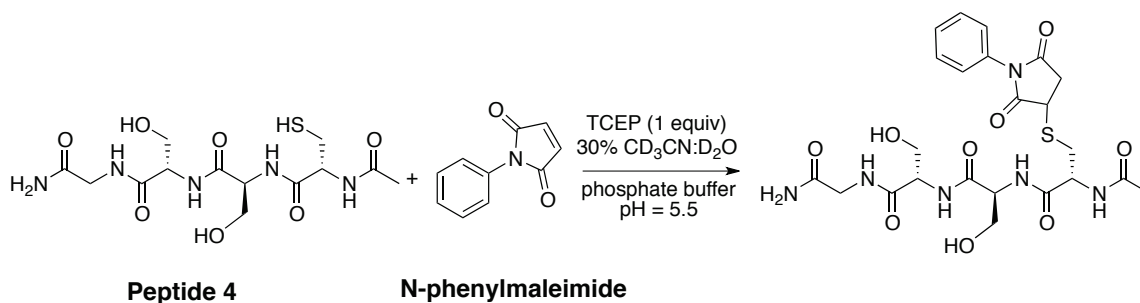


c)

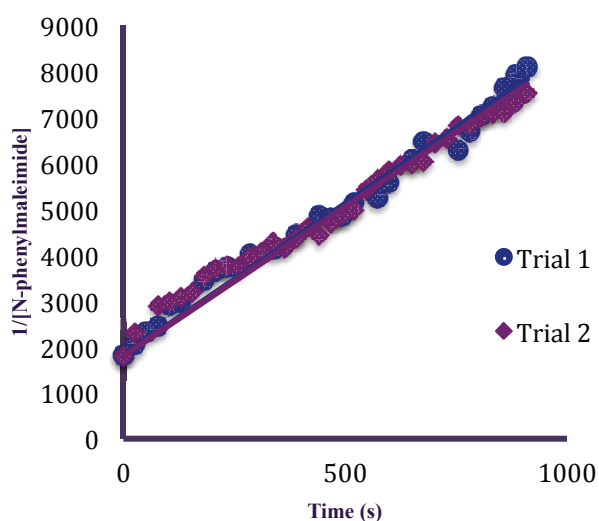
Trial	Rate ($M^{-1}s^{-1}$)	R^2
1	4.8	0.99
2	4.6	0.98
3	4.9	0.98

Average second order rate constant: $4.8 \pm 0.1 M^{-1}s^{-1}$

Figure 3-9: a) The reaction between 3-maleimidophenylboronic acid and peptide **4** was monitored at ~ 0.5 mM concentrations in 30 % $CD_3CN:D_2O$ by 1H NMR at room temperature. b) The second-order rate constant was calculated by plotting $1/[3\text{-maleimidophenylboronic}]$ as a function of time. The slope of the resulting line is the rate constant. Data is plotted to within 70% and 78% conversion to the product. c) Calculated second-order rate constants for each trial; average $k = 4.8 \pm 0.1 M^{-1}s^{-1}$



b)

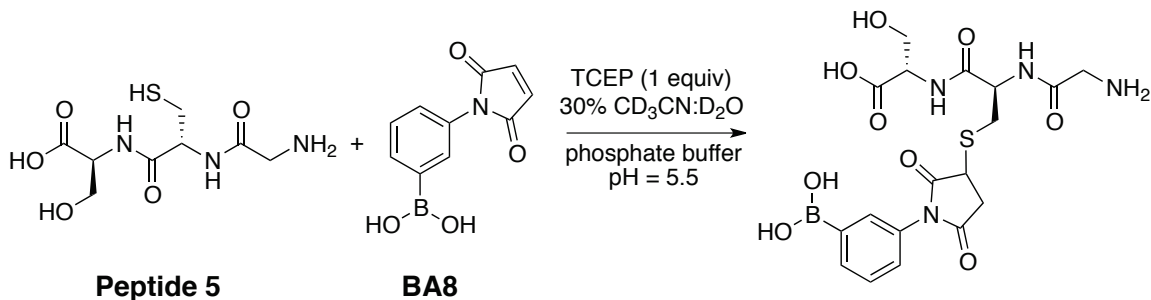


c)

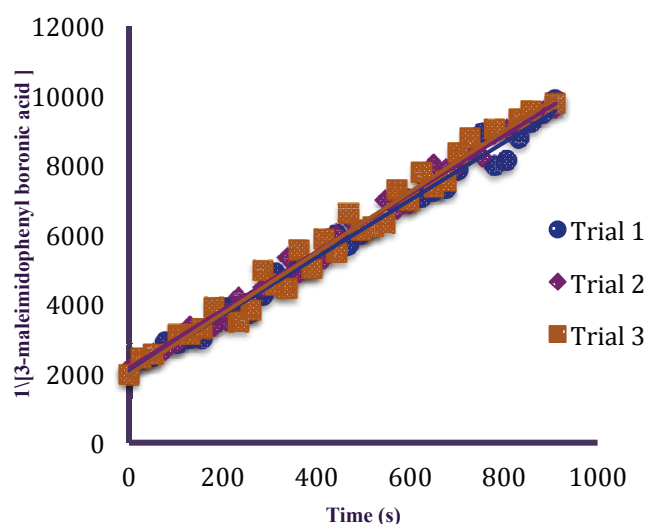
Trial	Rate ($M^{-1}s^{-1}$)	R^2
1	6.6	0.98
2	6.5	0.97

Average second order rate constant: $6.5 \pm 0.1 M^{-1}s^{-1}$

Figure 3-10: a) The reaction between N-phenylmaleimide and peptide **4** was monitored at ~ 0.5 mM concentrations in 30 % $CD_3CN:D_2O$ by 1H NMR at room temperature. b) The second-order rate constant was calculated by plotting $1/[N\text{-phenylmaleimide}]$ as a function of time. The slope of the resulting line is the rate constant. Data is plotted to within 76% and 81% conversion to the product. c) Calculated second-order rate constants for each trial; average $k = 6.5 \pm 0.1 M^{-1}s^{-1}$



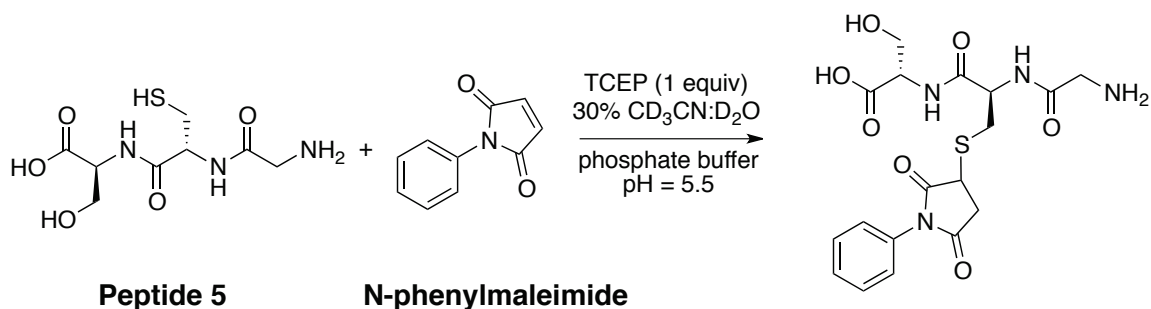
b)



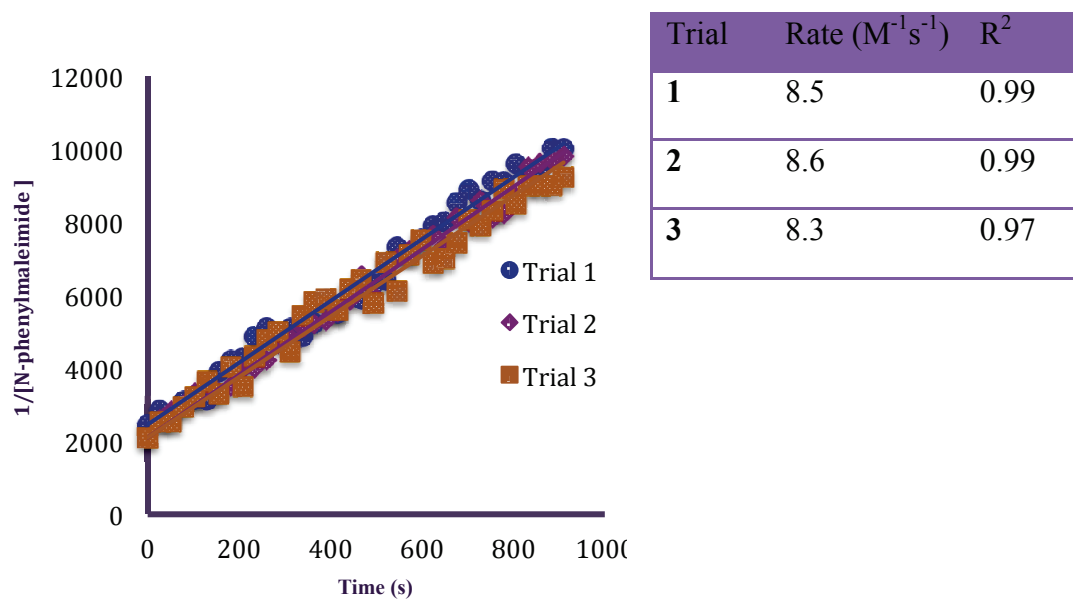
Trial	Rate (M ⁻¹ s ⁻¹)	R ²
1	8.3	0.99
2	8.4	0.99
3	8.8	0.97

Average second order rate constant: $8.5 \pm 0.3 \text{ M}^{-1}\text{s}^{-1}$

Figure 3-11: a) The reaction between 3-maleimidophenylboronic acid and peptide **5** was monitored at $\sim 0.5 \text{ mM}$ concentrations in 30 % CD₃CN: D₂O by ¹H NMR at room temperature. b) The second-order rate constant was calculated by plotting $1/[3\text{-maleimidophenylboronic acid}]$ as a function of time. The slope of the resulting line is the rate constant. Data is plotted to within 76% and 81% conversion to the product. c) Calculated second-order rate constants for each trial; average $k = 8.5 \pm 0.3 \text{ M}^{-1} \text{ s}^{-1}$



b)



c)

Average second order rate constant: $8.5 \pm 0.1 \text{ M}^{-1}\text{s}^{-1}$

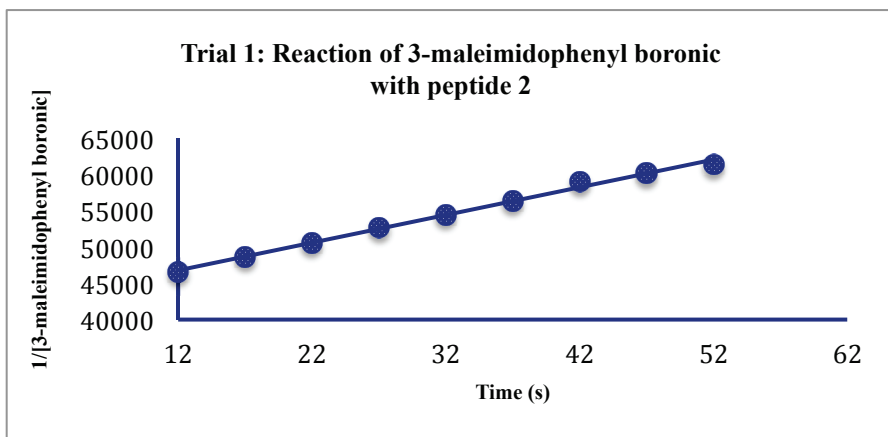
Figure 3-12: a) The reaction between N-phenylmaleimide and peptide **5** was monitored at $\sim 0.5 \text{ mM}$ concentrations in 30 % CD₃CN: D₂O by ¹H NMR at room temperature. b) The second-order rate constant was calculated by plotting $1/[\text{N-phenylmaleimide}]$ as a function of time. The slope of the resulting line is the rate constant. Data is plotted to within 76% and 81% conversion to the product. c) Calculated second-order rate constants for each trial; average $k = 8.5 \pm 0.1 \text{ M}^{-1}\text{s}^{-1}$

3.5 Kinetic study by HPLC-MS

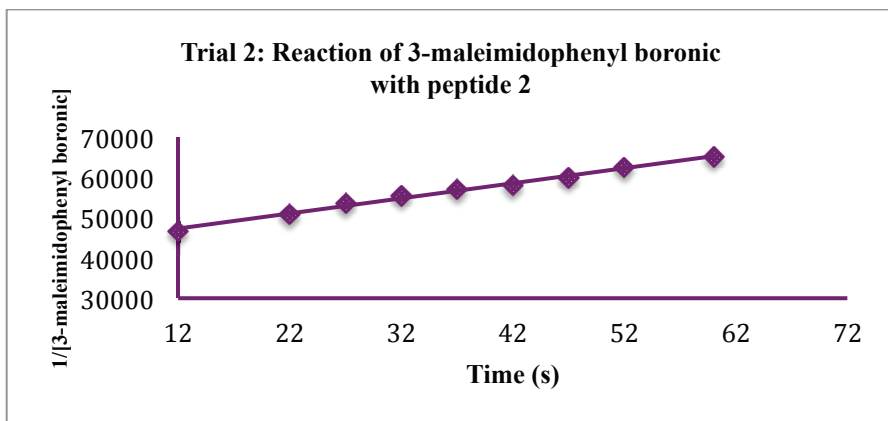
The kinetic study by ^1H NMR provided the first data pointing after 46 second so we were not able to obtain an accurate initial rate constant. To circumvent this issue, we decreased the concentration of solutions twenty times to be able to slow down the reaction and calculate the initial rate constant using HPLC-MS. This way, we were able to monitor the first sixty seconds of the reactions at room temperature. 3-Maleimidophenylboronic acid reacted with peptide **2** following second order kinetics with $k = 353.4 \pm 2.8 \text{ M}^{-1}\text{s}^{-1}$, and reaction of N-phenylmaleimide as a control molecule with the peptide **2** showed a second order kinetics with $k = 240.1 \pm 15.7 \text{ M}^{-1}\text{s}^{-1}$. The kinetics of reaction of 3-maleimidophenylboronic acid with peptide **2** was around one and half times faster than of N phenylmaleimide with peptide **2**. This result confirmed the ^1H NMR study and showed that the initial rate of 3-maleimidophenylboronic acid is higher than the control molecule. The kinetic study was performed in 30% acetonitrile: ammonium acetate buffer as a solvent to solubilize organic compounds and the pH was adjusted to 5.5 to decrease the reactivity.

For kinetic study, the reaction mixture was quenched with 5% TFA every five second started from 12 seconds and analyzed by HPLC-MS. Peak integration corresponding to the internal standard was applied to ensure the correct relative concentrations of each solution. Areas under the peaks of 3-maleimidophenylboronic acid or N-phenylmaleimide were normalized according to the area of peak of the internal standard. The second order rate constant for the reaction was determined in duplicate by plotting the $1/[\text{3-maleimidophenylboronic acid}]$ or $1/[\text{N-phenylmaleimide}]$ versus time and analyzing by linear regression. Details of the experiment will be discussed in the experimental section (Figures 3-13 and 3-14). Details of the experiment will be discussed in the experimental section.

a) $k = 356.2 \text{ M}^{-1}\text{s}^{-1}$, $R^2 = 0.99$



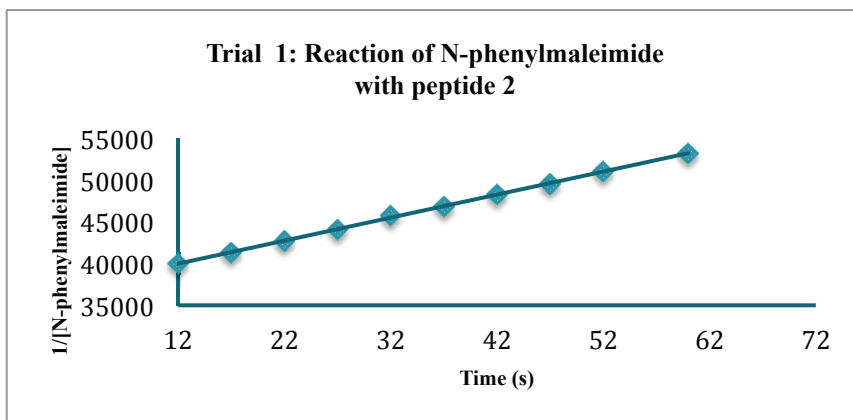
b) $k = 350.6 \text{ M}^{-1}\text{s}^{-1}$, $R^2 = 0.99$



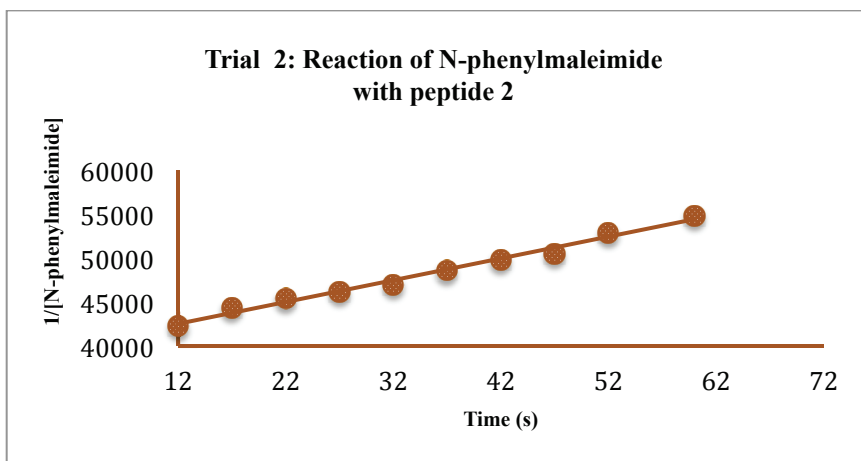
Average second order rate constant: $353.4 \pm 2.8 \text{ M}^{-1}\text{s}^{-1}$

Figure 3-13: Reaction between 1/[3-maleimidophenylboronic acid] and peptide 2 in ammonium acetate buffer (pH = 5.5) was monitored by HPLC by monitoring the disappearance of both starting materials and appearance of the product. N-Methylacetanilide was used as an internal standard. Second order rate constant for the reaction was determined by plotting the 1/[3-maleimidophenylboronic acid] versus time and analyzing by linear regression. Second order rate constant corresponds to the slope.
a) Trial 1 b) Trial 2

a) $k = 256.63 \text{ M}^{-1}\text{s}^{-1}$, $R^2 = 0.99$



b) $k = 225.17 \text{ M}^{-1}\text{s}^{-1}$, $R^2 = 0.99$



Average second order rate constant: $240.1 \pm 15.7 \text{ M}^{-1}\text{s}^{-1}$

Figure 3-14: Reaction between 1/[N-phenylmaleimide] and peptide 2 in ammonium acetate buffer (pH = 5.5) was monitored by HPLC by monitoring the disappearance of both starting materials and appearance of the product. N-Methylacetanilide was used as an internal standard. Second order rate constant for the reaction was determined by plotting the 1/[N-phenylmaleimide] versus time and analyzing by linear regression. Second order rate constant corresponds to the determined slope. a) Trial 1 b) Trial 2

3.6 Summary

In this chapter, we tried to develop site-specific Michael addition in an aqueous environment. Small boronic acid molecules with a Michael acceptor were designed and synthesized for the purpose of increasing site-specificity of the thiol-Michael addition reactions. After testing with the small peptides containing serine and cysteine residues, we found that 3-maleimidophenylboronic acid is more reactive towards terminal serine. We compare the reactivity of boronic acid with the control molecule, N-phenylmaleimide. Analysis of their reactivity was achieved by using ^1H NMR and HPLC-MS. Kinetic study by ^1H NMR showed that the rate constant for 3-maleimidophenylboronic acid is two times more than N-phenylmaleimide. Also, only a N-terminus serine showed higher activity, which could be studied in the future for selectivity towards N-terminal serine in larger library. Later, to calculate initial rate constant, we applied HPLC-MS and decreased the concentration of reactants 20 times compared to the ^1H NMR study. Data was collected within 60 seconds to calculate the initial rate constant, which showed that reaction between 3-maleimidophenylboronic acid and peptide **2** is around one and half times higher than N-phenylmaleimide. Thus, both methods showed similar result for 3-maleimidophenylboronic acid reactivity.

3.7 Future work

We have been able to show that the 3-maleimidophenylboronic acid can effectively recognize the N-terminal serine in small peptides, but there remains much room for improvement. Profluorescent boronic acid probe could be prepared to test the reactivity towards a larger library of peptides or proteins by using fluorescence spectroscopy. Also, one of our challenges was the high reactivity of cysteine in the peptide towards the maleimide Michael acceptor, which led us to decrease the pH of the solution to 5.5, and decreasing the concentration in HPLC to slow down the reactions. Thus, designing a boronic acid with the less reactivity in Michael acceptor part could be more effective to increase the selectivity by the presence of boronic acids.

3.8 Experimental

3.8.1 General information

All reagents used for the synthesis of boronic acids were purchased from Sigma-Aldrich or Combi-Blocks and used without further purification. Unless otherwise stated, all reactions were performed under a nitrogen atmosphere using flame-dried glassware. THF, dichloromethane and toluene were obtained from a MBraun MB SPS solvent system prior to use. Anhydrous 1,4-dioxane was purchased from Sigma-Aldrich, 99.8%, and it was deoxygenated with dry nitrogen for one hour before use. All peptides were synthesized manually using Fmoc-protected amino acids and Rink Amide resin from Novabiochem. Thin layer chromatography (TLC) was performed on Merck Silica Gel 60 F254 plates and was visualized with UV light and KMnO₄ stain. NMR spectra were recorded on Varian INOVA-400 or INOVA-500 MHz instruments. The residual solvent protons (¹H) or the solvent carbons (¹³C) were used as internal standards. ¹H NMR data is presented as follows: chemical shift in ppm (δ) downfield from tetramethylsilane (multiplicity, coupling constant, integration). The following abbreviations are used in reporting NMR data: s, singlet; br s, broad singlet; d, doublet; t, triplet; dd, doublet of doublets; m, multiplet. The boron-bound carbon was not detected. High-resolution mass spectra were recorded by the University of Alberta mass spectrometry services laboratory using either electron impact (EI) or electrospray ionization (ESI) techniques. Infrared spectra were obtained on a Nicolet Magna-IR instrument with frequencies expressed in cm⁻¹, with the range of wavenumber 650-4000 cm⁻¹ in microscope-FTIR, by using crystalized samples or dissolving in dichloromethane. Peptide analysis and purification and kinetic study by HPLC-MS were determined using Agilent 1100 HPLC-MS (UV-Vis fluorescence detector).

3.8.2 Synthesis of (*E*)-2-boronic acid-chalcone (BA5)

Benzaldehyde (530 mg, 5.00 mmol) and NaOH (2.5 M, 40 mL) were added to a stirred solution of *m*-bromoacethophenone (995 mg, 5.00 mmol) in EtOH (200 ml) at room

temperature. The mixture was stirred for 3 hours, neutralized with 1N HCl, and extracted three times with EtOAc. The organic layer was dried over anhydrous sodium sulfate, filtered and the solvents evaporated. The residue was purified by column chromatography on silica gel (Hexane/EtOAc = 8:2) to produce (*E*)-2-boronic acid-chalcone as a yellow solid (1.35 g, 95 %). Then, the general procedure in Chapter 2 for Miyaura reaction was applied to provide the related boronic acid. (*E*)-2-Boronic acid-chalcone (858 mg, 3.00 mmol), KOAc (294 mg 3.00 mmol), B₂pin₂ (915 mg 3.20 mmol) and PdCl₂dppf (40 mg, 0.05 mmol) in 1,4-dioxane (10 mL) afforded (*E*)-2-boronic ester-chalcone, which was purified by silica gel column chromatography (Hexane/EtOAc = 8:2). Finally, pinacol (*E*)-2-boronic ester-chalcone was hydrolyzed using the diethanolamine method to form (*E*)-2-boronic ester-chalcone as an ivory solid (375 mg, 50%).

¹H NMR (500 MHz, CDCl₃) δ 7.92 (m, 2H), 7.84 (d, *J* = 15.8 Hz, 1H), 7.66-7.68 (m, 4H), 7.52 (d, *J* = 15.7 Hz, 1H), 7.42-7.46 (m, 3H)

¹³C NMR (125 MHz, CDCl₃) δ 189.3, 145.4, 136.9, 134.7, 131.9, 130.7, 130.0, 129.0, 128.6, 127.9, 121.5 (The boron-bound carbon was not detected due to quadrupolar relaxation)

¹¹B NMR (128 MHz, CD₃OD) 29.5

IR (Microscope, cm⁻¹) 3401.60, 3060.13, 1654.91, 1621.86, 1478.50

HRMS (EI) for C₁₃H₇BrO: calcd. 252.0958; found 252.1043

M.P. 177- 178 °C

3.8.3 Synthesis of (*E*)-4-boronic acid-chalcone (BA6)

Benzaldehyde (530 mg, 5.00 mmol) and NaOH (2.5 M, 40 mL) were added to a stirred solution of *p*-bromoacetophenone (995 mg, 5.00 mmol) in EtOH (200 ml) at room temperature. The mixture was stirred for 3 hours, neutralized with 1 N HCl, and extracted three times with EtOAc. The organic layer was dried over anhydrous sodium sulfate, filtered and the solvents evaporated. The residue was purified by column chromatography on silica gel (Hexane/EtOAc = 8:2) to give (*E*)-2-boronic acid-chalcone as a yellow solid (1.35 g, 65 %). Then, the general procedure in Chapter 2 for Miyaura reaction was

applied to provide the related boronic acid. (*E*)-2-Boronic acid-chalcone (858 mg, 3.00 mmol), KOAc (294 mg, 3.00 mmol), B₂pin₂ (915 mg, 3.20 mmol) and PdCl₂dppf (40 mg, 0.05 mmol) in 1,4-dioxane (10 mL) afforded (*E*)-4-boronic ester-chalcone, which was purified by silica gel column chromatography (Hexane/EtOAc = 8:2). Next, pinacol (*E*)-4-boronic ester-chalcone was hydrolyzed by the diethanolamine method to form (*E*)-4-boronic ester-chalcone as an ivory solid (491 mg, 65%).

¹H NMR (400 MHz, DMSO-*d*₆) δ 8.28 (br s, B(OH)₂, 2H), 8.10 (m, 2H), 7.86-7.98 (m, 5H), 7.72 (m, 1H), 7.48 (m, 3H)

¹³C NMR (100 MHz, DMSO-*d*₆) δ 189.4, 143.9, 139.6, 138.6, 134.6, 134.3, 130.6, 128.9, 128.8, 127.3, 122.3, 122.2

¹¹B NMR (128 MHz, CDCl₃) 28.2

IR (Microscope, cm⁻¹) 3351, 3061, 1656, 1610, 1596

HRMS (EI) for C₁₃H₇BrO: calcd. 252.0958; found 252.1058

M.P. 188-190 °C

3.8.4 Synthesis of 3-acrylamidophenyl boronic acid (BA7)

3-Aminophenylboronic ester (1.1 g, 5.0 mmol) was dissolved in dry CH₂Cl₂ (10 mL) in a round bottom flask. The reaction mixture was cooled to 0 °C with an ice water bath, triethylamine (1 mL, 7 mmol) was added, and the solution was stirred for 30 min. A solution of acryloyl chloride (0.5 g, 5.5 mmol) in CH₂Cl₂ (5 mL) was added dropwise for 2 h at 0 °C, and the reaction was incubated for 24 h at room temperature. The solvent was removed under reduced pressure, and the crude solid product was suspended into ethyl acetate (200 mL) and stirred for 30 min followed by filtration to remove any solid particles. The organic layer was extracted with water (5 mL × 2), saturated aqueous sodium bicarbonate (5 mL × 2), water (5 mL × 2), and brine (5 mL × 2). The organic layer was dried over anhydrous sodium sulfate. After filtration, the solvent was removed under reduced pressure. The residue was purified by column chromatography on silica gel (Hexane/EtOAc = 8:2) to give 3-acrylamidophenyl boronic ester as a yellow solid (877 mg, 65% yield). Then 3-acrylamidophenyl boronic ester was hydrolyzed by the

diethanolamine method to form 3-acrylamidophenyl boronic acid as an ivory solid (50%).

¹H NMR (400 MHz, DMSO-*d*₆) δ 8.12 (s, B(OH)₂, 2H), 7.88 (s, 1H), 7.80 (m, 1H), 7.48 (dd, *J* = 1.1, 7.3 Hz, 1H), 7.28 (m, 1H), 6.44 (m, 1H), 6.27 (dd, *J* = 17.0, 2.0, 1H)

¹³C NMR (125 MHz, DMSO-*d*₆) δ 163.0, 138.1, 131.9, 129.3, 127.7, 126.6, 125.3, 121.3
(The boron-bound carbon was not detected due to quadrupolar relaxation)

¹¹B NMR (128 MHz, CDCl₃) 27.7

IR (Microscope, cm⁻¹) 3310.92, 3064.17, 1659.15, 1624.46, 1581.97, 1547.81

HRMS (EI) for C₁₃H₇BrO: calcd. 190.0754; found 190.0667

M.P. 143-145 °C

3.8.5 Synthesis of N-phenylmaleimide

Aniline (465 mg, 5.0 mmol) in toluene (5 mL) was added dropwise to a solution of maleic anhydride (600 mg, 6.00 mmol) in toluene (5 mL) at 35 °C. After addition was complete, the reaction was allowed to stir for 16 hours at room temperature. The crude acid was cooled and filtered under vacuum. This acid (765 mg, 4.00 mmol) was then dissolved in acetic anhydride (15 mL), sodium acetate (1.00 g, 13.2 mmol) was added, and the reaction heated at 80 °C for 5 hours. The reaction mixture was poured into water (30 mL) and extracted with dichloromethane (3 × 30 mL). The combined organic extracts were dried over anhydrous sodium sulfate and evaporated under reduced pressure. The residue was purified by column chromatography on silica gel (Hexane/EtOAc = 8:2) to give N-phenylmaleimide as a yellow solid (650 mg, 75% yield).

¹H NMR (500 MHz, DMSO-*d*₆) δ 7.74 (m, 2H), 7.38 (m, 1H), 7.62 (m, 2H), 7.16 (m, 2H)

¹³C NMR (100 MHz, DMSO-*d*₆) δ 169.8, 134.6, 131.5, 128.8, 127.6, 126.7

IR (Microscope, cm⁻¹) 3458, 3106, 1715, 1741, 1681.2, 1595.4

HRMS (EI) for C₁₃H₇BrO: calcd. 173.0477; found 173.0475

M.P. 80-82 °C

3.8.6 Synthesis of 3-maleimidophenylboronic acid (BA8)

3-Maleimidophenylboronic ester (1.1 g, 5.0 mmol) in toluene (5 mL) was added dropwise to a solution of maleic anhydride (600 mg, 6.00 mmol) in toluene (5 mL) at 35 °C. After addition was complete, the reaction was allowed to stir for 16 hours at room temperature. The crude acid was cooled and filtered under vacuum. This acid (1.2 g, 4.0 mmol) was then dissolved in acetic anhydride (15 mL), sodium acetate (1.00 g, 13.2 mmol) was added, and the reaction heated at 80 °C for 5 hours. The reaction mixture was poured into water (30 mL) and extracted with dichloromethane (3 × 30 mL). The combined organic extracts were dried over anhydrous sodium sulfate and evaporated under reduced pressure. The residue was purified by column chromatography on silica gel (Hexane/EtOAc = 8:2) to give 3-maleimidophenylboronic ester as a ivory solid (877 mg, 65% yield).

¹H NMR (400 MHz, DMSO-*d*₆) δ 8.2 (s, B(OH)₂, 2H), 7.8 (m, 1H), 7.68 (m, 1H), 7.42 (m, 1H), 7.34 (m, 1H), 7.16 (s, 2H)

¹³C NMR (100 MHz, DMSO-*d*₆) δ 170.5, 134.6, 133.4, 132.4, 130.9, 128.6, 127.9 (The boron-bound carbon was not detected due to quadrupolar relaxation)

¹¹B NMR (128 MHz, CD₃OH) 28.1

IR (Microscope, cm⁻¹) 3308.69, 3502.71, 3102.76, 1701.64, 1604.75, 1494.34

HRMS (EI) for C₁₃H₇BrO: calcd. 216.0546; found 216.0544

M.P. 210-212 °C

3.8.7 Synthesis of peptide 2

A solution of L-serine (500 mg, 5.00 mmol) in a mixture of t-BuOH (10 mL), water (25 mL), and NaOH (400 mg, 10.0 mmol) was stirred and cooled in an ice-water bath. Di-tert-butyl pyrocarbonate (1.1 g, 5.0 mmol) was added and stirring was continued at room temperature overnight. The solution was acidified with 5% HCl. The aqueous phase was extracted with ethyl acetate (3 × 30 mL). The combined organic extracts were dried over anhydrous sodium sulfate, filtered and evaporated *in vacuo*. N-Boc-L-serine (1.0 g, 4.8 mmol) was used without further purification. N-Boc-L-serine (1 g, 4.8 mmol), 1-

Hydroxy-7-azabenzotriazole (652 mg, 4.80 mmol), L-cysteine ethyl ester hydrochloride (895 mg, 4.87 mmol), and triethyl amine (950 mg, 9.70 mmol) were dissolved in dry CH_2Cl_2 (30 mL). The solution was cooled in an ice-water bath and stirred while DCC (1.1 g, 4.8 mmol) was added. Stirring was continued for 1 h at 0 °C then 3 hours at room temperature. The precipitated DCU was removed by filtration and the solvent was evaporated in vacuum (Scheme 3-4). The residue was purified by column chromatography on silica gel (EtOAc/Hexane 50:50) to give peptide **2** which was purified by reverse-phase HPLC (C8 column, 5 μm , 10 mm \times 250 mm) using a variable gradient of CH_3CN in H_2O (containing 0.1 % TFA) from 1 - 20 min and a flow rate of 3 mL/min (93% purity). HPLC-MS data is available in Appendices 2.

2.8.8 Synthesis of peptides by solid phase peptide synthesis

Standard Fmoc solid phase peptide synthesis as described in Chapter 2 was performed manually in 25 mL polypropylene tubes equipped with frit, solid phase synthesis reaction vessel. Rink amide resin on 0.69 mmol/g was used to provide the peptides **1**, **3**, and **4** following Fmoc-SPPS. Wang resin 0.93 mmol/g was used for the peptide **5**. For Wang resin, the general procedure for peptide synthesis began with coupling the first amino acid. First, Wang resin (0.279 mmol) swelled for 1 hour in 3 mL of DMF, before the solvent was drained off. HOAt (1.39 mmol, 5 equiv), DIC (1.395 mmol, 5 equiv) and DMAP (0.08 mmol, 0.3 equiv) were added to a solution of amino acid Fmoc-Ser(tBu)-OH (1.395 mmol, 5 equiv) in DCM:DMF (2:1). After 30 min of pre-activation, the mixture was added to the resin (300 mg, 0.279 mmol) and shaken for 3 hours at room temperature. The solvent was drained and the resin was washed with DMF (4 \times 4 mL), then DCM (4 \times 4 mL). To the peptide, Fmoc-SPPS was applied and provided peptide **5**. In the case of peptide **3** and **4**, the acetylation reaction was performed before the final cleavage. The dried resin was treated with TFA/ H_2O /phenol/TIPS (10 mL, 85/5/5/5 (v/v/v/v)) for 2 hours to cleave the peptide. The cleavage mixture was filtered from the resin, and precipitated in ice-cold diethyl ether for 20 min. The precipitate was then centrifuged (2000 g, 5 min) at 4 °C, washed three times with cold Et_2O , and dried under vacuum. The aqueous layer was flash-frozen, dried in a lyophilizer, and purified by HPLC (90-99% purity). HPLC-MS data is available in Appendices 2.

3.8.9 ¹H NMR kinetic analysis

Kinetic data for the reactions between 3-maleimidophenylboronic acid and the peptides **1-5** was obtained by ¹H NMR at room temperature using INOVA-400, INOVA-500 and INOVA-600 MHz instruments. A 30% CD₃CN/D₂O solution of 0.10 M sodium phosphate monobasic buffer was prepared as a stock solution and pH was adjusted to 5.5 by using dilute phosphoric acid. A 0.5 mM solution of 3-maleimidophenylboronic acid was prepared, and for each experiment, two or three separate NMR tubes were provided and 0.6 mL of the solution was added to each NMR tube. A 1.2 mM solution of 1,4-dinitrobenzene was used as an internal standard and proton integration relative to the internal standard was utilized to ensure the proper relative concentrations of each solution. Appropriate concentration of a peptide and TCEP in internal standard solution (50 μL) was added to each NMR tube containing 3-maleimidophenylboronic acid while monitoring the reaction. Resulting solutions containing 3-maleimidophenylboronic acid and peptide was finalized in a 1:1 ratio, then the proper ratio was confirmed by proton integration. The reaction solution was scanned once every 26 seconds after adding the peptide solution to the boronic acid over 30 minutes. This procedure was repeated for each of the remaining prepared NMR tubes. For each of the reactions tested, the disappearance of proton spectra in 7.2 ppm the related to the maleimide part of the molecule was monitored without any side products unless otherwise noted. The same method was used for monitoring and collecting data of the reaction between N-phenylmaleimide and peptides **1-5**. Prior to analysis, all spectra were subjected to baseline correction and phasing was corrected manually. Second order rate constants were calculated by plotting 1/[3-maleimidophenylboronic acid] as a function of time. The y-intercept of each plot was set to [starting 3-maleimidophenylboronic acid concentration]⁻¹. Plots show data collected to ~70-80% conversion to the product.

3.8.10 HPLC-MS kinetic analysis

The kinetic study was performed in 30% acetonitrile: ammonium acetate buffer as a solvent to solubilize organic compounds and the pH was adjusted to 5.5 to decrease the

reactivity. Stock solution A was prepared containing N-methylacetanilide as the internal standard (0.1 mM) and peptide **2** (0.1 mM). To a vial containing 600 μ L of the solution A, 600 μ L of the solution of 3-maleimidophenylboronic acid or N-phenylmaleimide (0.1 mM) was added to give a final concentration of 0.05 mM (both internal standard and reagents). Then the reaction mixture (90 μ L) was quenched with 5% TFA (90 μ L) and analyzed by HPLC-MS. Areas under the peaks of 3-maleimidophenylboronic acid or N-phenylmaleimide were normalized according to the area of peak of the internal standard. The second order rate constant for the reaction was determined in duplicate by plotting the $1/[3\text{-maleimidophenylboronic acid}]$ or $1/[N\text{-phenylmaleimide}]$ versus time and analyzing by linear regression.

3.8.11 References

- (1) Stenzel, H. M. (2013) Bioconjugation using thiols: old chemistry rediscovered to connect polymers with nature's building blocks. *ACS Macro Lett.* 2, 14–1.
- (2) Stephanopoulos, N., and Francis, B. M. (2011) Choosing an effective protein bioconjugation strategy. *Nat. Chem. Biol.* 7, 876–884.
- (3) Jones, W. M., Strickland, A. R., Schumacher, F. F., Caddick, S., Baker, R. J., Gibson, I. M., and Haddleton, M. D. (2012) Polymeric dibromomaleimides as extremely efficient disulfide bridging bioconjugation and pegylation agents. *J. Am. Chem. Soc.* 134, 1847–1852.
- (4) Adzima, J. B. and Bowman N. C. (2012) The emerging role of click reactions in chemical and biological engineering. *AIChE J.* 58, 10, 2952–2965.
- (5) Fei, D. X., Zhou, Z., Li, W., Zhu, M, Y., and Shen, K, J. (2012) Buchwald–Hartwig coupling/Michael addition reactions: one-pot synthesis of 1,2-disubstituted 4-quinolones from chalcones and primary amines. *Eur. J. Org. Chem.* 3001–3008.
- (6) Cheng, U., Zhang, X., Xiang, J., Wang, Y., Zheng, C., Lu, Z., and Li, C. (2012) Development of novel self-assembled poly (3-acrylamidophenylboronic acid)/poly (2 lactobionamidoethyl methacrylate) hybrid nanoparticles for improving nasal adsorption of insulin. *Soft Matter.* 8, 765-773.

-
- (7) Kim, Y., Ho, S. O., Gassman, N. R., Korlann, Y., Landorf, E.V., Collart, F. R., and Weiss, S. (2008) Efficient site-specific labeling of proteins *via* cysteines. *Bioconjugate Chem.* 19, 786–791.
- (8) Partis, M., Griffiths, D., Roberts, G., and Beechey, R. (1983) Cross-linking of protein by co-maleimido alkanoyl N-Hydroxysuccinimido esters. *J. Protein Chem.* 2, 263–277.
- (9) Kakwere, H., and Perrier, S. Orthogonal “relay” reactions for designing functionalized soft nanoparticles. (2009) *J. Am. Chem. Soc.* 131, 1889-95.
- (10) Corrie, J. E. T. (1994) Thiol-reactive fluorescent probes for protein labelling. *J. Chem. Soc., Perkin Trans. 1*, 297-2982.

Chapter 4

Thesis Summary, Conclusions and Future Perspectives

4.1 Thesis summary and conclusions

In the past two decades, boronic acids have occupied a special place in the design of fluorescent sensors for carbohydrates. However, there has been no progress using boronic acid sensors in the area of protein labeling. Work to better understand the use of non-toxic boronic acid compounds for the high selectivity and affinity recognition of proteins would be extremely valuable. RhoBo, the first reported rhodamine-derived bisboronic acid, has been synthesized as a nontoxic analogue of fluorescence derivative, which can function bioorthogonally to the tetraserine peptides as an affinity label.¹ This finding only was observed for the diboronic acid building block, although no binding affinity was observed for the monoboronic acid. The research presented in this thesis is centered on the synthesis of small monoboronic acids for the purpose of bioconjugation to proteins. In Chapter 2, I investigated the development of monoarylboronic acids with a potential ability of binding up to four covalent bonds. We hypothesized that serine and lysine amino acids in the peptide could contribute in binding to boronic acids containing ketone functionality. My results suggest that designed boronic acids are not able to covalently bind *via* the boronic acid and ketone motif to all the designed peptide sequence in which each serine is separated with different intervening from lysine amino acid in the peptide. Their reactivity was analyzed by using ARS colorimetric assay, UV spectrophotometry, fluorescence spectroscopy, HPLC-MS and mass spectrometric analysis.

In Chapter 3, we tried to develop site-specific probe operating by Michael addition in an aqueous environment. Small boronic acid molecules with a Michael acceptor part were designed and synthesized for the purpose of testing their binding affinity towards small peptides containing serine and cysteine amino acids. It was anticipated that boronate ester formation between serine and the boronic acid part of the molecule has the role to increase the rate and selectivity of nucleophilic addition of the cysteine to Michael

acceptor part of the molecule. After testing four different boronic acids containing a Michael acceptor unit, I found that 3-maleimidophenyl boronic acid was more reactive towards a cysteine containing peptide with a terminal serine in comparison to N-phenylmaleimide as a control molecule. By testing different small peptide libraries, I confirmed that N-terminus serine had higher activity towards 3-maleimidophenyl boronic acid in comparison to internal serine and C-terminus serine. Its reactivity is due to the forming of a stable five-member ring between boronic acid and N-terminal serine. However in C-terminal serine, six-member ring could form and is not stable. Their reactivity was analyzed by using ^1H NMR and HPLC-MS. Kinetic studies revealed that the rate constant for 3-maleimidophenylboronic acid was higher than N-phenylmaleimide.

4.2 Future perspectives

We tried to develop nontoxic, sequence-selective small molecule probes for proteins, which could act in a bioorthogonal studies. In Chapter 2, I have only tested a small array of eleven peptides to test their binding to the boronic acids, however nearly limitless combination of amino acid sequences is possible. Therefore, future work would be to create larger libraries of serine and lysine peptides and test the ability of boronic acids to target these sequences. Phage display is a widely used method that allows for the identification of useful ligands from a library of 10^9 random polypeptides and can be used to develop reactive peptide sequences, which are capable of forming covalent bonds.² Moreover, it is better to design a profluorescent boronic acid molecule, which is not fluorescent in the absence of its target, so it is possible to provide a turn-on mechanism, and monitoring of their activity would be easier in order to find one that induces a large fluorescent response.

In Chapter 3, we showed that the 3-maleimidophenyl boronic acid can effectively recognize N-terminus serine in the small peptide, but there remains much room for improvement in order to test the boronic acid reactivity towards larger peptide library. Again, phage display could be the option to find the highest binding affinity of peptide

tag. Also, profluorescent small molecules of boronic acid can be designed to test the reactivity towards proteins and *in vivo*. One of our challenges in this project was the high background reactivity of cysteine in the peptide towards Michael acceptor, which led us to decrease the pH of the reaction to 5.5, so we were able to compare the reactivity of 3-maleimidophenyl boronic acid and the control molecule. Moreover, a potential future direction could be the design of a small boronic acid with less reactivity in the Michael acceptor part, so that the boronic acid unit of the molecule could provide more selectivity with the interaction by serine residues of peptides. It is my hope that the information presented in this chapter will encourage the development of selective small-molecule fluorescent boronic acid sensors based on Michael acceptors for bioconjugation studies.

References

- (1) Halo, T. L., Appelbaum, J., Hobert, E. M., Balkin, D. M., and Schepartz, A. (2009) Selective recognition of protein tetraserine motifs with a cell-permeable, pro-fluorescent bis-boronic acid. *J. Am. Chem. Soc.* 131, 438–439.
- (2) Tanaka, F., Fuller, R., Asawapornmongkol, L., Warsinke, A., Gobuty, S., and Barbas, C. F. (2007) Development of a small peptide tag for covalent labeling of proteins. *Bioconjugate Chem.* 18,1318–1324.

Bibliography

- (1) Nienhaus, G. U. (2008) The green fluorescent protein: a key tool to study chemical processes in living cells. *Angew. Chem., Int. Ed.* *47*, 8992–8994.
- (2) Prescher, J. A., and Bertozzi, C. R. (2005) Chemistry in living systems. *Nat. Chem. Biol.* *1*, 13–21.
- (3) Kremers, G. J., Gilbert, S. G., and Cranfill, P. J. (2011) Fluorescent proteins at a glance. *J. Cell Sci.* *124*, 157–160.
- (4) Lisenbee, C. S., Karnik, S. K., and Trelease, R. N. (2003) Overexpression and mislocalization of a tail-anchored GFP redefines the identity of peroxisomal ER. *Traffic.* *4*, 491–501.
- (5) Marguet, D., Spiliotis, E. T., Pentcheva, T., and Lebowitz, M. (1999) Lateral diffusion of GFP-tagged H2L molecules and of GFP-TAP1 reports on the assembly and retention of these molecules in the endoplasmic reticulum. *Immunity.* *11*, 231–240.
- (6) Watanabe, S., Mizukami, S., and Hori, Y. (2010) Multicolor protein labeling in living cells using mutant β -lactamase-tag technology. *Bioconjugate Chem.* *21*, 2320–2326.
- (7) Carroll, L., Evans, H. L., and Aboagye, E. O. (2013) Bioorthogonal chemistry for pre-targeted molecular imaging—progress and prospects. *Org. Biomol. Chem.* *11*, 5772–5781.
- (8) Debets, M. F., Hest, J. C. M., and Rutjes, F. P. J. T. (2013) Bioorthogonal labelling of biomolecules: new functional handles and ligation methods. *Org. Biomol. Chem.* *11*, 6439–6455.
- (9) Agarwal, P., Kudirka, R., Albers, A. E., Barfield, R. M., de Hart, G. W., Drake, P. M., Jones, L. C., and Rabuka, D. (2013) Hydrazino-Pictet–Spengler ligation as a biocompatible method for the generation of stable protein conjugates. *Bioconjugate Chem.* *24*, 846–851.
- (10) Kalia, J., and Raines, R. T. (2008) Hydrolytic stability of hydrazones and oximes. *Angew. Chem., Int. Ed.* *120*, 7633–7636.
- (11) Cornish, V. W., Hahn, K. M., and Schultz, P. G. (1996) Site-specific protein modification using a ketone handle. *J. Am. Chem. Soc.* *118*, 8150–8151.

- (12) Lelle, M., and Peneva, K. (2014) An amino acid–based heterofunctional cross–linking reagent. *Amino Acids*. 46, 1243–1251.
- (13) Jencks, W. P. (1994) Reaction mechanisms, catalysis, and movement. *Protein Science*. 3, 2459–2464.
- (14) Vepřek, P., and Ježek, J. (1999) Peptide and glycopeptide dendrimers. Part II. *J. Pept. Sci.* 5, 203–220.
- (15) Wang, L., Zhang, Z., Brock, A., and Schultz, P. G. (2003) Addition of the keto functional group to the genetic code of *Escherichia coli*. *Proc. Nat. Acad. Sci. U.S.A.* 100, 56–61.
- (16) Mahal, L. K., Yarema, K. J., and Bertozzi, C. R. (1997) Engineering chemical reactivity on cell surfaces through oligosaccharide biosynthesis. *Science*. 276, 1125–1128.
- (17) Agarwal, P., Weijden, J. V., Sletten, E. M., Rabuka, D., and Bertozzi, C. R. (2013) A Pictet–Spengler ligation for protein chemical modification. *Proc. Nat. Acad. Sci. U.S.A.* 110, 46–51.
- (18) Tanaka, F., Fuller, R., Asawapornmongkol, L., Warsinke, A., and Gobuty, S. (2007) Development of a small peptide tag for covalent labeling of proteins. *Bioconjugate Chem.* 18, 1318–1324.
- (19) Gaietta, G., Deerinck, T. J., Adams, S. R., Bouwer, J., Tour, O., Laird, D. W., Sosinsky, G. E., Tsien, R. Y., and Ellisman, M. H. (2002) Multicolor and electron microscopic imaging of connexin trafficking. *Science*. 296, 503–507.
- (20) Griffin, B. A., Adams, S. R. J., and Tsien, R. Y. (1998) Specific covalent labeling of recombinant protein molecules inside live cells. *Science*. 281, 269–272.
- (21) Zürn, A., Klenk, C., Zabel, U., Reiner, S., Lohse, M. J., and Hoffmann, C. (2010) Site–specific, orthogonal labeling of proteins in intact cells with two small biarsenical fluorophores. *Bioconjugate chem.* 21, 853–859.
- (22) Guignet, E. G., Hovius, R., and Vogel, H. (2004) Reversible site–selective labeling of membrane proteins in live cells. *Nature Biotechnol.* 22, 440–444.
- (23) Bhagawati, M., Lata, S., Tampé, R., and Piehler, J. (2010) Native laser lithography of His–tagged proteins by uncaging of multivalent chelators. *J. Am. Chem. Soc.* 132, 5932–5933.

- (24) Marks, K. M., Rosinov, M., and Nolan, G. P. (2004) *In vivo* targeting of organic calcium sensors *via* genetically selected peptides. *Chem. Biol.* *11*, 347–356.
- (25) Franz, K. J., Nitz, M., and Imperiali, B. (2003) Lanthanide-binding tags as versatile protein coexpression probes. *ChemBioChem.* *4*, 265–271.
- (26) Sculimbrene B. R., and Imperiali, B. (2006) Lanthanide–Binding Tags as Luminescent Probes for Studying Protein Interactions. *J. Am. Chem. Soc.* *128*, 7346–52.
- (27) Giriat I., and Muir, T. W. (2003) Protein semi–synthesis in living cells. *J. Am. Chem. Soc.* *125*, 7180–7181.
- (28) Halo, T. L., Appelbaum, J., Hobert, E. M., Balkin, D. M., and Schepartz, A. (2009) Selective recognition of protein tetraserine motifs with a cell–permeable, pro–fluorescent bis–boronic acid. *J. Am. Chem. Soc.* *131*, 438–439.
- (29) Griffin, R. J (1994) The medicinal chemistry of the azido group. *Prog. Med. Chem.* *31*, 121–232.
- (30) Oyelere, A. K., Chen, P. C., and Yao, L. P. (2006) Heterogeneous diazo–transfer reaction: a facile unmasking of azide groups on amine–functionalized insoluble supports for solid–phase synthesis. *J. Org. Chem.* *71*, 9791–9796.
- (31) Kiick, K. L., Saxon, E., and Tirrell, D. A. (2002) Incorporation of azides into recombinant proteins for chemoselective modification by the Staudinger ligation. *Proc. Nat. Acad. Sci. U.S.A.* *99*, 19–24.
- (32) Xiao, J., and Tolbert, T. J. (2009) Synthesis of N–terminally linked protein dimers and trimers by a combined native chemical ligation–CuAAC click chemistry strategy. *Org. Lett.* *11*, 4144–4147.
- (33) Ngo, J. T., and Tirrell, D. A. (2011) Noncanonical amino acids in the interrogation of cellular protein synthesis. *Acc. Chem. Res.* *44*, 677–685.
- (34) Dieterich, D. C., Hodas, J. J. L., Gouzer, G., Shadrin, I. Y., Ngo, J. T., Triller, A., Tirrell, D. A., and Schuman, E. M. (2010) In situ visualization and dynamics of newly synthesized proteins in rat hippocampal neurons. *Nature Neuroscience.* *13*, 897–905.
- (35) Agard, N. J., and Bertozzi, C. R. (2009) Chemical approaches to perturb, profile, and perceive glycans. *Acc. Chem. Res.* *42*, 788–797.
- (36) Laughlin, S. T., Baskin, J. M., Amacher, L. S., and Bertozzi, C. R. (2008) *In vivo* imaging of membrane–associated glycans in developing zebrafish. *Science.* *320*, 664–

667.

(37) Kostiuk, M. A., Corvi, M. M., Keller, B. O., Plummer, G., Prescher, J. A., Hangauer, M. J., Bertozzi, C. R., Rajaiah, G., Falck, J. R., and Berthiaume, L. G. (2008) Identification of palmitoylated mitochondrial proteins using a bio-orthogonal azido-palmitate analogue. *FASEB J.* 22, 721–732.

(38) Heal, W. P., Jovanovic, B., Bessin, S., and Wright, M. H. (2011) Bioorthogonal chemical tagging of protein cholesterylation in living cells. *Chem Commun.* 47, 4081–4083.

(39) Salic, A., and Mitchison, T. J. (2008) A chemical method for fast and sensitive detection of DNA synthesis *in vivo*. *Proc. Nat. Acad. Sci. U.S.A.* 105, 415–2420.

(40) Martin, B. R., Wang, C., Adibekian, A., Tully, S. E., and Cravatt, B. F. (2012) Global profiling of dynamic protein palmitoylation. *Nature Methods.* 9, 84–89.

(41) Schieber, C., Bestetti, A., Lim, J. P., Ryan, A. D., Nguyen, T. L., Eldridge, R., White, A. R., Gleeson, P. A., Donnelly, P. S., Williams, S. J., and Mulvaney, P. (2012) Conjugation of transferrin to azide-modified CdSe/ZnS core-shell quantum dots using cyclooctyne click chemistry. *Angew. Chem., Int. Ed. Engl.* 51, 10523–10527.

(42) Köhn, M., and Breinbauer, R. (2004) The Staudinger ligation—a gift to chemical biology. *Angew. Chem., Int. Ed.* 43, 3106–16.

(43) Gololobov, Y. G., Zhmurova, I. N., and Kasukhin, L. F. (1981) Sixty years of Staudinger reaction. *Tetrahedron.* 37, 3437–472.

(44) Saxon, E., and Bertozzi, C. R. (2000) Cell surface engineering by a modified Staudinger reaction. *Science.* 287, 2007–2010.

(45) Fiona L Lin, Helen M Hoyt, Herman van Halbeek, Robert G Bergman, A., Carolyn R Bertozzi. (2005) Mechanistic investigation of the Staudinger ligation. *J. Am. Chem. Soc.* 127, 2686–2695.

(46) Sletten, E. M., and Bertozzi, C. R. (2011) From mechanism to mouse: a tale of two bioorthogonal reactions. *Acc. Chem. Res.* 44, 666–676.

(47) Carroll, L., Boldon, S., Bejot, R., Moore, J. E., Declerck, J., and Gouverneur, V. (2011) The traceless Staudinger ligation for indirect ¹⁸F-radiolabelling. *Org. Biomol. Chem.* 9, 136–140.

(48) Saxon, E., and Bertozzi, C. R. (2000) Cell surface engineering by a modified

Staudinger reaction. *Science*. 287, 2007–2010.

(49) Hang, H. C., Yu, C., Kato, D. L., and Bertozzi, C. R. (2003) A metabolic labeling approach toward proteomic analysis of mucin-type O-linked glycosylation. *Proc. Nat. Acad. Sci. U.S.A.* 100, 14846–14851.

(50) Vocadlo, D. J., Hang, H. C., Kim, E. J., Hanover, J. A., and Bertozzi, C. R. (2003) A chemical approach for identifying O-GlcNAc-modified proteins in cells. *Proc. Nat. Acad. Sci. U.S.A.* 100, 9116–9121.

(51) Sarah J Luchansky, Sulabha Argade, Bradley K Hayes, A., Carolyn R Bertozzi. (2004) Metabolic functionalization of recombinant glycoproteins. *Biochemistry*. 43, 12358–12366.

(52) Bradley L Nilsson, Laura L Kiessling, A., Ronald T Raines. (2000) Staudinger Ligation: a peptide from a thioester and azide. *Org. Lett.* 2, 1939–1941.

(53) Saxon, E., Armstrong, J. I., and Bertozzi, C. R. (2000) A “traceless” Staudinger ligation for the chemoselective synthesis of amide bonds. *Org. Lett.* 2, 2141–2143.

(54) Matthew B Soellner, Kimberly A Dickson, Bradley L Nilsson, A., Ronald T Raines. (2003) Site-specific protein immobilization by Staudinger ligation. *J. Am. Chem. Soc.* 125, 11790–11791.

(55) Köhn, M., Wacker, R., Peters, C., Schröder, H., Soulère, L., Breinbauer, R., Niemeyer, C. M., and Waldmann, H. (2003) Staudinger ligation: a new immobilization strategy for the preparation of small-molecule arrays. *Angew. Chem., Int. Ed.* 42, 5830–5834.

(56) Huisgen, R., Adelsberger, K., Aufderhaar, E., Knupfer, H., and Wallbillich, G. N. (1967) Unterschiedliche reaktivitäten substituierter nitrilimine. *Monatshefte für Chemie*. 98, 1618–1650.

(57) Agnew, H. D., Rohde, R. D., Millward, S. W., Nag, A., Yeo, W. S., Hein, J. E., Pitram, S. M., Tariq, A. A., Burns, V. M., Krom, R. J., Fokin, V. V., Sharpless, K. B., and Heath, J. R. (2009) Iterative in situ click chemistry creates antibody-like protein-capture agents. *Angew. Chem., Int. Ed.* 48, 4944–4948.

(58) Christian W Tornøe, Caspar Christensen, A., and Meldal, M. (2002) Peptidotriazoles on solid phase: [1,2,3]-triazoles by regiospecific copper(I)-catalyzed 1,3-dipolar cycloadditions of terminal alkynes to azides. *J. Org. Chem.* 67, 3057–3064.

- (59) Hao, Z., Hong, S., Chen, X., and Chen, P. R. (2011) Introducing bioorthogonal functionalities into proteins in living cells. *Acc. Chem. Res.* *44*, 742–51.
- (60) El-Sagheer, A. H., and Brown, T. (2012) Click nucleic acid ligation: applications in biology and nanotechnology. *Acc. Chem. Res.* *45*, 1258–1267.
- (61) Zhang, X., and Zhang, Y. (2013) Applications of azide–based bioorthogonal click chemistry in glycobiology. *Molecules.* *18*, 7145–7159.
- (62) Hong, V., Steinmetz, N. F., and Manchester, M. (2010) Labeling live cells by copper–catalyzed alkyne–azide click chemistry. *Bioconjugate Chem.* *21*, 1912–1916.
- (63) Hong, V., Presolski, S. I., Ma, C., and Finn, M. G. (2009) Analysis and optimization of copper-catalyzed azide–alkyne cycloaddition for bioconjugation. *Angew. Chem., Int. Ed.* *48*, 9879–9883.
- (64) Amo, D. S., Wang, W., Jiang, H., Besanceney, C., Yan, A. C., Levy, M., Liu, Y., Marlow, F. L., and Wu, P. (2010) Biocompatible copper(I) catalysts for *in vivo* imaging of glycans. *J. Am. Chem. Soc.* *132*, 16893–16899.
- (65) Wittig, G., and Krebs., A. (1961) On the existence of low–membered cycloalkynes. *Chem. Ber.* *94*, 3260–3275.
- (66) Nicholas J Agard, Jennifer A Prescher, A., and Bertozzi, C. R. (2004) A strain–promoted [3 + 2] azide–alkyne cycloaddition for covalent modification of biomolecules in living systems. *J. Am. Chem. Soc.* *126*, 15046–15047.
- (67) Turner, R. B., Jarrett, A. D., and Goebel, P. (1973) Heats of hydrogenation. IX. Cyclic acetylenes and some miscellaneous olefins. *J. Am. Chem. Soc.* *95*, 790–792.
- (68) Ning, X., Guo, J., Wolfert, M. A., and Boons, G. J. (2008) Visualizing metabolically labeled glycoconjugates of living cells by copper–free and fast Huisgen cycloadditions. *Angew. Chem., Int. Ed.* *47*, 2253–2255.
- (69) Baskin, J. M., Prescher, J. A., and Laughlin, S. T. (2007) Copper–free click chemistry for dynamic *in vivo* imaging. *Proc. Nat. Acad. Sci. U.S.A.* *104*, 16793–16797.
- (70) Agard, N. J., Prescher, J. A., and Bertozzi, C. R. (2004) A strain–promoted [3+ 2] azide–alkyne cycloaddition for covalent modification of biomolecules in living systems. *J. Am. Chem. Soc.* *126*, 15046–15047.
- (71) Ning, X., Temming, R. P., Dommerholt, J., Guo, J., Ania, D. B., Debets, M. F., Wolfert, M. A., Boons, G. J., and van Delft, F. L. (2010) Protein modification by strain–

- promoted alkyne–nitronc cycloaddition. *Angew. Chem., Int. Ed.* *49*, 3065–3068.
- (72) Marks, S. I., Kang, S. J., Jones, T. B., Landmark, J. K., and Cleland, J. A. (2011) Strain-promoted “click” chemistry for terminal labeling of DNA. *Bioconjugate Chem.* *22*, 1259–1263.
- (73) Jewett, J. C., Sletten, E. M., and Bertozzi, C. R. (2010) Rapid Cu–free click chemistry with readily synthesized biarylazacyclooctynones. *J. Am. Chem. Soc.* *132*, 3688–3690.
- (74) Blackman, M. L., Royzen, M., and Fox, J. M. (2008) Tetrazine ligation: fast bioconjugation based on inverse–electron–demand Diels–Alder reactivity. *J. Am. Chem. Soc.* *130*, 13518–13519.
- (75) Selvaraj, R., and Fox, J. M. (2013) Trans–cyclooctene—a stable, voracious dienophile for bioorthogonal labeling. *Curr. Opin. Chem. Biol.* *17*, 753–760.
- (76) Bach, R. D. (2009) Ring strain energy in the cyclooctyl system. The effect of strain energy on [3 + 2] cycloaddition reactions with azides. *J. Am. Chem. Soc.* *131*, 5233–5243.
- (77) Rossin, R., Bosch, S. M., and Hoeve, W. T. (2013) Highly Reactive trans–cyclooctene tags with improved stability for Diels–Alder chemistry in living systems. *Bioconjugate chem.* *24*, 1210–1217.
- (78) Devaraj, N. K., Thurber, G. M., Keliher, E. J., Marinelli, B., and Weissleder, R. (2012) Reactive polymer enables efficient *in vivo* bioorthogonal chemistry. *Proc. Nat. Acad. Sci. U.S.A.* *109*, 4762–4767.
- (79) Rossin, R., Verkerk, P. R., van den Bosch, S. M., Vulderson, R. C. M., Verel, I., Lub, J., and Robillard, M. S. (2010) *In vivo* chemistry for pretargeted tumor imaging in live mice. *Angew. Chem., Int. Ed.* *49*, 3375–3378.
- (80) Budin, G., Chung, H. J., Lee, H., and Weissleder, R. (2012) A magnetic Gram stain for bacterial detection. *Angew. Chem., Int. Ed.* *51*, 7752–7755.
- (81) Devaraj, N. K., Weissleder, R., and Hilderbrand, S. A. (2008) Tetrazine–based cycloadditions: application to pretargeted live cell imaging. *Bioconjugate Chem.* *19*, 2297–2299.
- (82) Patterson, D. M., Nazarova, L. A., and Xie, B. (2012) Functionalized cyclopropenes as bioorthogonal chemical reporters. *J. Am. Chem. Soc.* *134*, 18638–18643.

- (83) Cole, C. M., Yang, J., Šečkutė, J., and Devaraj, N. K. (2013) Fluorescent live-cell imaging of metabolically incorporated unnatural cyclopropene-mannosamine derivatives. *ChemBioChem*. *14*, 205–208.
- (84) Li, Q., Dong, T., Liu, X., and Lei, X. (2013) A bioorthogonal ligation enabled by click cycloaddition of *o*-quinolinone quinone methide and vinyl thioether. *J. Am. Chem. Soc.* *135*, 4996–4999.
- (85) Patterson, D. M., Nazarova, L. A., and Prescher, J. A. (2014) Finding the right Bioorthogonal chemistry. *ACS. Chem. Biol.* *9*, 592–605.
- (86) Jelinek, R., and Kolusheva, S. (2004) Carbohydrate biosensors. *Chem. Rev.* *104*, 5987–6015.
- (87) Cao, H., and Heagy, M. D. (2004) Fluorescent chemosensors for carbohydrates: A decade's worth of bright spies for saccharides in review. *J. Fluoresc.* *14*, 569–584.
- (88) James, T. D., Linnane, P., and Shinkai, S. (1996) Fluorescent saccharide receptors: a sweet solution to the design, assembly and evaluation of boronic acid derived PET sensors. *Chem. Commun.* 281–288.
- (89) Hall, D. G. (2012) Boronic Acids: Preparation and applications in organic synthesis, medicine and materials.
- (90) Lorand, J. P., and Edwards, J. O. (1959) Polyol Complexes and structure of the benzenboronate ion. *J. Org. Chem.* *24*, 769–774.
- (91) Springsteen, G., and Wang, B. (2002) A detailed examination of boronic acid-diol complexation. *Tetrahedron.* *58*, 5291–5300.
- (92) Yan, J., Springsteen, G., Deeter, S., and Wang, B. (2004) The relationship among pKa, pH, and binding constants in the interactions between boronic acids and diols—it is not as simple as it appears. *Tetrahedron.* *60*, 11205–11209.
- (93) James, T. D., Sandanayake, K. R. A. S., and Shinkai, S. (1994) Novel photoinduced electron-transfer sensor for saccharides based on the interaction of boronic acid and amine. *J. Am. Chem. Soc.* *117*, 8982–8987.
- (94) Tong, A. J., Yamauchi, A., Hayashita, T., and Zhang, Z. Y. (2001) Boronic acid fluorophore/ β -cyclodextrin complex sensors for selective sugar recognition in water. *Anal. Chem.* *73*, 1530–1536.
- (95) Larkin, J. D., Fossey, J. S., James, T. D., Brooks, B. R., and Bock, C. W. (2010) A

computational investigation of the nitrogen–boron interaction in *o*–(N,N–dialkylaminomethyl)arylboronate systems. *J. Phys. Chem.* *114*, 12531–12539.

(96) Collins, B. E., Metola, P., and Anslyn, E. V. (2013) On the rate of boronate ester formation in ortho–aminomethyl–functionalised phenyl boronic acids. *Supramol Chem.* *25*, 79–86.

(97) Cao, H., and Heagy, M. D. (2004) Fluorescent chemosensors for carbohydrates: a decade's worth of bright spies for saccharides in review. *J. Fluoresc.* *14*, 569–584.

(98) James, T. D., Sandanayake, K. R. A. S., and Shinkai, S. (1994) A glucose-selective molecular fluorescence sensor. *Angew. Chem., Int. Ed.* *33*, 2207–2209.

(99) James, T. D., Sandanayake, K. R. A. S., and Shinkai, S. (1995) Chiral discrimination of monosaccharides using a fluorescent molecular sensor. *Nature.* *374*, 345–347.

(100) Wulff, G. (1995) Molecular imprinting in cross-linked materials with the aid of molecular templates—a way towards artificial antibodies. *Angew. Chem., Int. Ed.* *34*, 1812–1832.

(101) Tsukagoshi, K., and Shinkai, S. (1991) Specific complexation with mono– and disaccharides that can be detected by circular dichroism. *J. Org. Chem.* *56*, 4089–4091.

(102) Eggert, H., Frederiksen, J., Morin, A. C., and Norrild, C. J. (1999) A new glucose–selective fluorescent bisboronic acid. First report of strong α –furanose complexation in aqueous solution at physiological pH. *J. Org. Chem.* *64*, 3846–3852.

(103) Liu, Y., Deng, C., Tang, L., Qin, A., and Hu, R. (2010) Specific detection of D–glucose by a tetraphenylethene–based fluorescent sensor. *J. Am. Chem. Soc.* *133*, 660–663.

(104) Pal, A., Bérubé, M., and Hall, D. G. (2010) Design, synthesis, and screening of a library of peptidyl bis(boroxoles) as oligosaccharide receptors in water: identification of a receptor for the tumor marker TF–antigen disaccharide. *Angew. Chem., Int. Ed.* *49*, 1492–1495.

(105) Stones, D., Manku, S., and Lu, X. (2004) Modular solid-phase synthetic approach to optimize structural and electronic properties of oligoboronic acid receptors and sensors for the aqueous recognition. *Chem. Eur. J.* *10*, 92–100.

(106) Bérubé, M., Dowlut, M., and Hall, D. G. (2008) Benzoboroxoles as efficient glycopyranoside–binding agents in physiological conditions: structure and selectivity of

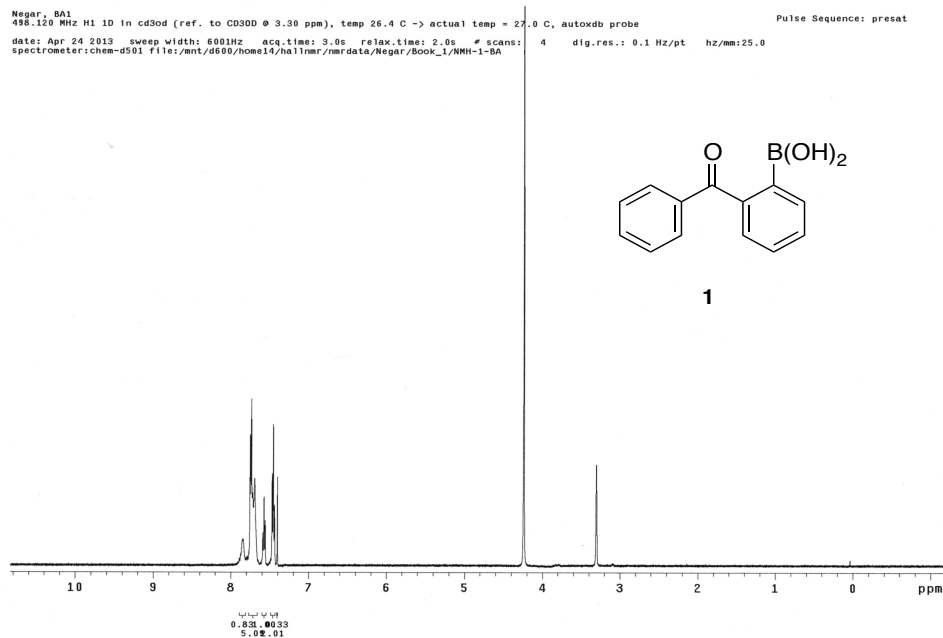
- complex formation. *J. Org. Chem.* 73, 6471–6479.
- (107) Huang, Y. J., Ouyang, W. J., Wu, X., Li, Z., Fossey, J. S., James, T. D., and Jiang, Y. B. (2013) Glucose sensing *via* aggregation and the use of “knock-out” binding to improve selectivity. *J. Am. Chem. Soc.* 135, 1700–1703.
- (108) Huang, L. L., Jin, Y. J., Zhao, D., Yu, C., Hao, J., and Xie, H. Y. (2014) A fast and biocompatible living virus labeling method based on sialic acid–phenylboronic acid recognition system. *Anal. Bioanal. Chem.* 406, 2687–2693.
- (109) Cal, P. M. S. D., Vicente, J. B., Pires, E., Coelho, A. V., Veiros, L. F., Cordeiro, C., and Gois, P. M. P. (2012) Iminoboronates: a new strategy for reversible protein modification. *J. Am. Chem. Soc.* 134, 10299–10305.
- (110) McFarland J. M., and Francis, M. B. (2005) Reductive alkylation of proteins using iridium catalyzed transfer hydrogenation. *J. Am. Chem. Soc.* 127, 13490–13491.
- (111) Raindlová, V., Pohl, R., and Hocek, M. (2012) Synthesis of aldehyde-linked nucleotides and DNA and their bioconjugations with lysine and peptides through reductive amination. *Chem. Eur. J.* 18, 4080–4087.
- (112) Smith, M. E. B., Schumacher, F. F., Ryan, C. P., Tedaldi, L. M., Papaioannou, D., Waksman, G., Caddick, S., and Baker, J. R. (2010) Protein modification, bioconjugation, and disulfide bridging using bromomaleimides. *J. Am. Chem. Soc.* 132, 1960–1965.
- (113) Zhu, L., Shabbir, S. H., Gray, M., and Lynch, V. M. (2006) A structural investigation of the NB interaction in an *o*-(N, N-dialkylaminomethyl) arylboronate system. *J. Am. Chem. Soc.* 128, 1222–1232.
- (114) Cal, P. M. S. D., Frade, R. F. M., Chudasama, V., Cordeiro, C., Caddick, S., and Gois, P. M. P. (2014) Targeting cancer cells with folic acid–iminoboronate fluorescent conjugates. *Chem. Commun.* 50, 5261–5263.
- (115) Halo, T. L., Appelbaum, J., Hobert, E. M., Balkin, D. M., and Schepartz, A. (2009) Selective recognition of protein tetraserine motifs with a cell-permeable, pro-fluorescent bis-boronic acid. *J. Am. Chem. Soc.* 131, 438–439.
- (116) Cal, P. M. S. D., Vicente, J. B., Pires, E., Coelho, A. V., Veiros, L. F., Cordeiro, C., and Gois, P. M. P. (2012) Iminoboronates: a new strategy for reversible protein modification. *J. Am. Chem. Soc.* 134, 10299–10305.
- (117) Cal, P. M. S. D., Frade, R. F. M., Chudasama, V., Cordeiro, C., Caddick, S., and

- Gois, P. M. P. (2014) Targeting cancer cells with folic acid–iminoboronate fluorescent conjugates. *Chem. Commun.* 50, 5261–5263.
- (118) Zheng, H., Lejkowski, M., and Hall, G. D. (2011) Mild and selective boronic acid catalyzed 1,3-transposition of allylic alcohols and Meyer-Schuster rearrangement of propargylic alcohols. *Chem. Sci.* 2, 1305-1310.
- (119) Wada, T., Muckerman, T. J., Fujitab, E., Tanaka, K. (2011) Substituents dependent capability of bis (ruthenium-dioxolene-terpyridine) complexes toward water oxidation. *Dalton Trans.* 40, 2225-2233.
- (120) Adeogun, A. I., Odozi, N. W., Obiegbedi N. O., and Bello O. S. (2008) Solvents effect on $n \rightarrow \pi^*$ and $\pi \rightarrow \pi^*$ transition of 9-fluorenone. *Afr. J. Biotechnol.* 7, 2736-2738.
- (121) Cleavage, deprotection, and isolation of peptides after fmoc synthesis. *Applied Biosystems.*
- (122) Cochran, A. G., Skelton, N. J., and Starovasnik, M. A. (2001) Tryptophan zippers: stable, monomeric β -hairpins. *Proc. Nat. Acad. Sci.* 98, 5578–5583.
- (123) Cheng, Z., Campbell, E. R. (2009) An engineered tryptophan zipper type peptide as a molecular recognition scaffold. *J. Pept. Sci.* 15, 523–532.
- (124) Dewar, J. S. M., Zoebisch, G. E., Healy, F. E., and Stewart, J. P. J. (1985) Development and use of quantum mechanical molecular models. 76. AM1: a new general purpose quantum mechanical molecular model. *J. Am. Chem. Soc.* 107, 3902–3909.
- (125) Suenaga, M. (2005) Facio: new computational chemistry environment for PC GAMESS. *J. Comput. Chem. Jpn.* 4, 25-32.
- (126) Schmidt, W. M., Baldrige, K. K., Boatz, A. J., Elbert, T. S., Gordon, S. M., Jensen, H. J., Koseki, S., Matsunaga, N., Nguyen, A. H., Su, S., Windus, L. T., Dupuis, M., and Montgomery A. J. (1993) General atomic and molecular electronic structure system. *J. Comput. Chem.* 14, 1347-1363.
- (127) Springsteen, G., and Wang, B. (2002) A detailed examination of boronic acid–diol complexation. *Tetrahedron.* 58, 5291–5300.
- (128) Stenzel, H. M. (2013) Bioconjugation using thiols: old chemistry rediscovered to connect polymers with nature’s building blocks. *ACS Macro Lett.* 2, 14–1.
- (129) Stephanopoulos, N., and Francis, B. M. (2011) Choosing an effective protein bioconjugation strategy. *Nat. Chem. Biol.* 7, 876–884.

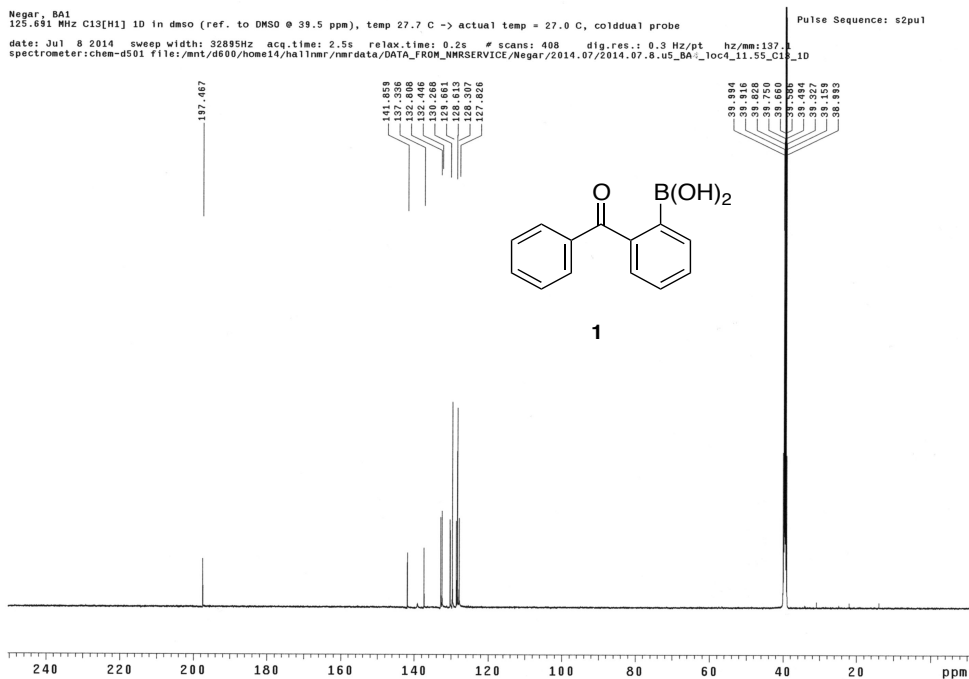
- (130) Jones, W. M., Strickland, A. R., Schumacher, F. F., Caddick, S., Baker, R. J., Gibson, I. M., and Haddleton, M. D. (2012) Polymeric dibromomaleimides as extremely efficient disulfide bridging bioconjugation and pegylation agents. *J. Am. Chem. Soc.* 134, 1847–1852.
- (131) Adzima, J. B. and Bowman N. C. (2012) The emerging role of click reactions in chemical and biological engineering. *AIChE J.* 58, 10, 2952–2965.
- (132) Fei, D. X., Zhou, Z., Li, W., Zhu, M, Y., and Shen, K, J. (2012) Buchwald–Hartwig coupling/Michael addition reactions: one-pot synthesis of 1,2-disubstituted 4-quinolones from chalcones and primary amines. *Eur. J. Org. Chem.* 3001–3008.
- (133) Cheng, U., Zhang, X., Xiang, J., Wang, Y., Zheng, C., Lu, Z., and Li, C. (2012) Development of novel self-assembled poly (3-acrylamidophenylboronic acid)/poly (2 lactobionamidoethyl methacrylate) hybrid nanoparticles for improving nasal adsorption of insulin. *Soft Matter.* 8, 765-773.
- (134) Kim, Y., Ho, S. O., Gassman, N. R., Korlann, Y., Landorf, E.V., Collart, F. R., and Weiss, S. (2008) Efficient site-specific labeling of proteins *via* cysteines. *Bioconjugate Chem.* 19, 786–791.
- (135) Partis, M., Griffiths, D., Roberts, G., and Beechey, R. (1983) Cross-linking of protein by co-maleimido alkanoyl N-Hydroxysuccinimido esters. *J. Protein Chem.* 2, 263–277.
- (136) Kakwere, H., and Perrier, S. Orthogonal “relay” reactions for designing functionalized soft nanoparticles. (2009) *J. Am. Chem. Soc.* 131, 1889-95.
- (137) Corrie, J. E. T. (1994) Thiol-reactive fluorescent probes for protein labelling. *J. Chem. Soc., Perkin Trans. 1*, 297-2982.
- (138) Halo, T. L., Appelbaum, J., Hobert, E. M., Balkin, D. M., and Schepartz, A. (2009) Selective recognition of protein tetraserine motifs with a cell-permeable, pro-fluorescent bis-boronic acid. *J. Am. Chem. Soc.* 131, 438–439.
- (139) Tanaka, F., Fuller, R., Asawapornmongkol, L., Warsinke, A., Gobuty, S., and Barbas, C. F. (2007) Development of a small peptide tag for covalent labeling of proteins. *Bioconjugate Chem.* 18,1318–1324.

Appendix 1 Selected copies of NMR spectra

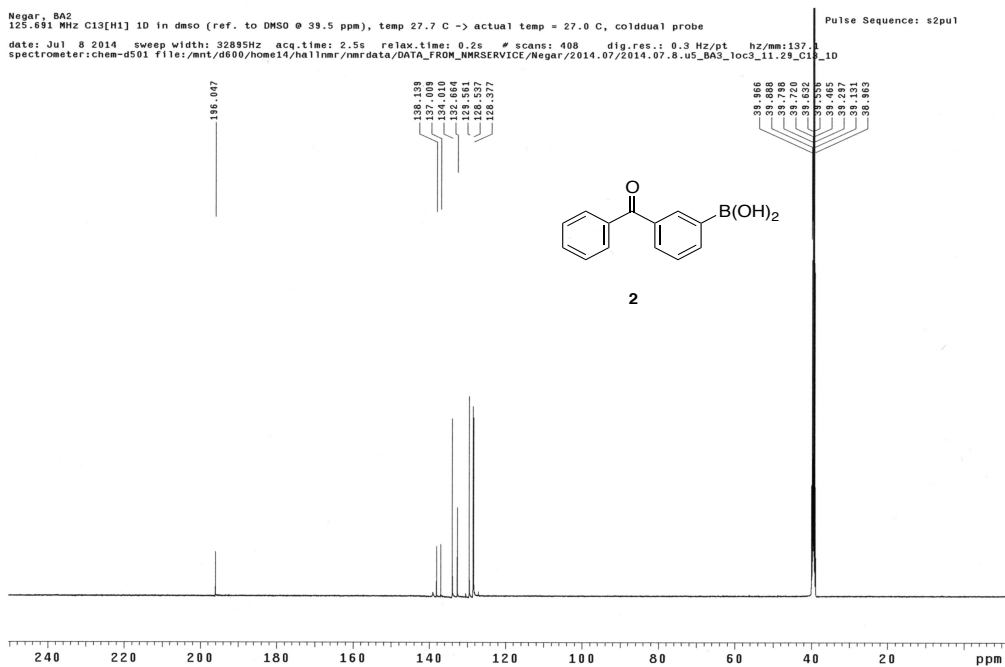
^1H NMR of 2-benzoylphenyl boronic acid in CD_3OD (one drop D_2O) at 25°C



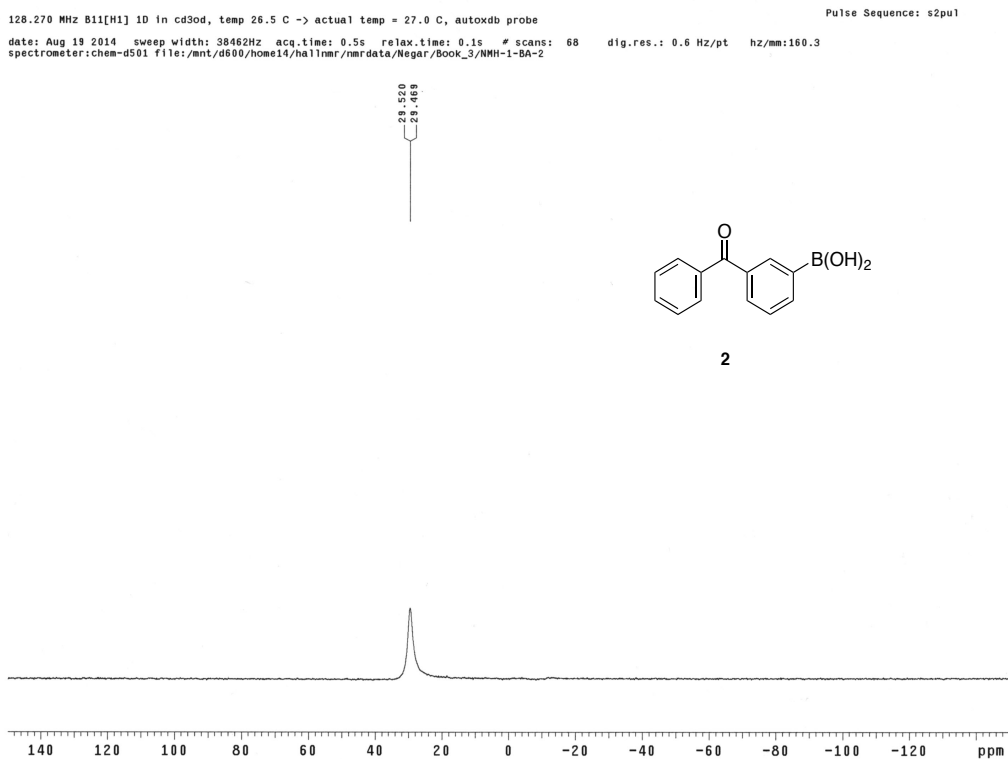
^{13}C NMR of 2-benzoylphenyl boronic acid in $\text{DMSO}-d_6$ (one drop D_2O) at 25°C



¹³C NMR of 3-benzoylphenyl boronic acid in DMSO-*d*₆ (one drop D₂O) at 25 °C

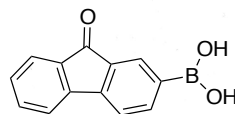
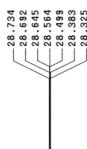


¹¹B NMR of 3-benzoylphenyl boronic acid in CD₃OD (one drop D₂O) at 25 °C

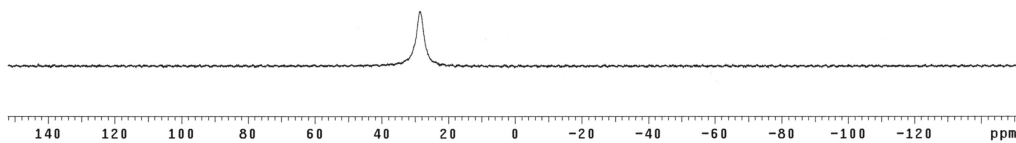


¹³B NMR of 9-fluorenone-2-boronic acid (4) in CD₃OD (one drop D₂O) at 25 °C

BA4
128.331 MHz B11[H1] 1D in cd3od, temp 25.9 C -> actual temp = 27.0 C, onenmr probe Pulse Sequence: s2pu1
date: Jul 30 2013 sweep width: 39062Hz acq.time: 1.0s relax.time: 0.1s # scans: 64 dig.res.: 0.3 Hz/pt hz/mm:162.8
spectrometer:chem-d501 file:/mnt/d600/home14/hallnmr/nmrdata/Negar/BOOK_1/NMH-1-176bnmr

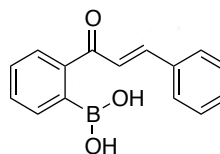


4

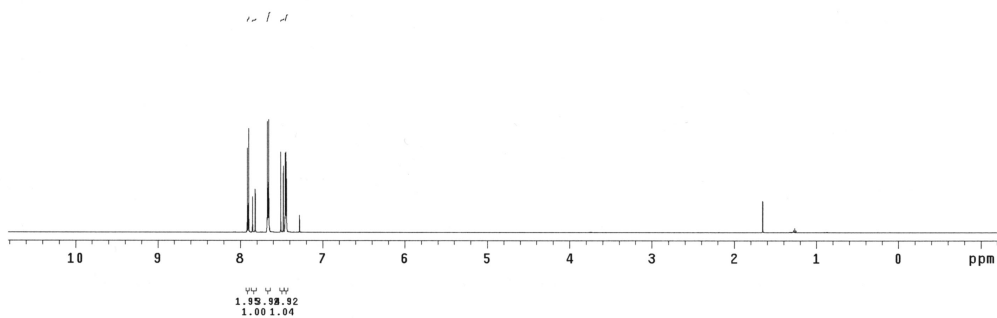


¹H NMR of (*E*)-2-boronic acid-chalcone (1) in CDCl₃ (one drop D₂O) at 25 °C

Negar, NMH-2-1
400.118 MHz H1 1D in cdc13 (ref. to CDC13 @ 7.26 ppm), temp 26.4 C -> actual temp = 27.0 C, autotdb probe Pulse Sequence: s2pu1
date: Aug 1 2013 sweep width: 6001Hz acq.time: 5.0s relax.time: 0.1s # scans: 16 dig.res.: 0.1 Hz/pt hz/mm:25.0
spectrometer:chem-d501 file:/mnt/d600/home14/hallnmr/nmrdata/Negar/NMH-1-184HNMR

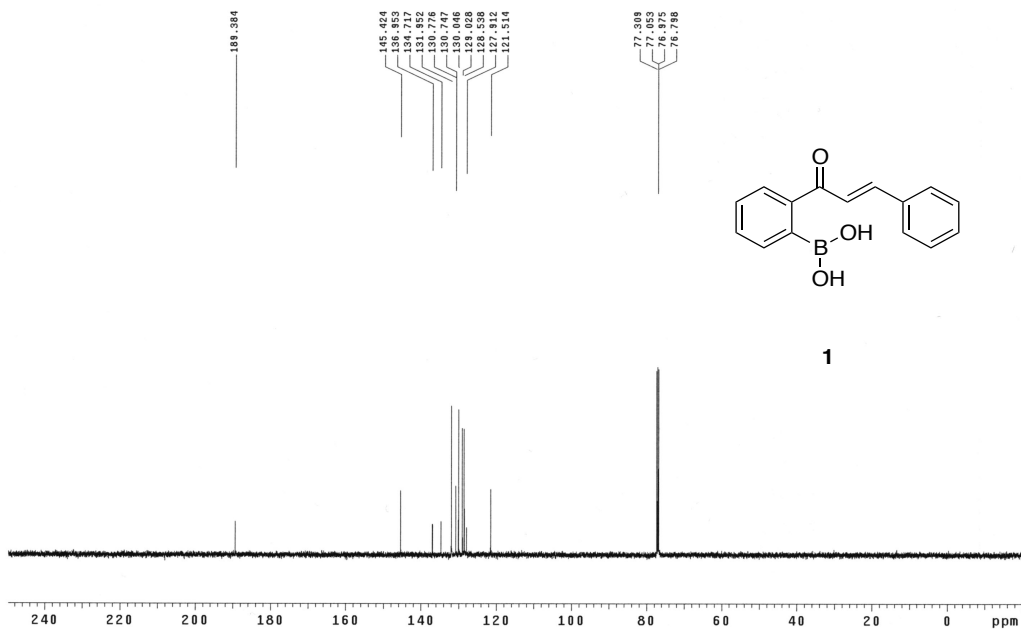


1



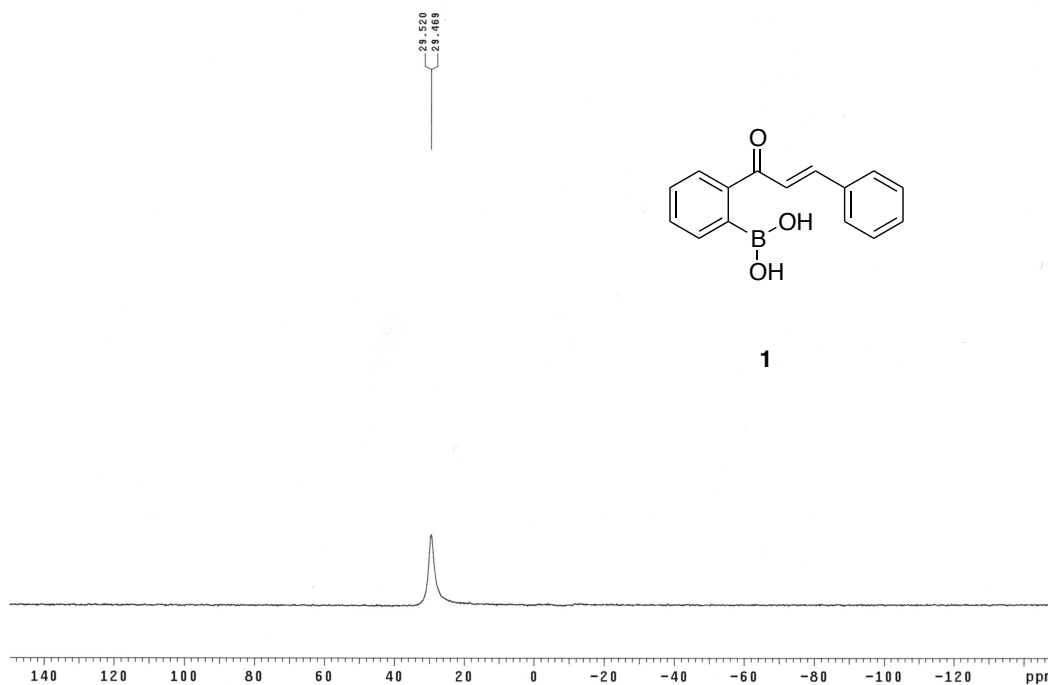
¹³C NMR of (*E*)-2-boronic acid-chalcone (1) in CDCl₃ (one drop D₂O) at 25 °C

Negar, NMH-2-1
125.266 MHz C13[H1] 1D in cdc13 (ref. to CDC13 @ 77.06 ppm), temp 26.4 C -> actual temp = 27.0 C, autotdb probe Pulse Sequence: s2pu1
date: Aug 1 2013 sweep width: 33827Hz acq.time: 2.5s relax.time: 0.1s # scans: 44 dig.res.: 0.3 Hz/pt hz/mm:140.9
spectrometer:chem-d501 file:/mnt/d600/home14/hallnmr/nmrdata/Negar/NMH-1-184CNMR



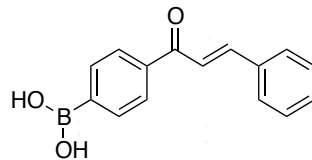
¹¹B NMR of (*E*)-2-boronic acid-chalcone (1) in CD₃OD (one drop D₂O) at 25 °C

Negar, NMH-2-1
128.270 MHz B11[H1] 1D in cd3od, temp 26.5 C -> actual temp = 27.0 C, autotdb probe Pulse Sequence: s2pu1
date: Aug 19 2014 sweep width: 38462Hz acq.time: 0.5s relax.time: 0.1s # scans: 68 dig.res.: 0.6 Hz/pt hz/mm:160.3
spectrometer:chem-d501 file:/mnt/d600/home14/hallnmr/nmrdata/Negar/Book_3/NMH-1-BA-2

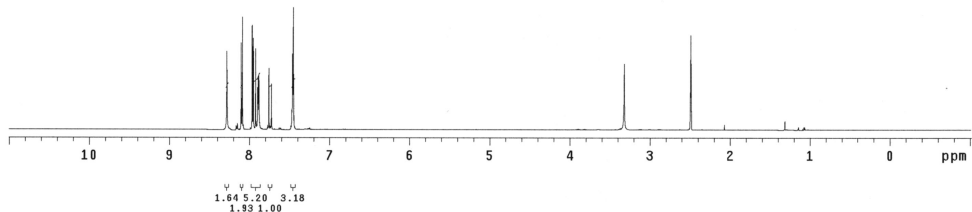


¹H NMR of (*E*)-4-boronic acid-chalcone (3) in DMSO-*d*₆ (one drop D₂O) at 25 °C

Negar, NMH-2-2
499.809 MHz H1 PRESAT in dms0 (ref. to DMSO @ 2.49 ppm), temp 27.7 C -> actual temp = 27.0 C, colddual probe Pulse Sequence: PRESAT
date: Aug 6 2014 sweep width: 6010Hz acq.time: 5.0s relax.time: 2.1s # scans: 52 dig.res.: 0.2 Hz/pt hz/mm:25.0
spectrometer:chem-d501 file:/mnt/d600/home14/hallnmr/nmrdata/DATA_FROM_NMRSERVICE/Negar/2014.08/2014.08.6.u5_NMH-2-3_loc6_03.10_H1_1D

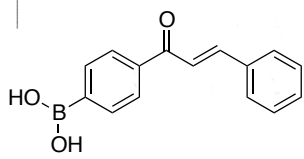


2

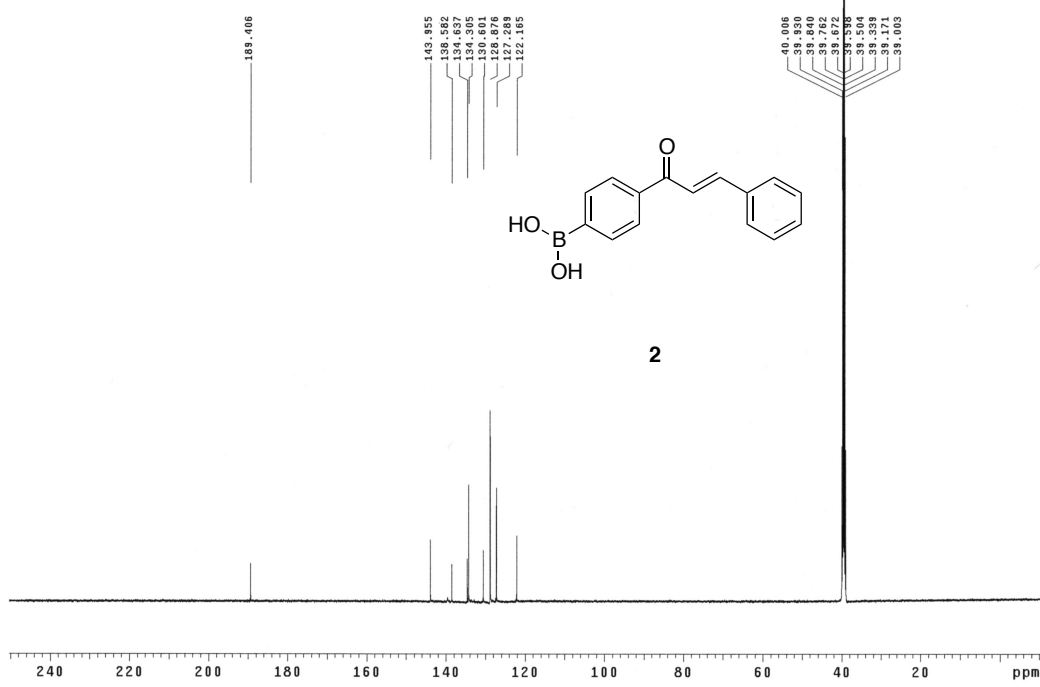


¹³C NMR of (*E*)-4-boronic acid-chalcone (3) in DMSO-*d*₆ (one drop D₂O) at 25 °C

Negar, NMH-2-2
125.691 MHz C13[H1] 1D in dms0 (ref. to DMSO @ 39.5 ppm), temp 27.7 C -> actual temp = 27.0 C, colddual probe Pulse Sequence: s2pu1
date: Aug 6 2014 sweep width: 32895Hz acq.time: 2.5s relax.time: 0.2s # scans: 188 dig.res.: 0.3 Hz/pt hz/mm:137.1
spectrometer:chem-d501 file:/mnt/d600/home14/hallnmr/nmrdata/DATA_FROM_NMRSERVICE/Negar/2014.08/2014.08.6.u5_NMH-2-3_loc6_03.15_C13_1D

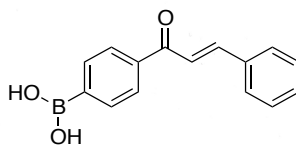


2

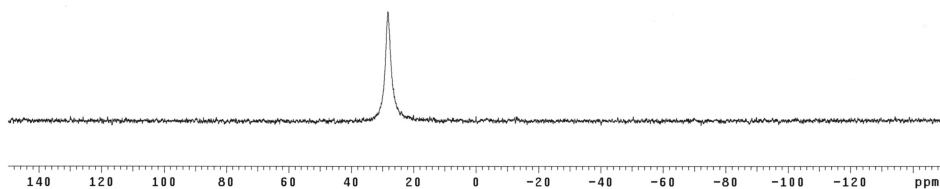


^{11}B NMR of (*E*)-4-boronic acid-chalcone (3) in CD_3OD (one drop D_2O) at 25 $^\circ\text{C}$

Negar, NMH-2-2
129.270 MHz ^{11}B in cd_3od , temp 26.5 C -> actual temp = 27.0 C, autotxdr probe Pulse Sequence: s2pu1
date: Aug 19 2014 sweep width: 38462Hz acq.time: 0.5s relax.time: 0.1s # scans: 56 dig.res.: 0.6 Hz/pt hz/mm:100.3
spectrometer:chem-d501 file:/mnt/d600/home14/hallnmr/nmrdata/Negar/BocK_3/NMH-1-5A-3

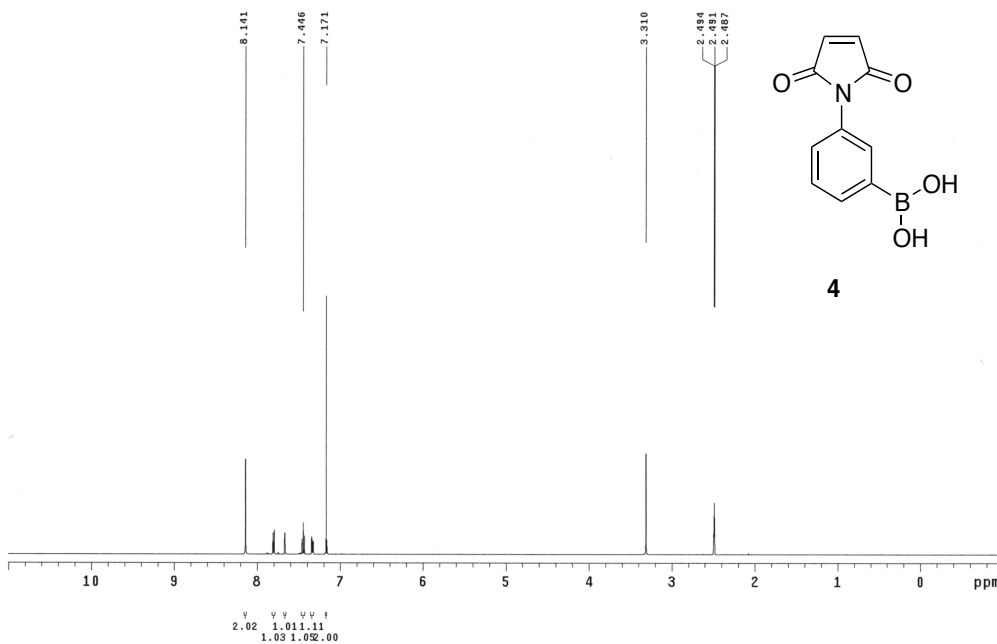


2

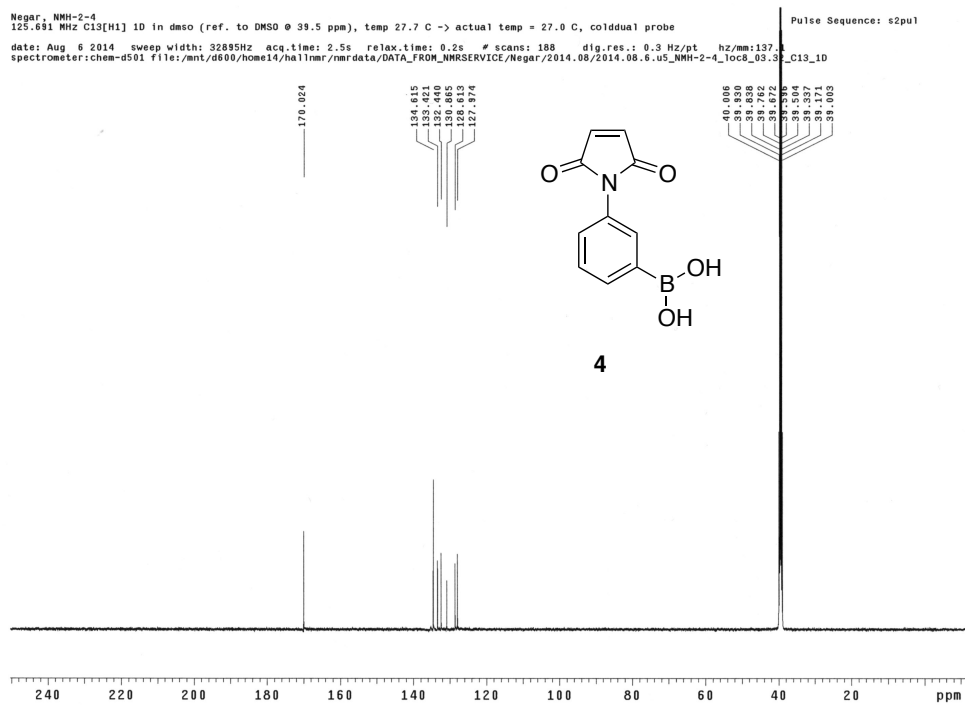


^1H NMR of 3-maleimidophenylboronic acid (4) in $\text{DMSO}-d_6$ (one drop D_2O) at 25 $^\circ\text{C}$

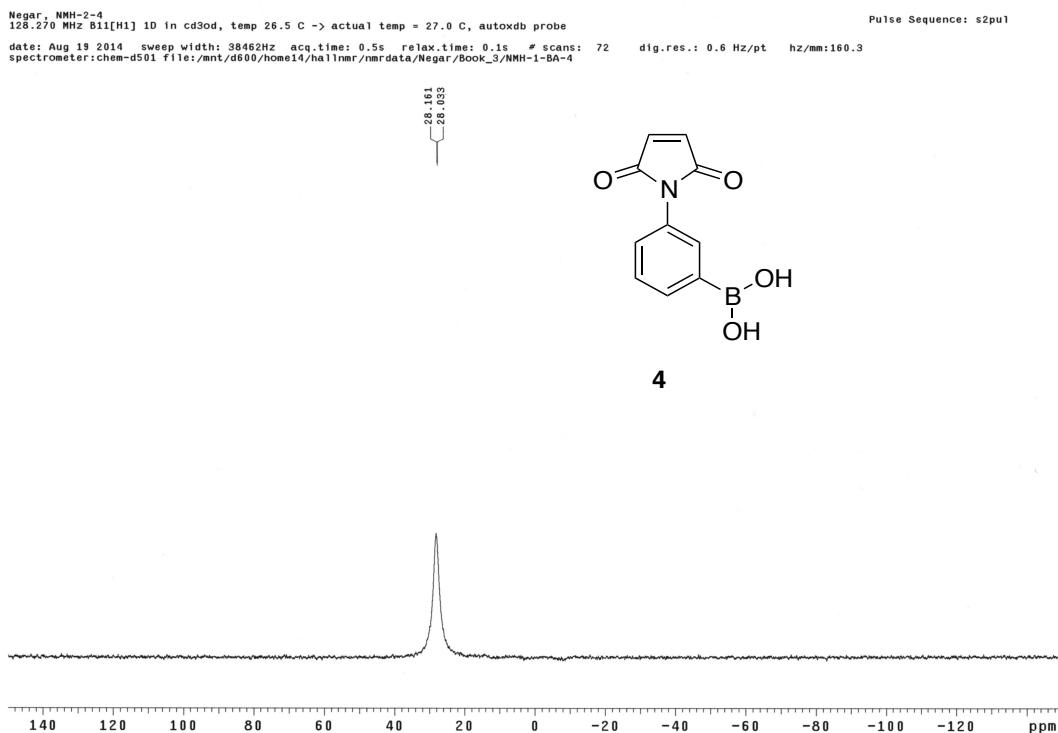
Negar, NMH-2-4
499.809 MHz ^1H PRESAT in dmsO (ref. to DMSO δ 2.49 ppm), temp 27.7 C -> actual temp = 27.0 C, colddual probe Pulse Sequence: PRESAT
date: Aug 6 2014 sweep width: 6010Hz acq.time: 5.0s relax.time: 2.1s # scans: 52 dig.res.: 0.2 Hz/pt hz/mm:25.0
spectrometer:chem-d501 file:/mnt/d600/home14/hallnmr/nmrdata/DATA_FROM_NMRSERVICE/Negar/2014.08/2014.08.6.us_NMH-2-4_Toc8_03.28_H1_10



¹³C NMR of 3-maleimidophenylboronic acid (4) in DMSO-*d*₆ (one drop D₂O) at 25 °C



¹¹B NMR of 3-maleimidophenylboronic acid (4) in CD₃OD (one drop D₂O) at 25 °C

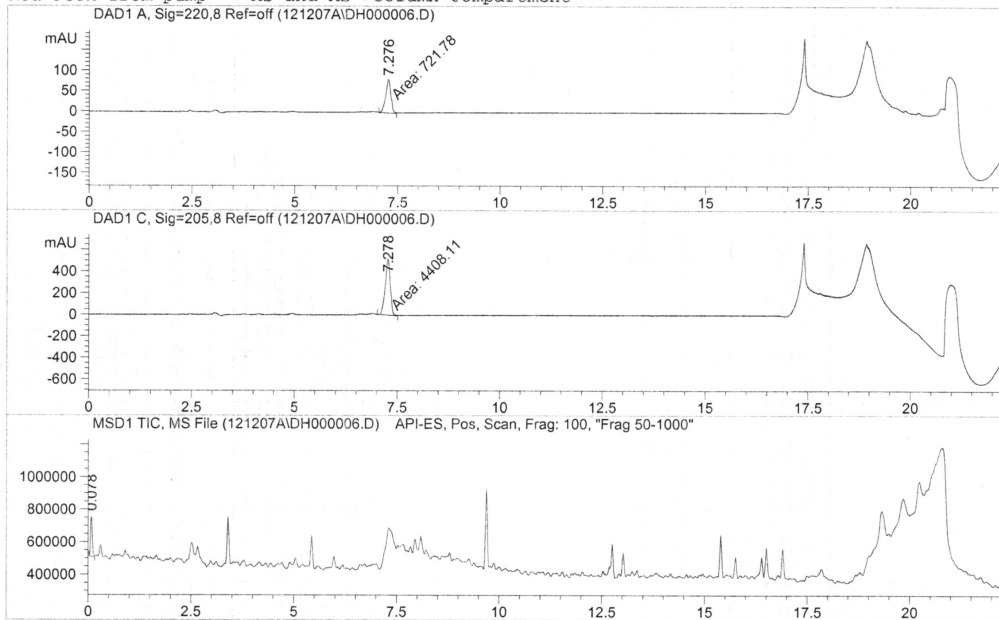


Appendix 2: HPLC-MS data for peptides

HPLC data for Chapter 2

Peptide 1: Ac-KSGSSGG-NH₂

```
=====  
Injection Date : 12/10/2012 8:35:00 PM      Seq. Line : 6  
Sample Name    : NH-pep-01                  Location  : P1-C-05  
Acq. Operator  : Ed                        Inj      : 1  
Acq. Instrument: 1100LC                     Inj Volume: 1 µl  
Different Inj Volume from Sequence !      Actual Inj Volume : 10 µl  
Acq. Method    : C:\HPCHEM\1\METHODS\GEN_ANRR.M  
Last changed   : 12/10/2012 8:22:20 PM by Ed  
Analysis Method: C:\HPCHEM\1\METHODS\GEN_ANRR.M  
Last changed   : 12/4/2012 1:45:11 AM by Ed  
Agilent SB-C18 2.1*30mm, 3.5µm; 1mL/min, 40°C  
M.P.A:0.1%GAA/FA in H2O M.P.B:0.1%GAA/FA in ACN  
Red Peek from pump -> AS and AS->column compartment  
=====
```



Fraction Information

Fraction collection off

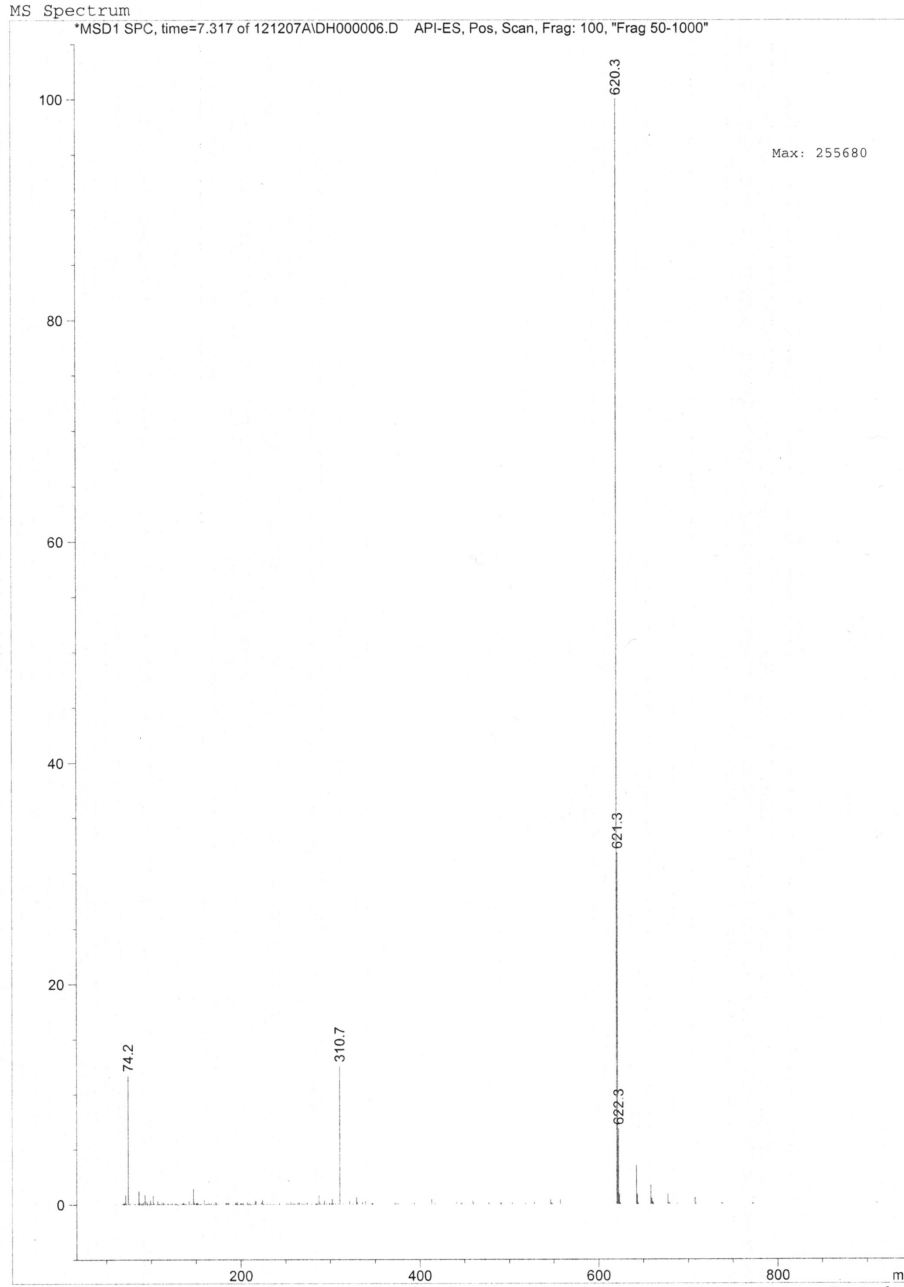
No Fractions found.

Area Percent Report

```
Sorted By      :      Signal  
Multiplier     :      1.0000  
Dilution       :      1.0000  
Use Multiplier & Dilution Factor with ISTDs
```

Mass Spectrum of peptide 1 (ES, Pos)

Print of window 80: MS Spectrum



1100LC 12/10/2012 9:32:32 PM Ed

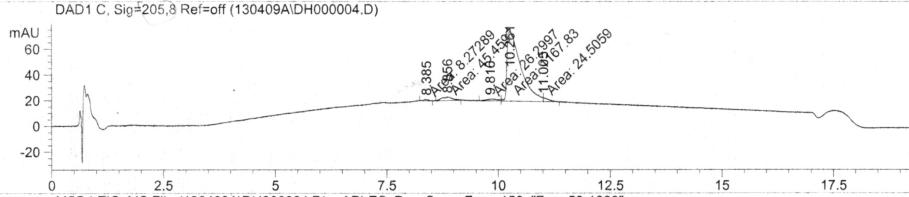
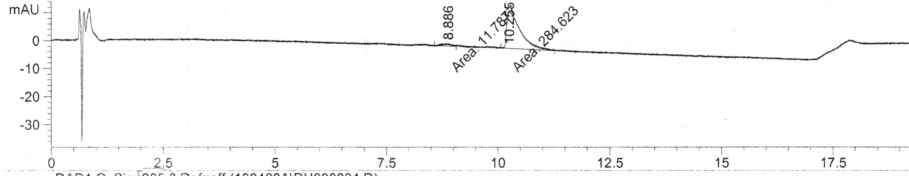
Page 1 of 1

Peptide 2: Ac-KSPSSGG-NH₂

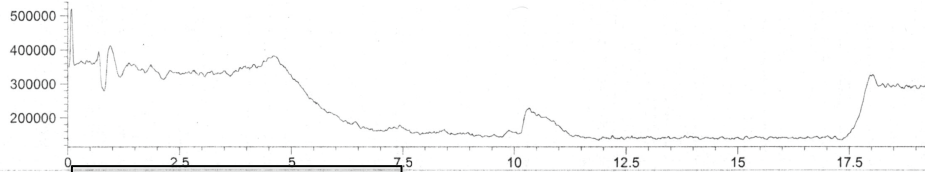
NMH-01-098 H2O and ACN GEN_HIL.m Apr 09, 2013

=====
Injection Date : 4/9/2013 2:34:33 PM Seq. Line : 4
Sample Name : NMH-01-098 Location : P1-D-01
Acq. Operator : Ed Inj : 1
Acq. Instrument : 1100LC Inj Volume : 1 µl
Different Inj Volume from Sequence ! Actual Inj Volume : 10 µl
Acq. Method : C:\HPCHEM\1\METHODS\GEN_HIL.M
Last changed : 4/9/2013 2:10:37 PM by Ed
 (modified after loading)

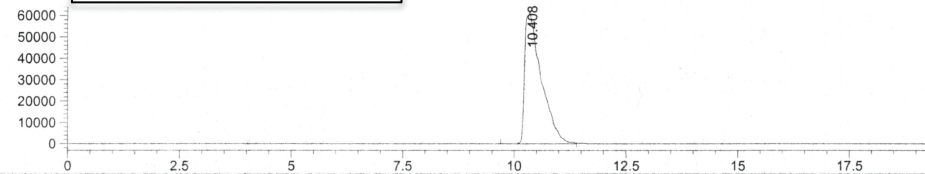
Analysis Method : C:\HPCHEM\1\METHODS\GEN_ANRR.M
Last changed : 4/9/2013 8:19:08 AM by Ed
Agilent SB-C18 2.1*30mm, 3.5µm; 1mL/min, 40'C
M.P.A:0.1%GAA/FA in H2O M.P.B:0.1%GAA/FA in ACN
Red Peak from pump -> AS and AS->column compartment
DAD1 A, Sig=220,8 Ref=off (130409AIDH000004.D)



MSD1 TIC, MS File (130409AIDH000004.D) API-ES, Pos. Scan, Frag: 150, "Frag 50-1000"



MSD1 660, EIC=859.7:860.7 (130409AIDH000004.D) API-ES, Pos. Scan, Frag: 150, "Frag 50-1000"

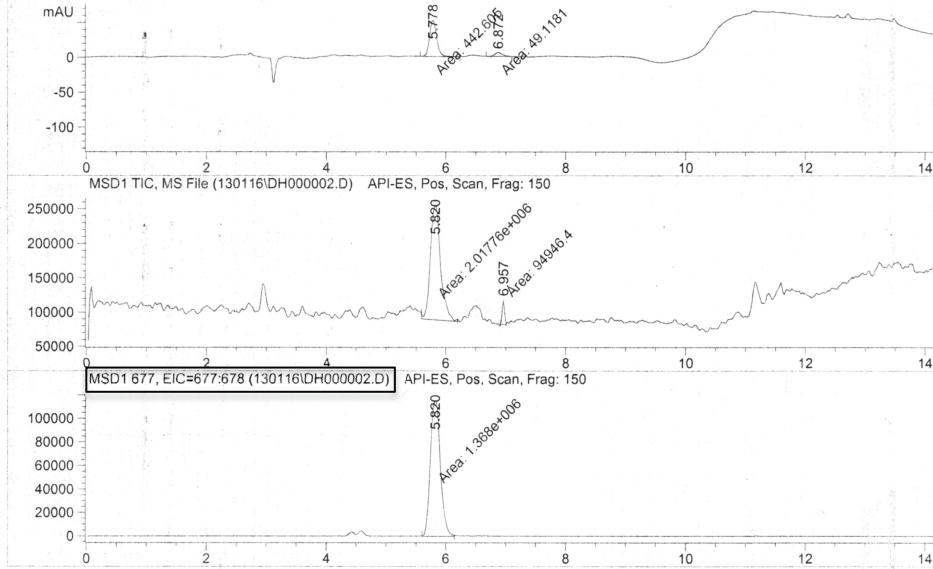


=====
Fraction Information
=====
Fraction collection off
=====
No Fractions found.
=====

Peptide 3: Ac-KSGGSSGG-NH₂

NMH-01-71 0.1% TFA in H2O and ACN GEN_ANA3.m Jan 16, 2013

```
=====
Injection Date   : 1/16/2013 10:24:15 PM      Seq. Line   :    2
Sample Name     : NMH-01-71                  Location    : P1-C-02
Acq. Operator   : Ed                        Inj         :    1
Acq. Instrument : 1100LC                    Inj Volume  : 15 µl
Different Inj. Volume from Sequence !      Actual Inj Volume : 10 µl
Acq. Method    : C:\HPCHEM\1\METHODS\GEN_ANA3.M
Last changed   : 1/16/2013 10:19:56 PM by Ed
Analysis Method : C:\HPCHEM\1\METHODS\GEN_ANRR.M
Last changed   : 1/14/2013 10:53:55 PM by Ed
Agilent SB-C18 2.1*30mm, 3.5µm; 1mL/min, 40°C
M.P.A:0.1%GAA/FA in H2O M.P.B:0.1%GAA/FA in ACN
Red Peak from pump -> AS and AS->column compartment
DAD1 A, Sig=220.8 Ref=off (130116\DH000002.D)
=====
```



Fraction Information

Fraction collection off

No Fractions found.

Area Percent Report

```
Sorted By      :      Signal
Multiplier     :      1.0000
Dilution       :      1.0000
Use Multiplier & Dilution Factor with ISTDs
```

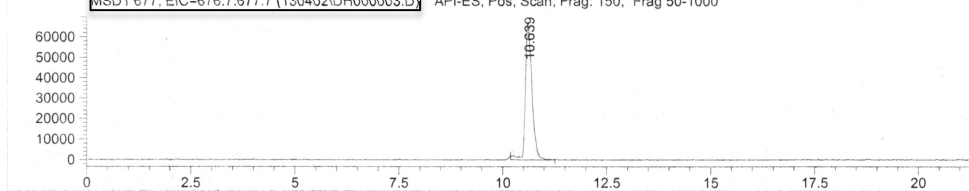
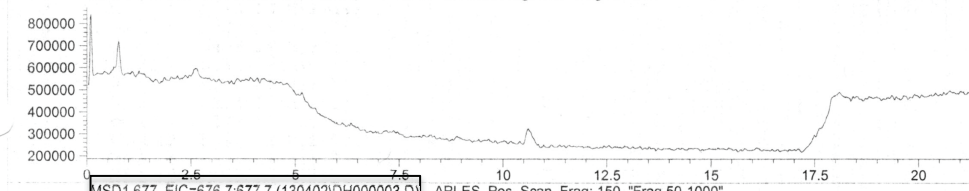
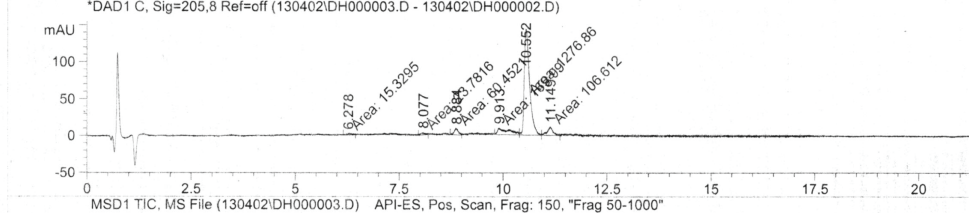
Peptide 4: AcKGGSSSSGG-NH₂

Data File C:\HPCHEM\1\DATA\130402\DH000003.D

Sample Name: NMH-01-1

NMH-01-105 H2O and ACN GEN_HIL.M Apr 02, 2013

=====
Injection Date : 4/2/2013 8:14:25 AM Seq. Line : 3
Sample Name : NMH-01-105 Location : P1-A-01
Acq. Operator : Ed Inj : 1
Acq. Instrument : 1100LC Inj Volume : 1 µl
Different Inj Volume from Sequence ! Actual Inj Volume : 2 µl
Acq. Method : C:\HPCHEM\1\METHODS\GEN_HIL.M
Last changed : 4/2/2013 7:46:06 AM by Ed
(modified after loading)
Analysis Method : C:\HPCHEM\1\METHODS\GEN_ANRR.M
Last changed : 4/2/2013 7:28:51 AM by Ed
(modified after loading)
Agilent SB-C18 2.1*30mm, 3.5µm; 1mL/min, 40°C
M.P.A:0.1%GAA/FA in H2O M.P.B:0.1%GAA/FA in ACN
Red Peak from pump -> AS and AS->column compartment
*DAD1 C, Sig=205.8 Ref=off (130402\DH000003.D - 130402\DH000002.D)



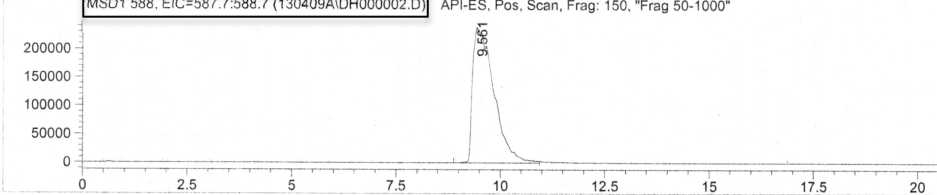
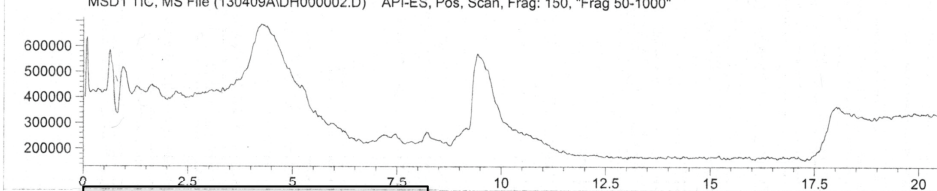
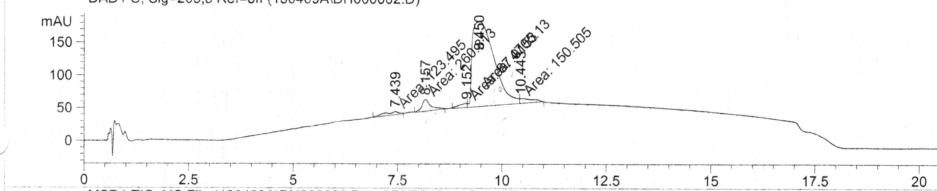
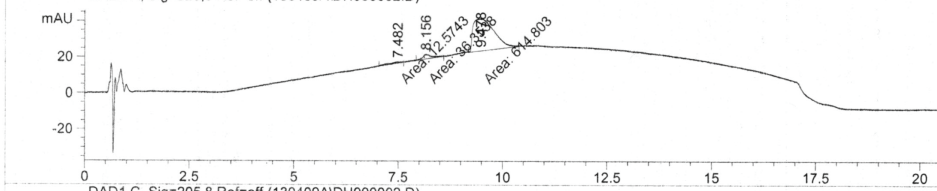
=====
Fraction Information
=====
Fraction collection off
=====
No Fractions found.
=====

=====
Area Percent Report
=====
Sorted By : Signal
Multiplier : 1.0000
Dilution : 1.0000
Use Multiplier & Dilution Factor with ISTDs

Peptide 6: Ac-KAGSGAG-NH₂

NMH-01-099 H2O and ACN GEN_HIL.m Apr 09, 2013

```
=====
Injection Date : 4/9/2013 1:48:55 PM      Seq. Line : 2
Sample Name    : NMH-01-099                Location  : P1-D-02
Acq. Operator  : Ed                        Inj      : 1
Acq. Instrument : 1100LC                    Inj Volume : 1 µl
Different Inj Volume from Sequence !      Actual Inj Volume : 10 µl
Acq. Method    : C:\HPCHEM\1\METHODS\GEN_HIL.M
Last changed   : 4/9/2013 2:10:37 PM by Ed
                (modified after loading)
Analysis Method : C:\HPCHEM\1\METHODS\GEN_ANRR.M
Last changed   : 4/9/2013 8:19:08 AM by Ed
Agilent SB-C18 2.1*30mm, 3.5µm; 1mL/min, 40'C
M.P.A:0.1%GAA/FA in H2O M.P.B:0.1%GAA/FA in ACN
Red Peak from pump -> AS and AS->column compartment
DAD1 A, Sig=220,8 Ref=off (130409A\DH000002.D)
=====
```

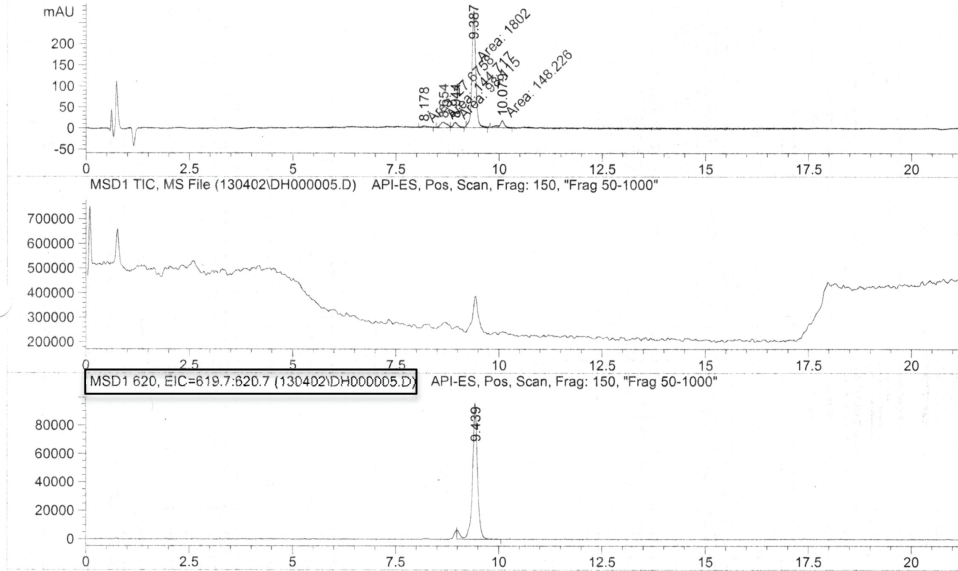


```
=====
Fraction Information
=====
Fraction collection off
=====
No Fractions found.
=====
```

Peptide 7: Ac-ASGGSSGG-NH₂

NMH-01-108 H2O and ACN GEN_HIL.m Apr 02, 2013

```
=====  
Injection Date : 4/2/2013 9:01:17 AM      Seq. Line : 5  
Sample Name    : NMH-01-108              Location  : P1-A-03  
Acq. Operator  : Ed                      Inj      : 1  
Acq. Instrument : 1100LC                 Inj Volume : 1 µl  
Different Inj Volume from Sequence !      Actual Inj Volume : 2 µl  
Acq. Method    : C:\HPCHEM\1\METHODS\GEN_HIL.M  
Last changed   : 4/2/2013 7:46:06 AM by Ed  
                (modified after loading)  
Analysis Method : C:\HPCHEM\1\METHODS\GEN_ANRR.M  
Last changed   : 4/2/2013 7:28:51 AM by Ed  
                (modified after loading)  
Agilent SB-C18 2.1*30mm, 3.5µm; 1mL/min, 40'C  
M.P.A:0.1%GAA/FA in H2O M.P.B:0.1%GAA/FA in ACN  
Red Peek from pump -> AS and AS->column compartment  
*DAD1 C, Sig=205.8 Ref=off (130402\DH000005.D - 130402\DH000002.D)
```



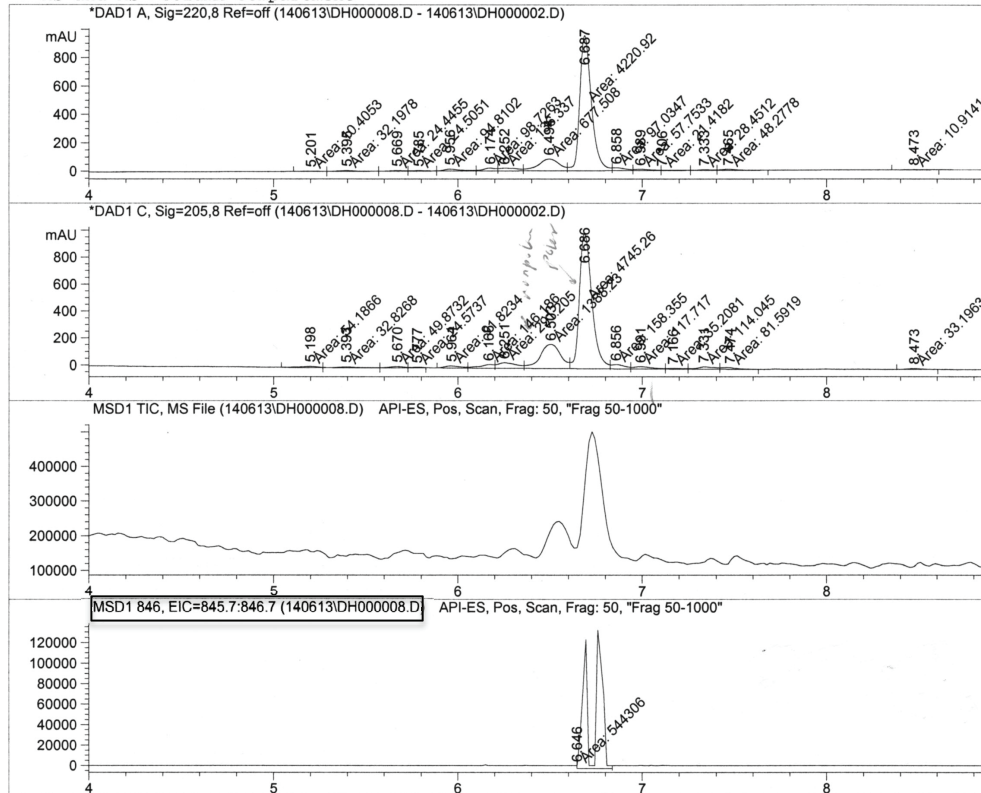
```
=====  
Fraction Information  
=====  
Fraction collection off  
=====  
No Fractions found.  
=====  
Area Percent Report  
=====  
Sorted By      : Signal  
Multiplier    : 1.0000  
Dilution      : 1.0000  
Use Multiplier & Dilution Factor with ISTDs
```


Peptide 9: AcWKPGSSSG-NH₂

NMH-1-133-S 0.1% TFA in aq and ACN GEN_HIL.M Jun 13, 2014

```

=====
Injection Date : 6/13/2014 12:45:09 PM      Seq. Line : 8
Sample Name    : NMH-1-133-S                Location  : Pl-B-05
Acq. Operator  : Ed                        Inj       : 1
Acq. Instrument: 1100LC                     Inj Volume: 1 µl
Different Inj Volume from Sequence !      Actual Inj Volume : 3 µl
Acq. Method    : C:\HPCHEM\1\METHODS\GEN_HIL.M
Last changed   : 6/13/2014 10:51:27 AM by Ed
                (modified after loading)
Analysis Method: C:\HPCHEM\1\METHODS\GEN_HIL.M
Last changed   : 6/13/2014 1:21:14 PM by Ed
                (modified after loading)
Agilent Hilic 4.6*50mm, 3.5µm; 1mL/min, 40'C
M.P.A:0.1%GAA/FA in H2O M.P.B:0.1%GAA/FA in ACN
-> AS and AS->column compartment
    
```

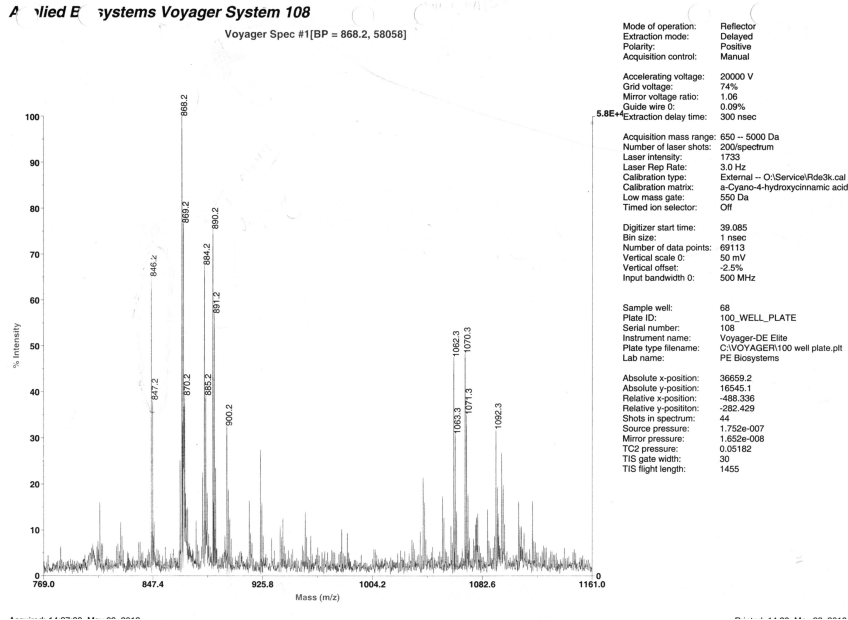


```

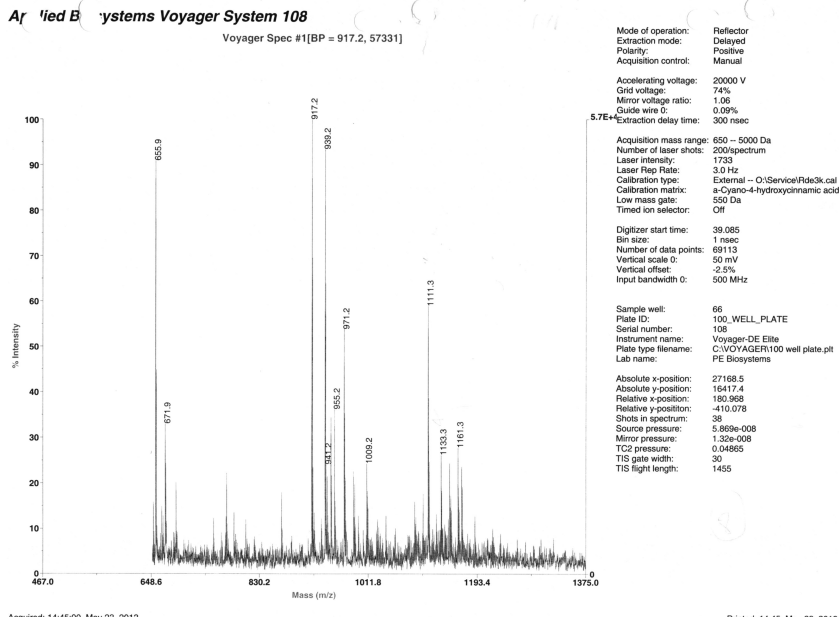
=====
Fraction Information
=====
Fraction collection off
=====
No Fractions found.
=====
    
```

MALDI-TOF data for reaction of peptide 8 and peptide 9 with 9-fluorenone-2-boronic acid (4)

Peptide 8 + 9-fluorenone-2-boronic acid (4)



Peptide 9 + 9-fluorenone-2-boronic acid (4)



Reaction of Peptide 10: KWTWSSGKWTWS + 9-fluorenone-2-boronic acid (4)

Data File C:\HPCHEM\1\DATA\130523A\DH000056.D

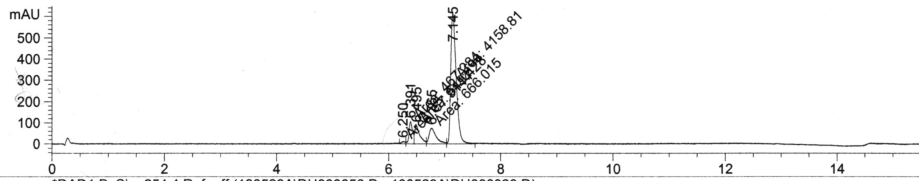
Sample Name: NMH-01-

NMH-01-145 0.1% TFA in H2O and ACN CR_C18MS.m May 24, 2013

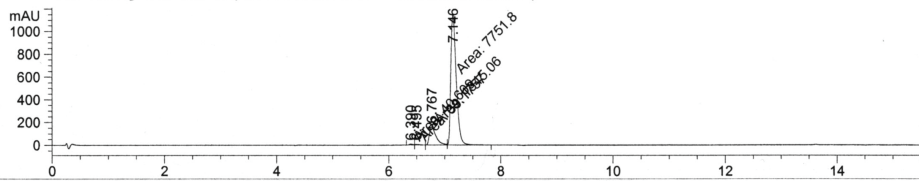
=====
Injection Date : 5/24/2013 10:14:26 AM Seq. Line : 56
Sample Name : NMH-01-145 Location : Pl-F-06
Acq. Operator : Ed Inj : 1
Acq. Instrument : 1100LC Inj Volume : 1 µl
Acq. Method : C:\HPCHEM\1\METHODS\CR_C18MS.M
Last changed : 5/24/2013 9:52:59 AM by Ed
analysis Method : C:\HPCHEM\1\METHODS\GEN_ANRR.M
Last changed : 5/24/2013 8:34:34 AM by Ed
(modified after loading)

Agilent SB-C18 2.1*30mm, 3.5µm; 1mL/min, 40'C
M.P.A:0.1%GAA/FA in H2O M.P.B:0.1%GAA/FA in ACN
Red Peak from pump -> AS and AS->column compartment

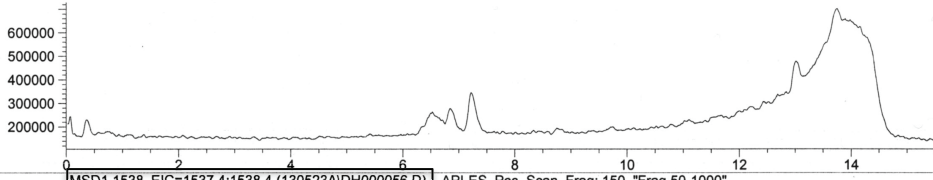
*DAD1 A, Sig=210,4 Ref=off (130523A\DH000056.D - 130523A\DH000020.D)



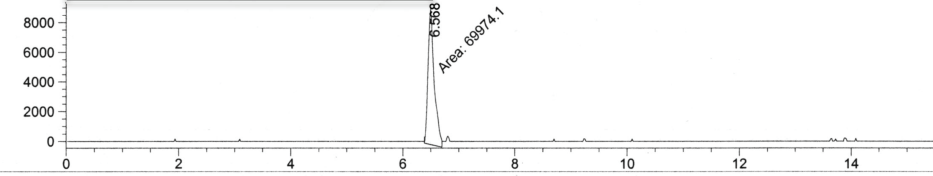
*DAD1 B, Sig=254,4 Ref=off (130523A\DH000056.D - 130523A\DH000020.D)



MSD1 TIC, MS File (130523A\DH000056.D) API-ES, Pos, Scan, Frag: 150, "Frag 50-1000"



MSD1 1538, EIC=1537.4:1538.4 (130523A\DH000056.D) API-ES, Pos, Scan, Frag: 150, "Frag 50-1000"



Fraction Information

Fraction collection off

No Fractions found.

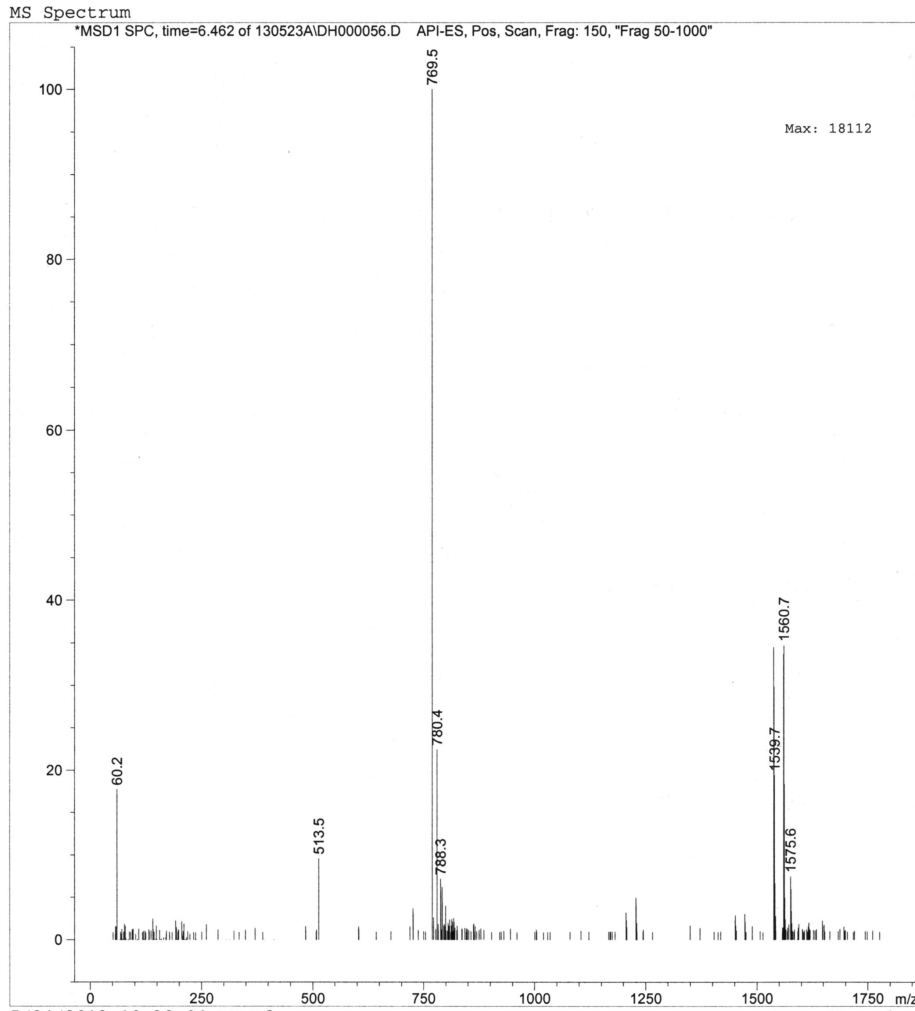
1100LC 5/24/2013 10:37:44 AM Ed

Page 1 of 2

Mass spectrum of Peptide 10 (ES, Positive)

Print of window 80: MS Spectrum
NMH-01-145 0.1% TFA in H2O and ACN CR_C18MS.m May 24,
2013

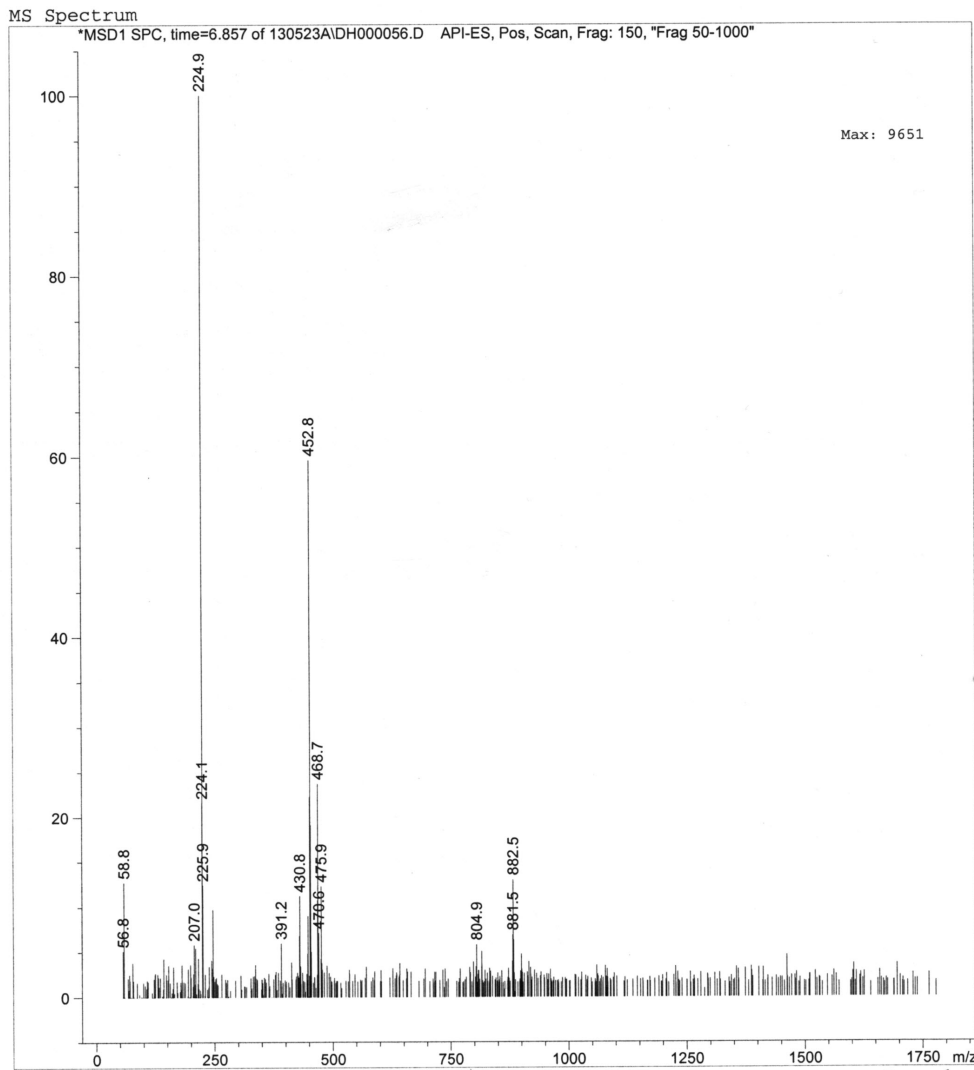
```
=====
Injection Date : 5/24/2013 10:14:26 AM      Seq. Line : 56
Sample Name    : NMH-01-145                  Location  : P1-F-06
An Operator    : Ed                          Inj      : 1
An Instrument  : 1100LC                      Inj Volume: 1 µl
Ac Method     : C:\HPCHEM\1\METHODS\CR_C18MS.M
Last changed  : 5/24/2013 9:52:59 AM by Ed
An Analysis Method: C:\HPCHEM\1\METHODS\GEN_ANRR.M
La changed    : 5/24/2013 8:34:34 AM by Ed
                (modified after loading)
Agilent SB-C18 2.1*30mm, 3.5µm; 1mL/min, 40°C
M.P.A:0.1%GAA/FA in H2O M.P.B:0.1%GAA/FA in ACN
Red Peek from pump -> AS and AS->column compartment
=====
```



Mass spectrum of 9-fluorenone-2-boronic acid (4) (ES, Positive)

Print of window 80: MS Spectrum
NMH-01-145 0.1% TFA in H2O and ACN CR_C18MS.M May 24,
2013

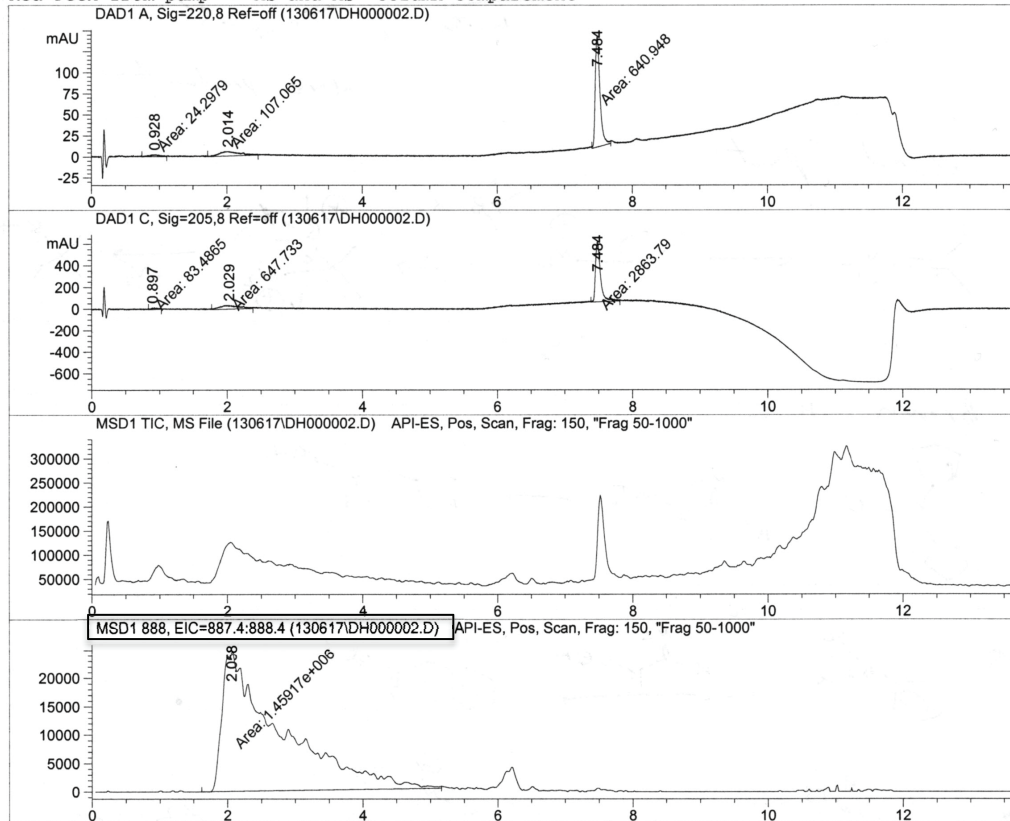
```
=====
Injection Date : 5/24/2013 10:14:26 AM      Seq. Line : 56
Sample Name    : NMH-01-145                  Location  : P1-F-06
Acq. Operator  : Ed                          Inj      : 1
Acq. Instrument: 1100LC                      Inj Volume: 1 µl
Acq. Method    : C:\HPCHEM\1\METHODS\CR_C18MS.M
Last changed   : 5/24/2013 9:52:59 AM by Ed
Analysis Method: C:\HPCHEM\1\METHODS\GEN_ANRR.M
Last changed   : 5/24/2013 8:34:34 AM by Ed
                (modified after loading)
Agilent SB-C18 2.1*30mm, 3.5µm; 1mL/min, 40'C
M.P.A:0.1%GAA/FA in H2O M.P.B:0.1%GAA/FA in ACN
Red Peek from pump -> AS and AS->column compartment
=====
```



Reaction of Peptide 11: AKAAASAASAA-NH₂ + 9-fluorenone-2-boronic acid (4)

NMH-1-157 0.1 % TFA in H₂O and ACN GEN_ANRR.M Jun 17, 2013

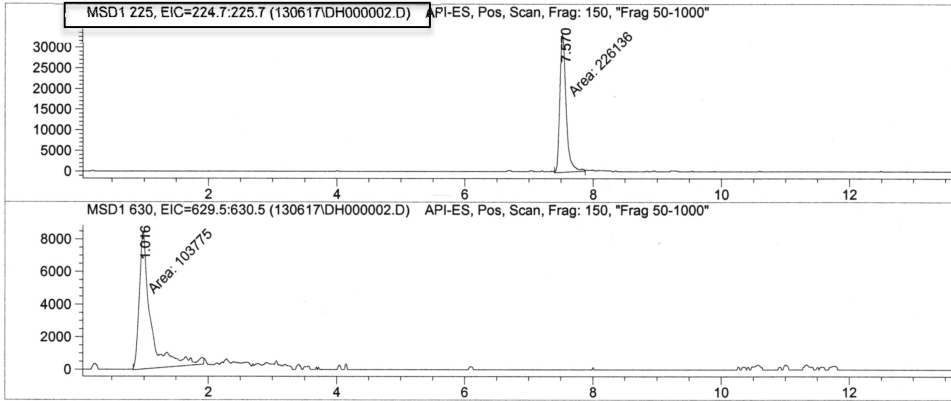
=====
Injection Date : 6/17/2013 10:20:32 AM Seq. Line : 2
Sample Name : NMH-1-157 Location : P1-D-08
Acq. Operator : Ed Inj : 1
Acq. Instrument : 1100LC Inj Volume : 1 µl
Different Inj Volume from Sequence ! Actual Inj Volume : 2 µl
Acq. Method : C:\HPCHEM\1\METHODS\GEN_ANRR.M
Last changed : 6/17/2013 10:03:48 AM by Ed
 (modified after loading)
Analysis Method : C:\HPCHEM\1\METHODS\NMH01149.M
Last changed : 6/11/2013 12:12:38 PM by Ed
Agilent SB-C18 2.1*30mm, 3.5µm; 1mL/min, 40'C
M.P.A:0.1%GAA/FA in H₂O M.P.B:0.1%GAA/FA in ACN
Red Peek from pump -> AS and AS->column compartment



Peptide 11: AKAAASAASAA-NH₂ + 9-fluorenone-2-boronic acid (4)

Data File C:\HPCHEM\1\DATA\130617\DH000002.D

Sample Name: NMH-1-1



```

=====
                        Fraction Information
=====
Fraction collection off
=====
No Fractions found.
=====

```

```

=====
                        Area Percent Report
=====

Sorted By      :      Signal
Multiplier     :      1.0000
Dilution       :      1.0000
Use Multiplier & Dilution Factor with ISTDs

```

Signal 1: DAD1 A, Sig=220,8 Ref=off

Peak #	RetTime [min]	Type	Width [min]	Area [mAU*s]	Height [mAU]	Area %
1	0.928	MM	0.1728	24.29795	2.41838	3.1461
2	2.014	MM	0.3386	107.06464	5.27050	13.8629
3	7.484	MM	0.0814	640.94763	131.22972	82.9910
Totals :				772.31021	138.91860	

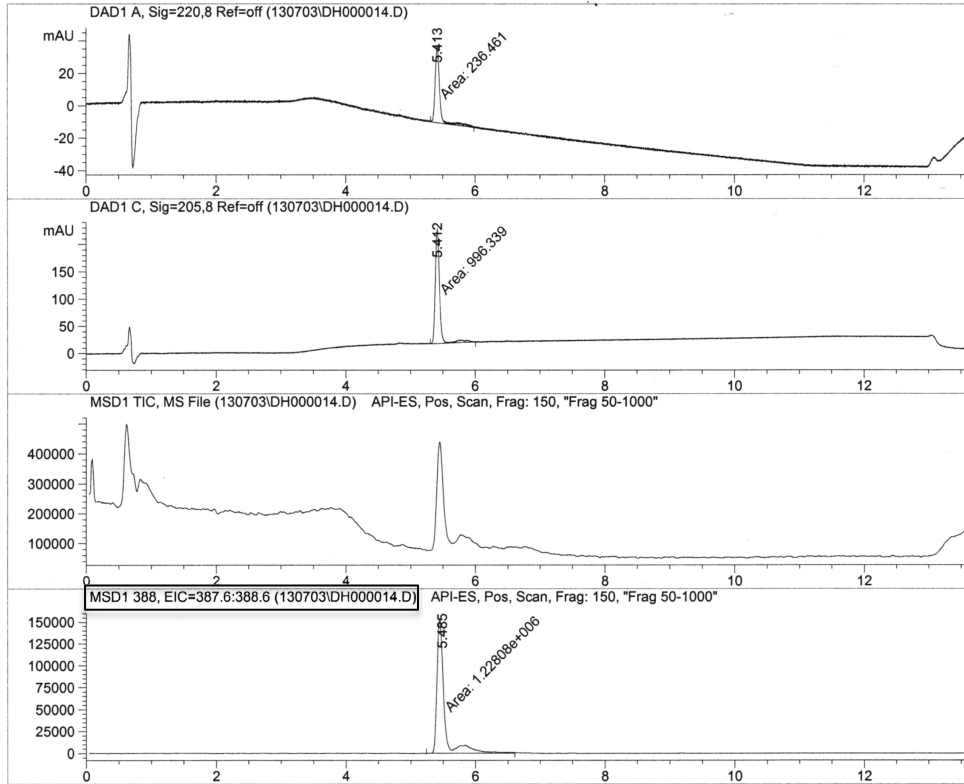
Signal 2: DAD1 C, Sig=205,8 Ref=off

Peak #	RetTime [min]	Type	Width [min]	Area [mAU*s]	Height [mAU]	Area %
1	0.897	MM	0.0810	83.48646	14.66496	2.3223
2	2.029	MM	0.3177	647.73303	33.98145	18.0176
3	7.484	MM	0.0851	2863.78540	560.56396	79.6601
Totals :				3595.00489	609.21038	

Peptide: Ac-SPGS-NH₂

SFH-02-164 0.05% AA in H2O and ACN GEN_HIL.m Jul 03, 2013

=====
Injection Date : 7/3/2013 3:32:24 PM Seq. Line : 14
Sample Name : NMH-1-164 Location : P1-E-06
Acq. Operator : Ed Inj : 1
Acq. Instrument : 1100LC Inj Volume : 1 µl
Different Inj Volume from Sequence ! Actual Inj Volume : 5 µl
Acq. Method : C:\HPCHEM\1\METHODS\GEN_HIL.M
Last changed : 6/19/2013 11:51:42 AM by Ed
Analysis Method : C:\HPCHEM\1\METHODS\CR_C18.M
Last changed : 6/21/2013 3:56:22 PM by Ed
Agilent SB-C18 2.1*30mm, 3.5µm; 0.5mL/min, 40°C
M.P.A.:H2O M.P.B: ACN
=====



=====
Area Percent Report
=====

Sorted By : Signal
Multiplier : 1.0000
Dilution : 1.0000
Use Multiplier & Dilution Factor with ISTDs

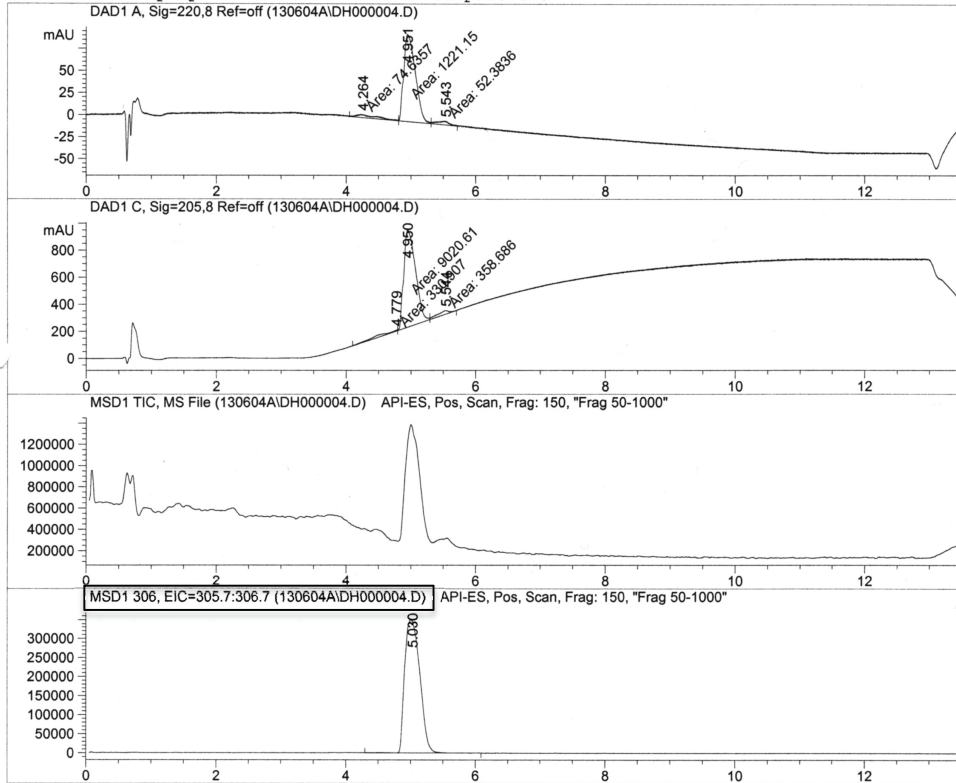
Peptide GGSS-NH₂

Data File C:\HPCHEM\1\DATA\130604A\DH000004.D

Sample Name: NMH-01-

NMH-01-135 0.1% TFA in H₂O and ACN GEN_HIL.m Jun 04, 2013

=====
Injection Date : 6/4/2013 1:40:45 PM Seq. Line : 4
Sample Name : NMH-01-135 Location : P1-A-02
Acq. Operator : Ed Inj : 1
Acq. Instrument : 1100LC Inj Volume : 1 µl
Different Inj Volume from Sequence ! Actual Inj Volume : 10 µl
Acq. Method : C:\HPCHEM\1\METHODS\GEN_HIL.M
Last changed : 6/4/2013 1:38:33 PM by Ed
Analysis Method : C:\HPCHEM\1\METHODS\GEN_ANRR.M
Last changed : 5/31/2013 1:22:52 PM by Ed
Agilent SB-C18 2.1*30mm, 3.5µm; 1mL/min, 40°C
M.P.A:0.1%GAA/FA in H₂O M.P.B:0.1%GAA/FA in ACN
Red Peak from pump -> AS and AS->column compartment

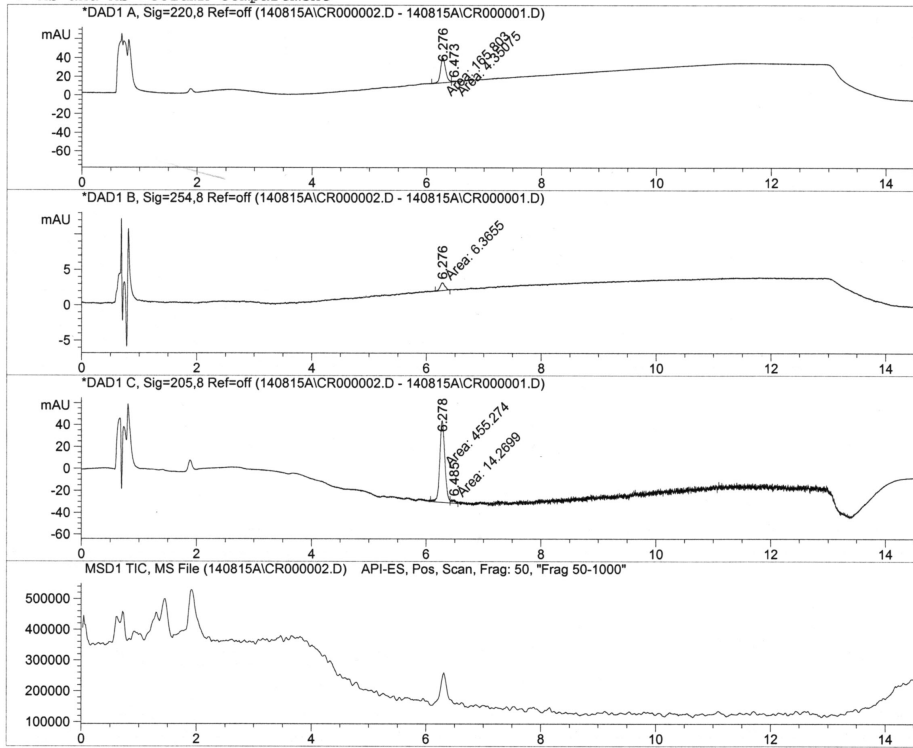


HPLC data for Chapter 3:

Peptide 1

0.1% TFA in aq and ACN GEN_HIL.m Aug 15, 2014

```
=====  
Injection Date : 8/15/2014 3:53:12 PM      Seq. Line : 2  
Sample Name    : NMH-1-183                 Location  : P1-A-01  
Acq. Operator  : Ed                       Inj      : 1  
Acq. Instrument: 1100LC                    Inj Volume: 1 µl  
Method         : C:\HPCHEM\1\METHODS\GEN_HIL.M  
Last changed   : 4/30/2014 3:38:45 PM by Ed  
Agilent Hilic 4.6*50mm, 3.5µm; 1mL/min, 40°C  
M.P.A:0.1%GAA/FA in H2O M.P.B:0.1%GAA/FA in ACN  
-> AS and AS->column compartment  
=====
```

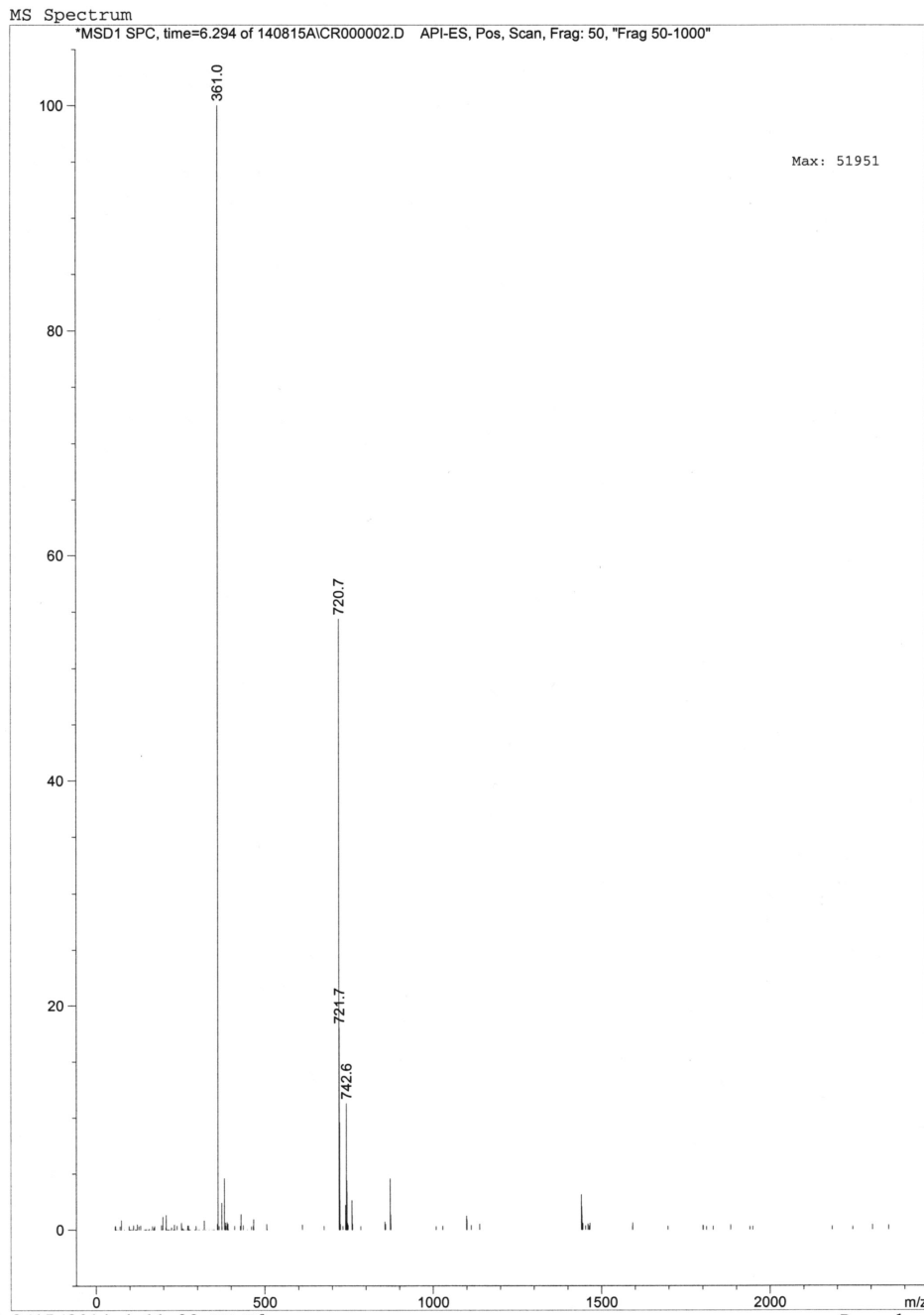


Area Percent Report

```
=====  
Sorted By      :      Signal  
Multiplier     :      1.0000  
Dilution       :      1.0000  
Use Multiplier & Dilution Factor with ISTDs  
=====
```

Mass of peptide 1 (ES, Positive)

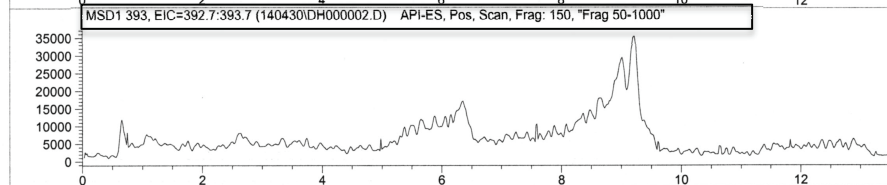
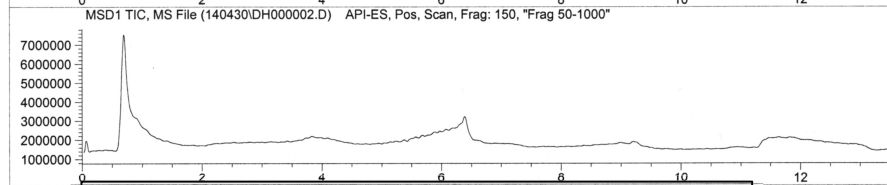
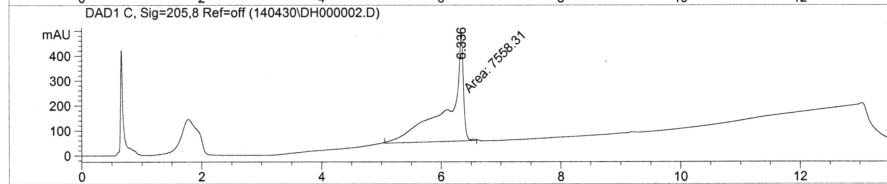
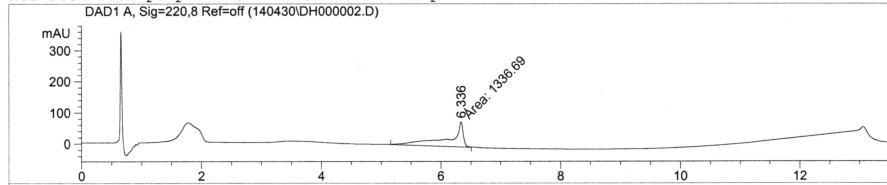
Print of window 80: MS Spectrum



Peptide 3

NMH SSC c1 0.1% AA in aq and ACN GEN_HIL.m Apr 30, 201
4

```
=====
Injection Date : 4/30/2014 10:25:08 AM      Seq. Line : 2
Sample Name    : NMH SSC c1                  Location  : P1-B-01
Acq. Operator  : Ed                          Inj       : 1
Acq. Instrument: 1100LC                       Inj Volume: 1 µl
Different Inj Volume from Sequence !      Actual Inj Volume : 20 µl
Acq. Method    : C:\HPCHEM\1\METHODS\GEN_HIL.M
Last changed   : 9/18/2013 2:47:44 PM by Ed
Analysis Method: C:\HPCHEM\1\METHODS\GEN_ANRR.M
Last changed   : 5/2/2014 4:22:35 PM by Ed
Agilent SB-C18 2.1*30mm, 3.5µm; 1mL/min, 40°C
M.P.A:0.1% AA/FA in H2O M.P.B:0.1% AA/FA in ACN
Red Peak from pump -> AS and AS->column compartment
=====
```

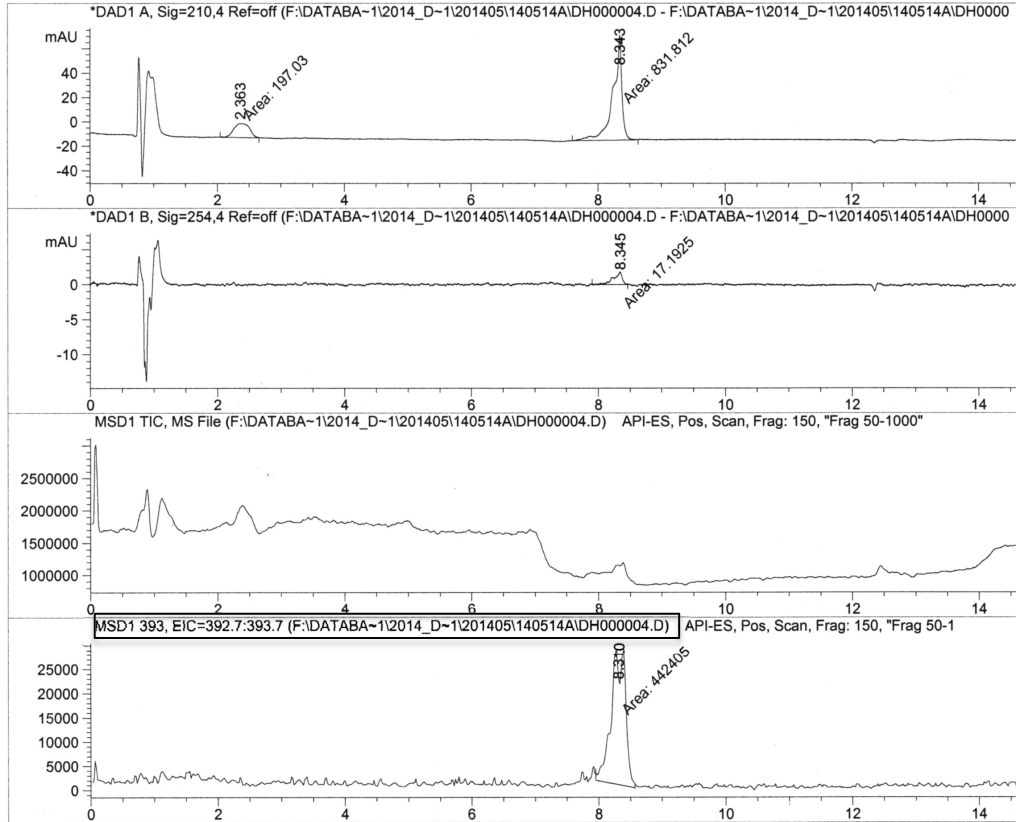


```
=====
Fraction Information
=====
Fraction collection off
=====
No Fractions found.
=====
```

Peptide 4

NMH_SCSc 0.1% AA in aq and ACN CR_HILIC.m May 14, 2014

```
=====
Injection Date : 5/14/2014 12:04:06 PM      Seq. Line : 4
Sample Name    : NMH_SCSc                    Location  : P1-D-02
Acq. Operator  : Ed                          Inj       : 1
Acq. Instrument: 1100LC                       Inj Volume: 1 µl
Different Inj Volume from Sequence !      Actual Inj Volume : 10 µl
Acq. Method    : C:\HPCHEM\1\METHODS\CR_HILIC.M
Last changed   : 2/21/2014 8:56:40 AM by Ed
Analysis Method : C:\HPCHEM\1\METHODS\CR_C18MS.M
Last changed   : 7/25/2014 11:19:16 AM by Ed
Agilent SB-C18 2.1*30mm, 3.5µm; 0.5mL/min, 40'C
M.P.A.:H2O M.P.B: ACN
=====
```



```
=====
Fraction Information
=====
Fraction collection off
=====
No Fractions found.
=====
```

Peptide 5

0.1% AA in aq and ACN CR_C18MS.m Jul 10, 2014

```
=====
Injection Date : 7/11/2014 11:17:07 AM      Seq. Line : 102
Sample Name    : NMH-1-Wang                  Location  : P2-F-03
Acq. Operator  : Ed                         Inj      : 1
Acq. Instrument: 1100LC                     Inj Volume: 1 µl
Different Inj Volume from Sequence !      Actual Inj Volume : 10 µl
Acq. Method    : C:\HPCHEM\1\METHODS\CR_C18MS.M
Last changed   : 5/27/2014 10:16:01 AM by Ed
Analysis Method: C:\HPCHEM\1\METHODS\CR_C18.M
Last changed   : 7/11/2014 11:35:58 AM by Ed
              (modified after loading)
Agilent SB-C18 2.1*30mm, 3.5µm; 0.5mL/min, 40°C
M.P.A:H2O M.P.B: ACN
=====
```

